DAYTIME RADIATION REGIMES WITHIN A CORN CANOPY

DAYTIME RADIATION REGIMES WITHIN A CORN CANOPY

by

WILLIAM JOHN KYLE, B.Sc.

A Thesis

Submitted to the Faculty of Graduate Studies

in Partial Fulfillment of the Requirements

for the Degree

Master of Science

McMaster University

May 1971

MASTER OF SCIENCE (1971)
(Geography)

McMASTER UNIVERSITY
Hamilton, Ontario

TITLE: Daytime Radiation Regimes within a Corn Canopy

AUTHOR: William John Kyle, B.Sc. (University of Nottingham)

SUPERVISOR: Professor J. A. Davies

NUMBER OF PAGES: xiii, 140

SCOPE AND CONTENTS:

A micrometeorological investigation was conducted over and within a crop of corn (Zea mays, var. Seneca Chief). The purpose of the experiment was to observe net radiation profiles within the canopy and to determine their behavior with respect to crop density. Discussion of the construction and evaluation of linear net radiometers for use in this study is included. The net radiation profiles are examined and compared with existing theoretical models. The form of the profiles is studied and a new model of net global radiation profiles based on micrometeorological data and crop parameters is discussed.

ACKNOWLEDGEMENTS

This study was supported by a research grant from the National Research Council of Canada.

Special acknowledgement goes to Dr. J. A. Davies, as Research Director, whose guidance and support throughout this study has been gratefully appreciated. Thanks also to other members of the Department of Geography for assistance and useful comment during the investigation. In particular, I am grateful to Mr. M. Nunez who was responsible for the initial development of the radiation model described in Chapter VII.

The assistance of Dr. G. Collin, Director of the Ontario Horticultural Experiment Station, and his co-workers, in preparing the site is gratefully acknowledged.

The figures were prepared with the assistance of Mr. H Fritz and the final draft was typed by Miss J. Hillen to whom grateful thanks are extended.

Final acknowledgement is to my wife, Ina, for her encouragement and perseverance during my studies.

TABLE OF CONTENTS

LIST OF PLATES

LIST OF TABLES

LIST OF FIGURES

LIST OF SYMBOLS

a	leaf absorption coefficient	(dimensionless)
D	diffuse component of global radiation	($W\ m^{-2}$)
F	leaf-area-index	($cm^2\ cm^{-2}$)
Fc	cumulative leaf-area-index = $\int_x^h F(z)\ dz$	(dimensionless)
F'/F	Wilson-Reeve leaf-area ratio	(dimensionless)
h	height of crop canopy	(cm)
I	direct component of global radiation	($W\ m^{-2}$)
j	foliage angle of plants	(deg)
k	Monsi and Saeki extinction coefficient for short-wave radiation	(dimensionless)
K	transmission coefficient for thermal energy	($m^2\ s^{-1}$)
Ld	downward long-wave radiation	($W\ m^{-2}$)
Ln	net long-wave radiation	($W\ m^{-2}$)
Lo	net long-wave radiation at zero global radiation	($W\ m^{-2}$)
Lu	upward long-wave radiation	($W\ m^{-2}$)
m	angle of penetration of direct solar radiation	(deg)
r	correlation coefficient	(dimensionless)
Rn	net all-wave radiation (radiation balance)	($W\ m^{-2}$)
ε	Monteith's fraction of incident radiation which passes unintercepted through a layer	(dimensionless)

S	incoming short-wave (global) radiation	($W\ m^{-2}$)
Sn	net short-wave (global) radiation	($W\ m^{-2}$)
t	Student's t value = $(a - b)/\sqrt{\left[2/(N - 1)\right]}$	
T	temperature	(^{o}C)
Ta	air temperature	(^{o}C)
Tb	temperature of sensor bottom surface	(^{o}C)
Tm	mean temperature	(^{o}C)
Tt	temperature of sensor top surface	(^{o}C)
z	depth of measurement in canopy	(cm)
α	reflection coefficient	(dimensionless)
αg	ground reflection coefficient	(dimensionless)
β	"surface heating coefficient"	(dimensionless)
ε	emissivity of a surface	(dimensionless)
ζ	solar zenith angle	(deg)
κ	extinction coefficient for net radiation	(dimensionless)
λ	wavelength of radiation	(nm)
π	3.14159265	
σ	Stefan-Boltzman constant = 5.67×10^{-8}	($W\ m^{-2}\ deg^{-4}K$)
τ	leaf transmission coefficient	(dimensionless)
ϕ	solar azimuth angle	(deg)
$\frac{\partial(\ )}{\partial(\ )}$	partial derivative	
Δ	finite difference operator	

CHAPTER I

INTRODUCTION

1. Radiation and crops

The determination of radiation regimes within crop canopies is a central problem in agricultural meteorology because the microclimate of a plant community is largely controlled by the energy balance. Transpiration and photosynthesis, the two major processes in the crop canopy are closely coupled to the energy balance. Transpiration is governed to a considerable extent by the net radiation within the crop, which is the main source of energy available for the evaporation of water from leaves. Photosynthesis is the principle form of plant nutrition. Yields are first of all intimately dependent on the rates and results of the photosynthetic activity of plant crops, which in turn is associated with the amount of photosynthetically-active radiation intercepted by the leaves, and to the carbon dioxide available in the canopy.

Following Monteith (1965a) three aspects of radiation can be considered to be biologically significant. The first is radiation intensity which describes the amount of energy received by unit surface in unit time. The second is the spectral distribution of the energy which governs photochemical reactions such as photosynthesis. Finally there is the distribution of energy in time, important for a wide range of photoperiodic phenomena.

The radiation regime of a plant community may be considered as a budget containing two major terms, radiation income and radiation losses. Income consists of solar radiation and atmospheric radiation. The radiant energy from the sun consists of wavelengths between 0.3 and 4.0 μm and hence is known as short-wave radiation; roughly half of this energy is contained within the visible portion of the spectrum (0.4 - 0.7 μm). The spectral distribution is dependent on solar altitude. When the sun is directly overhead visible radiation constitutes about half of the direct radiation. At a solar altitude of 20^{o} only 30% of the radiation is in the visible portion. Solar radiation that penetrates the atmosphere without being scattered reaches the earth as a direct beam. Superimposed on the solar spectrum are the absorption bands of the atmospheric gases; 1. ozone mainly in the ultra-violet region 2. water vapour in the near infra-red bands centered at 0.93, 1.13, 1.42, and 1.47 μm, and 3. carbon dioxide in the near infra-red bands at 2.7 μm (Chang, 1968). Figure 1 shows a typical depleted solar spectrum reaching the ground surface from a solar zenith angle of 60^{o} as a plot of irradiance against the equivalent wave number, the reciprocal of wavelength. This plot has the advantage of accomodating the full spectrum without the long-wavelength tail.

Solar radiation absorbed by atmospheric gases is reemitted as long-wave radiation at wavelengths between 3 and 100 μm. However, total atmospheric absorption, and therefore emission, is much greater for long than short wavelengths. This is chiefly because water vapour absorbs strongly over certain wavelength bands prominent in the terrestrial long-wave spectrum. This absorption of the earth's outgoing radiation results

FIG. 1. *SPECTRAL DISTRIBUTION OF SOLAR RADIATION (after Brooks, 1956).*

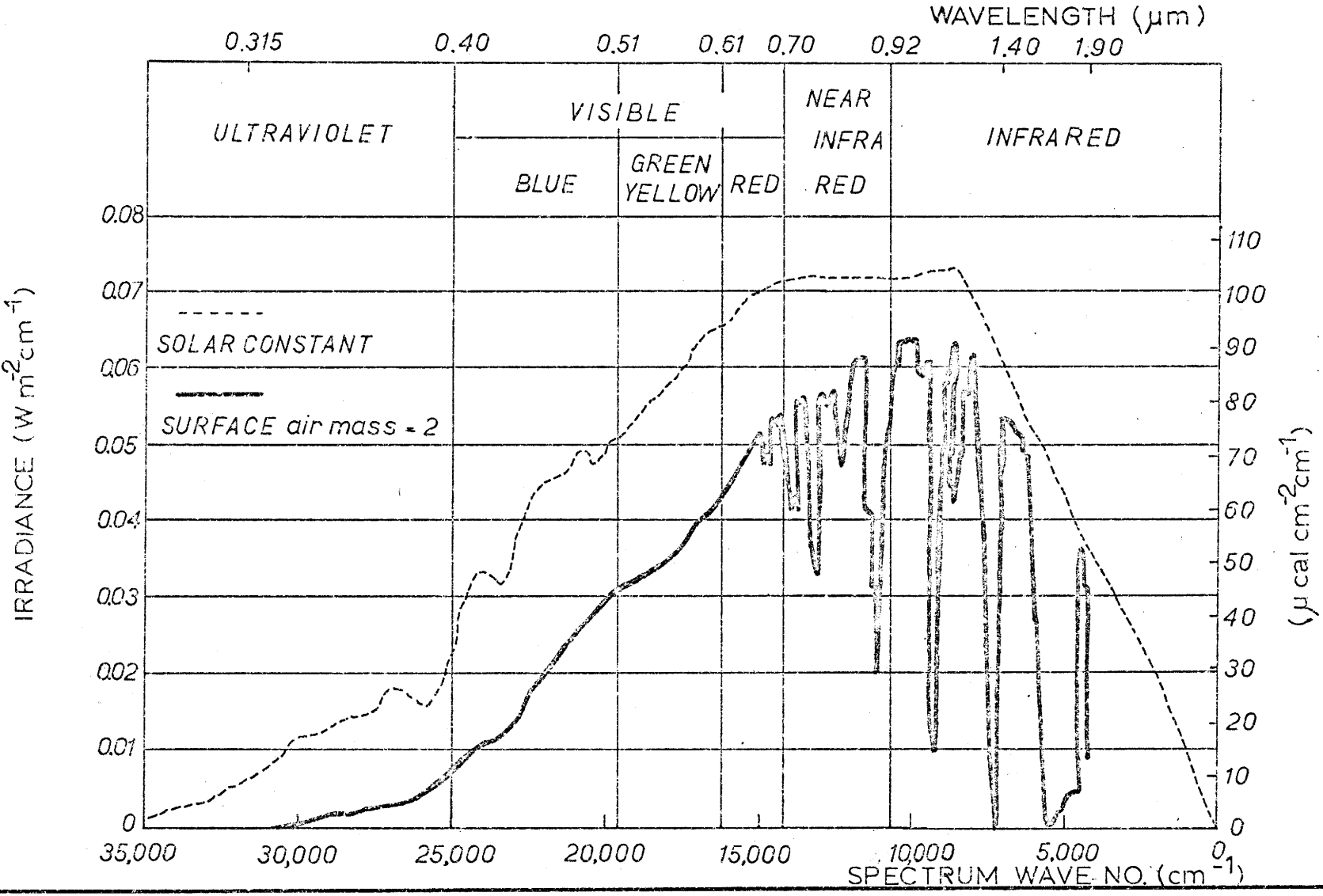

in a considerable downward flux of long-wave radiation back to the earth's surface from the atmosphere.

Radiation losses are due to reflection of solar radiation, transmission and absorption in the canopy, and long-wave radiation emission. Studies by Gates (1965) show that for single leaves reflection and transmission spectra are very similar (Fig. 2). Visible light between 0.4 and 0.7 μm is strongly absorbed by leaf pigments such as chlorophyll. Little radiation is absorbed beyond 0.7 μm in the near infra-red. At 1.5 μm and 2.0 μm and beyond 3.0 μm, leaf spectra exhibit the absorption bands of liquid water. Over the whole spectrum the incident radiation can be multiplied by a reflection coefficient to obtain the intensity of reflected radiation. When leaves form the canopy of a field crop, some radiation is trapped between them by multiple reflection so that the reflection coefficient for the canopy as a whole is less than for single leaves, and seldom exceeds 25% (Monteith, 1959a).

Below the top of the crop, some radiation reaches the ground in the form of sunflecks that are spectrally unchanged. Some, mainly infra-red, also reaches the soil surface by transmission and reflection downwards by leaves. These terms are important since any radiant energy not absorbed by leaves must be considered when calculating transpiration or photosynthesis. Since leaves absorb radiation they therefore emit long-wave radiation virtually as black bodies, the intensity of emitted radiation being proportional to the fourth power of their absolute temperature.

A model of radiation transmission through the elements of a plant community is necessary in gaining knowledge of the use made by the crop of the incident radiation. It is likely to be related to the amount of

FIG. 2. *SPECTRAL REFLECTANCE, TRANSMITTANCE AND ABSORPTANCE OF LEAVES OF Populus deltoides (after Gates, 1965)*

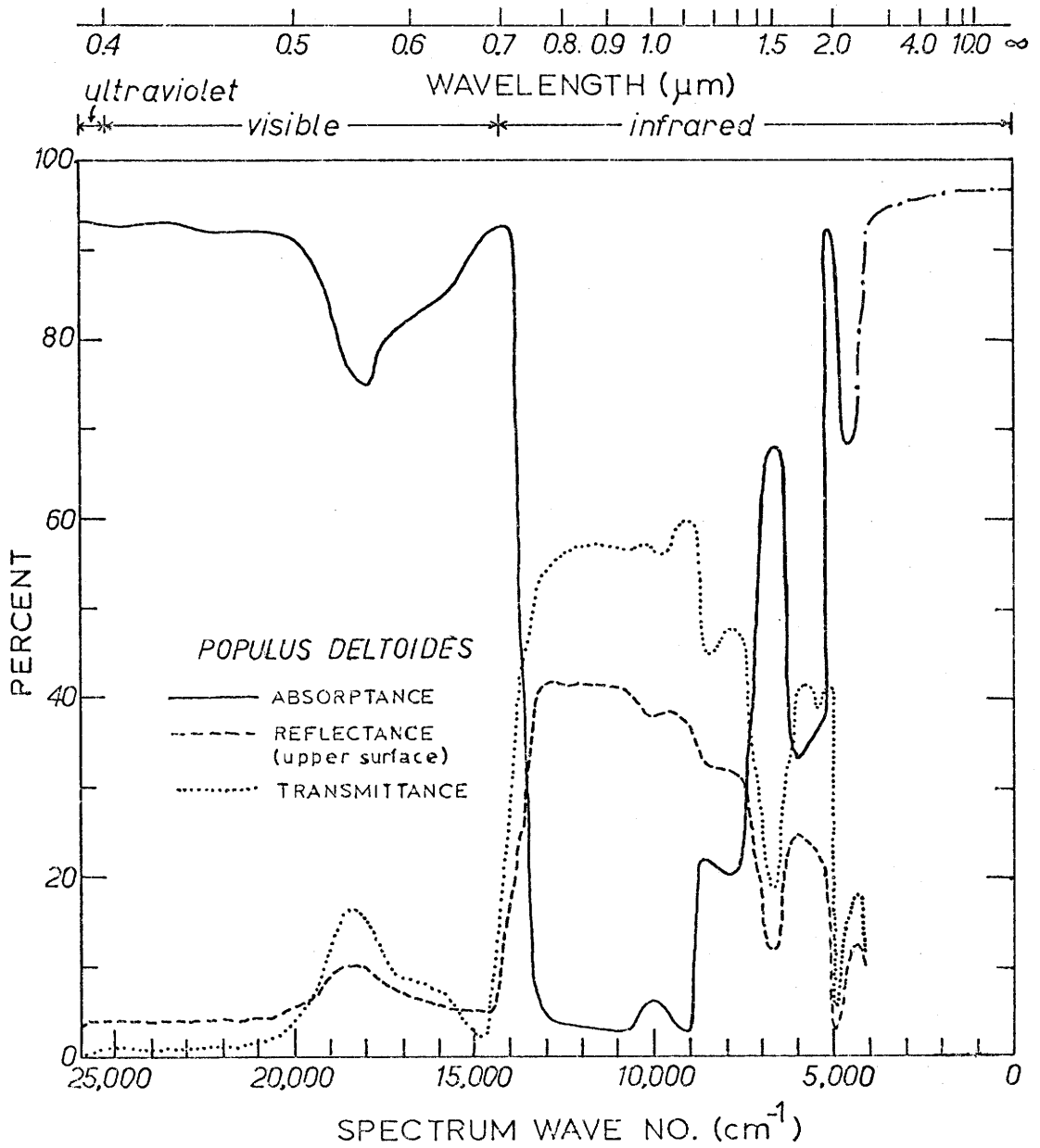

IDEALISED LEAF SPECTRA

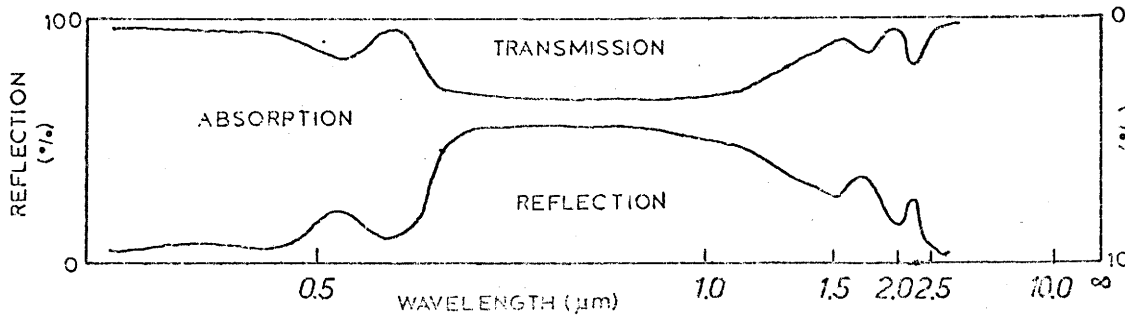

foliage in a stand of plants as specified by leaf density. Most studies have neglected processes within canopies and considered energy exchanges at uniform horizontal planes. In the air layers next to such planes vertical divergence of any flux is negligible. However, within canopies marked flux divergence is present at all times. Clearly, divergence strongly depends upon the structure of the canopy.

The net amount of radiation absorbed by a plant community or its radiation balance, Rn, is the difference between radiation gained from the sun and atmosphere, and that lost by reflection, transmission, and emission. For a plane some distance above the canopy this can be expressed as

$$Rn = (S - \alpha S) + (Ld - Lu). \qquad (1)$$

In the case of a cropped surface this is of course an oversimplification. From the top of the canopy downwards we are dealing with a zone of flux divergence. To illustrate this point consider a crop canopy as Figure 3. Equation 1 would apply to a plane at height z3. At the plane z2 near the top of the canopy the radiation balance, Rn_2, is

$$Rn_2 = (1 - \alpha)\, S_{z2} + \left[Ld_{z2} - Lu_{z2}\right], \qquad (2)$$

and in the plane z1 nearer the bottom

$$Rn_1 = (1 - \alpha)\, S_{z1} + \left[Ld_{z1} - Lu_{z1}\right]. \qquad (3)$$

There is a divergence of the flux between the planes z1 and z2 as shown by the profile of net radiation. Source and sink distributions (vertical divergence) of Rn can be calculated by differentiation of the vertical

FIG. 3. *RADIATION BALANCE IN A PLANT CANOPY*

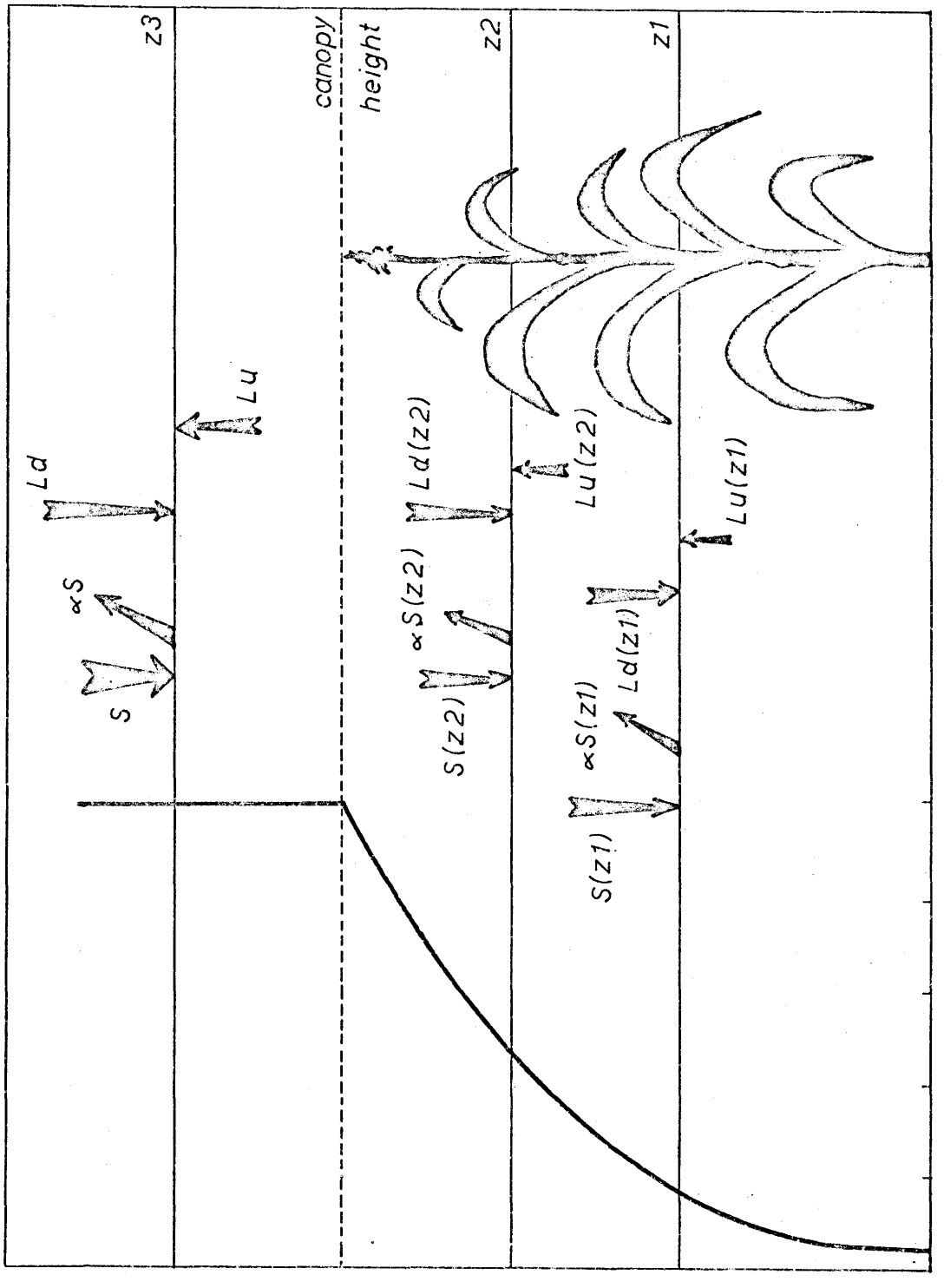

fluxes with height

$$\frac{\partial Rn}{\partial z} = (1 - \alpha) \frac{\partial S}{\partial z} + \left[\frac{\partial Ld}{\partial z} - \frac{\partial Lu}{\partial z} \right] . \qquad (4)$$

Since a canopy is composed of a large number of these planes, the complexity of a canopy radiation regime becomes apparent. Previous workers have approached the problem by layering the canopy and obtaining an empirical extinction coefficient for each layer. Such studies are useful, particularly for prediction purposes, but they do not treat the crop as a complete optical system since they use bulk parameters.

2. Objectives of present study

The main purpose of this investigation is to provide observations of net all-wave radiation and net short-wave radiation over and within a crop of corn, to evaluate canopy effects, and to test existing models of radiation profiles in canopies. The specific aims of the study were:

1. to construct and evaluate linear net radiation sensors,

2. to obtain simultaneous observations of radiation above the crop and at several levels within the canopy, and

3. to evaluate the performance of existing models and, if necessary, to suggest modifications.

CHAPTER II

RADIATION AND CROP ARCHITECTURE

1. Radiation above the canopy

1. The radiation balance

The source of all energy for physical and biological processes is global radiation. The importance of global radiation to agriculture has been expressed concisely by Monteith (1958):

> "....agriculture is an exploitation of solar energy, made possible by an adequate supply of water and nutrients to maintain plant growth".

Net global radiation and the net long-wave radiation constitute the net radiation at the surface of the earth, a fundamental meteorological variable. In general terms the radiation balance of a surface may be expressed, using the principle of conservation of energy, as

$$Rn = S(1 - \alpha) + Ln, \qquad (5)$$

where Ln, the balance between the long-wave radiation of the surface and atmosphere, is usually negative. Eq. 5 shows the dependence of net radiation on the global radiation, a reflection coefficient, and the net long-wave radiation (Fig. 4). This radiation balance at land surfaces covered by agricultural crops is very important in determining the water loss and dry matter accumulation of the vegetation as well as many features

FIG. 4. *COMPONENTS OF THE DAYTIME ENERGY BALANCE (after Rose, 1966)*

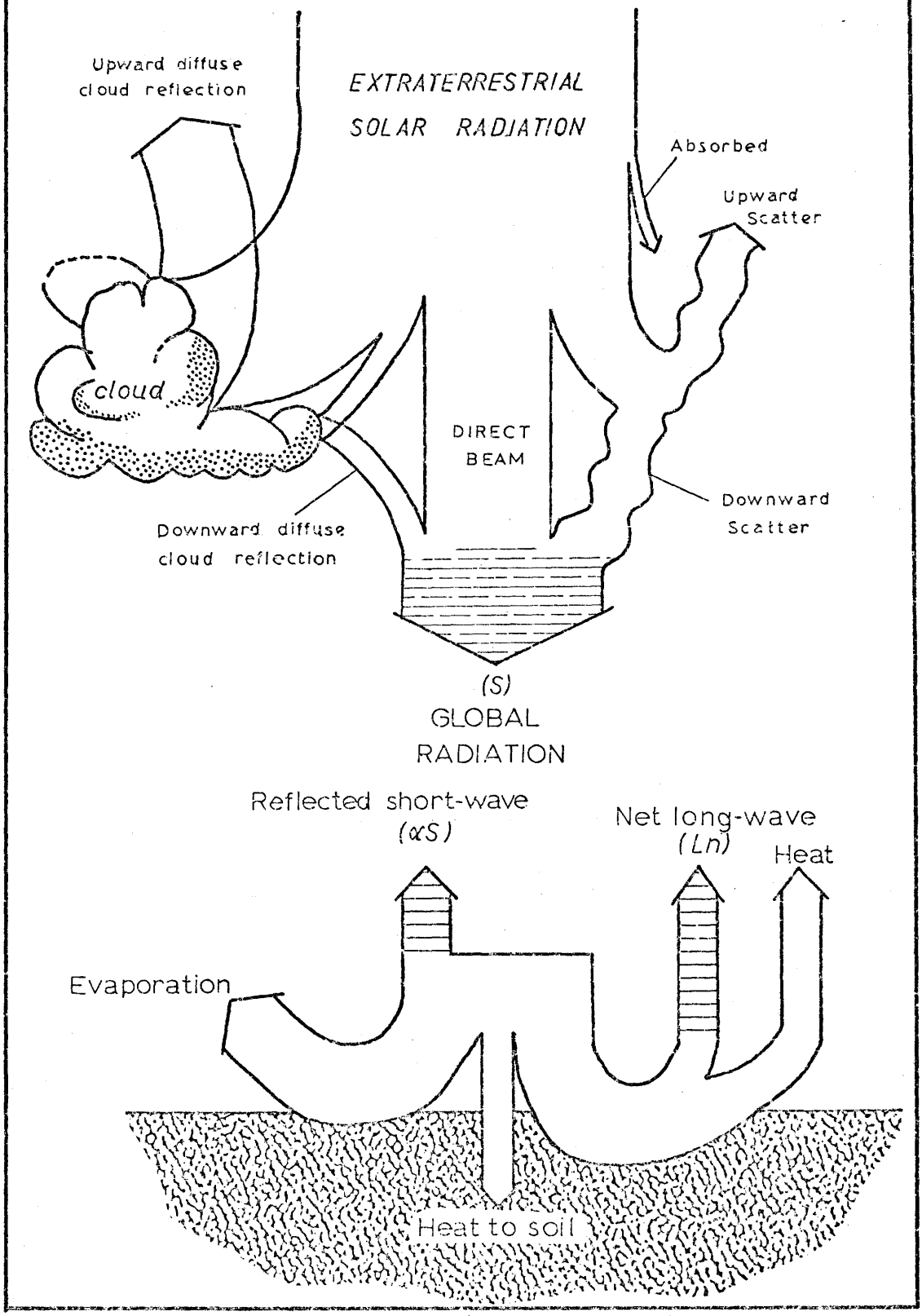

of the microclimate.

The net radiation absorbed by a surface was only seriously investigated in the 1960's. Penman (1948) emphasised its importance in determining crop evaporation but at that time climatological records comparable with those for short-wave radiation did not exist. Monteith and Szeicz (1961, 1962) have shown that the radiative characteristics of agricultural surfaces can be very closely approximated by an empirical equation. Plots of Rn against S $(1 - \alpha)$ are linear and can be fitted by simple regression to give

$$Rn = a\,(1 - \alpha)\,S + b. \qquad (6)$$

Simultaneous solution of Eq. 5 and 6 yields

$$Ln = b/a - \beta Rn, \qquad (7)$$

where $\beta = (1 - a)/a = \partial Ln / \partial Rn$. Monteith and Szeicz (1962) considered β as a surface "heating coefficient" with characteristic values between 0.10 and 0.20. Assuming that b defines the net long-wave flux when $S = 0$

$$Rn = \left[(1 - \alpha) / (1 + \beta)\right] S + Lo. \qquad (8)$$

This method of deriving the radiation balance of natural surfaces from measurements of global radiation is potentially very useful. However, values of α, β, and Lo are needed to parameterise surface types according to their vegetation cover. Further work by Stanhill, Hofstede and Kalma (1966) confirmed the linear relationship between net and global radiation. They found reflection to be the most important discriminant in

the relationship. Surprisingly low values of the "heating coefficient" were also obtained. In the literature negative values of β have been quoted (Ekern, 1965). These values may be contrasted with those suggested by Monteith and Szeicz (1962).

Several attempts have been made to explain this variation in β with little success. Linacre (1968) infers that the coefficient b in Eq. 6 depends on the degree to which the sky is overcast and thus avoids the use of β. He proceeds to explain that the differences in previously published data are mainly due to various degrees of temperature and cloudiness, and attempts to derive relationships from measurements of sunshine hours and mean temperatures. The controversy about β is, of course, not resolved with this approach.

Idso (1968) analyses the heating coefficient concept and concludes that there is no justification for the use of Eq. 8. The reason for the failure of the concept, according to Idso, is that the derivation of Monteith and Szeicz (1961) depends on the physically unrealistic assumption that net long-wave loss is a linear function of net radiation (Eq. 7). He noted that although the correlation coefficients are very high, net long-wave radiation is a small difference between two larger quantities and this reduces the reliability of Eq. 7. His conclusion is that Eq. 8 has no advantage over Eq. 6. Fritschen (1967), Davies (1967), and Davies and Buttimor (1969) found Eq. 6 to have no advantage over the simple equation

$$Rn = a\,S + b, \qquad (9)$$

hence, the use of β and a reflection coefficient may not improve the

estimate of net radiation.

2. Reflection coefficient

Not all the global radiation is retained by the surface. Some is reflected, the quantity depending on its albedo. The term albedo has generally been used to denote the reflectivity of either the total short-wave or the visible spectrum. To eliminate confusion, Monteith (1959a) suggested that albedo be used exclusively for visible light, and the term reflection coefficient for total short-wave radiation.

The reflection coefficient of a crop surface is dependent upon its colour, the moisture conditions, the density of the crop cover, leaf arrangement, and the angle of the sun. Changes of reflection coefficient during the course of a day may be expected because at high zenith angles the solar beam strikes the surface at more acute angles and a higher reflection is likely. Short-wave radiation is also trapped between the elements of a crop canopy and this tends to lower the reflection coefficient (Monteith, 1966). The amount of trapping increases with irregularity of the surface and with solar elevation since radiation penetrates further into the canopy as the sun approaches the zenith. Observations by Monteith and Szeicz (1961), Davies and Buttimor (1969), Impens and Lemeur (1969) and others confirm this.

In many cases it is difficult to show whether this diurnal variation may be completely attributed to solar elevation changes. When measurements are required over small plots, an inverted pyranometer normally used to measure reflection of short-wave radiation, can be positioned close to the crop surface so that only a small part of the

radiation reaches the sensor from outside the area. This procedure necessarily reduces the area sampled and may lead to biased results, particularly in row crops or crops with non-uniform cover. Hence the pyranometer must be sited so that its field of view is sufficiently large to sample a representative area of the cropped surface. This means that at high zenith angles there is a strong possibility that some incoming radiation will impinge on the sensor thus overestimating the reflected radiation intensity. This implies that the increase in reflection coefficient at high zenith angles may be completely instrumental.

Investigations undertaken by Brown, Rosenberg and Doraiswamy (1970), revealed that by shading the pyranometer to reduce the field of view the ratio of unshaded to shaded measured reflection was about 1.3 during the mid-day period (zenith angle = 25° - 40°) and was as large as 1.6 at high zenith angles. They concluded that to achieve proper measurement of the reflected short-wave radiation it is necessary to prevent radiation from entering the glass bulb of an inverted pyranometer at high zenith angles.

A considerable amount of work has been done in obtaining measurements of reflection coefficients for a wide variety of surfaces thus underlining the importance of this component of the radiation balance. Table 1 summarises a number of observations of the reflection coefficients of field crops at various sites around the world. It will be seen that in the middle and high latitudes, the maximum reflection coefficients for mature crops that completely cover the ground are approximately 0.25 (Monteith, 1959a); whereas in the tropics, the values are much lower. Two recent papers by Oguntoyinbo (1970a and 1970b) confirm this trend

TABLE ONE

REFLECTION COEFFICIENTS OF FIELD CROPS

LOCALITY	CROPS	REF. COEFF.	REFERENCE
England 51°50'N	Grass, lucerne, potatoes, sugar beet, spring wheat	0.25-0.27	Monteith (1959b)
USSR	Rye	0.10-0.25	Budyko (1958)
	Potatoes, meadow grass	0.15-0.25	
	Cotton	0.20-0.25	
Canada 43°30'N	Corn	0.12-0.21	Graham and King (1961)
England 51°50'N	Short grass	0.25-0.27	Monteith and Szeicz (1961)
	Long grass	0.26	
	Kale	0.19-0.28	
Hawaii 20°N	Sugar cane	0.05-0.18	Chang (1961)
	Pineapple	0.05-0.08	Ekern (1965)
New York 42°30'N	Corn	0.235	Allen and Brown (1965)
Australia 15°42'S	Irrigated cotton	0.17-0.20	Fitzpatrick and Stern (1965)
Canada 42°50'N	Corn	0.22-0.25	Davies and Buttimor (1969)
	Wheat	0.21-0.25	
	Tobacco	0.24	
	Grass	0.23-0.24	
Belgium 51°03'N	Sunflower	0.23-0.32	Impens and Lemeur (1969a)
	Beans	0.20-0.28	
	Corn	0.20-0.30	
Israel 13°N	Cotton (irrigated)	0.13-0.19	Stanhill et al., (1968)
Nigeria 7°30'N	Tobacco	0.15-0.23	Oguntoyinbo (1970b)
	Corn	0.17	
	Yams, vegetables, melons	0.13-0.20	

and strengthen the assertion that it is not a satisfactory procedure to use albedo values taken from higher latitudes to obtain values of the radiation balance in the tropics. The low reflectivity in the tropics may, in part, be due to greater solar elevations at these latitudes.

2. Radiation profiles in crop canopies

1. Introduction

The ability to characterise the radiation regime in crop canopies is essential to the understanding of plant community activity in such processes as evaporation, heat exchange, and photosynthesis. Consequently attempts have been made to evaluate those conditions which make it possible to produce crops that absorb the greatest amount of energy from solar radiation and most efficiently use it for photosynthesis and for the production of useful yields. In order to accomplish this the crop must be studied in detail as a complete optical system.

In the last 20 years a number of studies have appeared and material has been accumulated so that some general conclusions may be drawn. Some of the earliest work are the studies made by the Japanese (Monsi and Saeki, 1953; Kasanaga and Monsi, 1954) who divided the biomass into 10 cm layers and considered the illumination at the interfaces of successive layers. Since these initial studies were concerned with short-wave radiation or part of that spectrum this aspect of the radiation regime will be considered first before dealing with themore complex problem of net radiation.

2. Short-wave profiles

Using the layer technique, Monsi and Saeki (1953) found that the

relative radiation intensity (the percentage of radiation incident upon a plant stand which is recorded at a level inside the canopy) decreases exponentially with increasing leaf-area-index. Their exponential model is

$$S(z) = S(h).\ \exp(-kF), \qquad (10)$$

in which, S(h) is the radiation incident upon the canopy, S(z) is the radiation received at a given level where the L A I is F, and k is an extinction coefficient. The calculated values of k from Eq. 10 were for a model plant stand in which foliage was inclined at a constant angle j to the horizontal and showed no preferred orientation. A further assumption was that the stand was illuminated by an isotropic sky. When calculated in terms of the radiation incident on a horizontal surface, k was found to be 1 for stands where j = 0 and to decrease with increasing values of j. What this means, in effect, is that more radiation penetrates the canopy when the leaves are nearly vertical than when they are horizontal. Although a simple model this appeared to work quite well and they used k with considerable success to predict maximum photosynthetic production. However, this may be because the further expressions for production are insensitive to changes in the value of k.

The assumptions in the model have been subject to considerable criticism particularly by Anderson (1966, 1969b). Monsi and Saeki suggested that k can be treated as effectively constant in a stand with constant leaf inclination. Their plots of log (S(z) / S(h)) against F for an isotropic sky were however, not strictly linear, but concave upwards, except when j = 0. The departure from linearity was most marked at larger values of j but Monsi and Saeki concluded that the curvature was

not sufficient to invalidate Eq. 10. Anderson disputes this assertion by saying that the slope of the line of best fit to the semi-logarithmic plot will decrease as larger maximum values of F are considered, and, although the departure from linearity in terms of log (S(z) / S(h)) may not be great, the real values of (S(z) / S(h)) may be very different from those predicted.

Values of k vary widely for direct but little for diffuse radiation. Unfortunately in crop radiation studies we have to deal with both cases. Anderson (1966) showed that when relative intensity of direct beam radiation must be considered over a range of angles of penetration m, k is not constant unless j = 0 when k = 1. From her analysis Anderson arrives at the following relationships

$$k = \cos j \qquad m \geq j \qquad (11)$$

$$k = (\cos j).\ 1 + 2(\tan\theta - \theta) / \pi \qquad m < j < \pi/2 \qquad (12)$$

$$k = 2 \cot m / \pi \qquad j = \pi/2 \qquad (13)$$

In Eq. 12

$$\theta = \cos^{-1} (\tan m / \tan j). \qquad (14)$$

Clearly k is a function of both j and m, (Fig. 5) and this necessitates a more stringent treatment of these variables thus supporting the need to treat direct and diffuse beam radiation separately. This is the approach favoured by Duncan, Loomis, Williams and Hanau (1967). They use the following plant properties,

1. leaf area,
2. leaf angle,

FIG. 5. *k AS A FUNCTION OF FOLIAGE ANGLE (j) AND ANGLE OF PENETRATION (m) (after Anderson, 1966)*

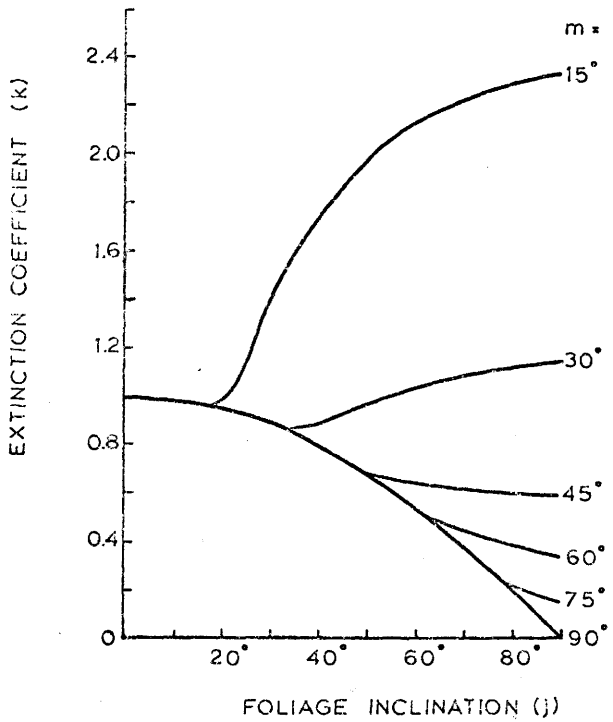

(a) THE EXTINCTION COEFFICIENT, k, AS A FUNCTION OF FOLIAGE INCLINATION, j, AT 15° INTERVAL VALUES OF m, ANGLE OF PENETRATION

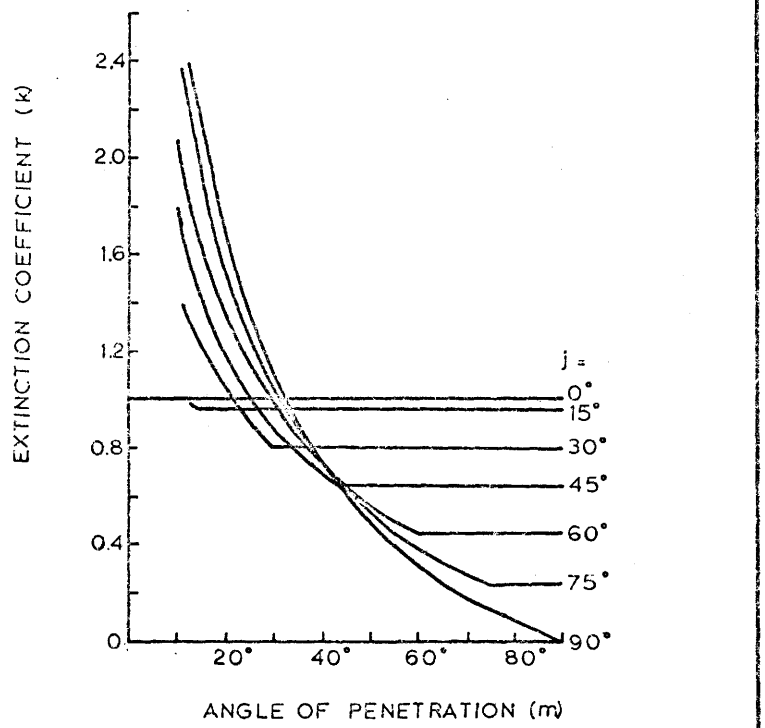

(b) THE EXTINCTION COEFFICIENT, k, AS A FUNCTION OF ANGLE OF PENETRATION, m, AT 15° INTERVAL VALUES OF j, FOLIAGE INCLINATION

3. vertical position,
4. radiation reflected from leaves,
5. radiation transmitted through leaves.

Assumptions are made that leaves grow equally in all directions around the individual stems. This is likely to be the case with plants with 180^{o} phyllotaxis such as corn. Leaf area and position are described as leaf-area-index within each layer. Further assumptions include; 1. leaves are vertically separated enough in relation to their width to permit uniform penetration of skylight; 2. leaves act as Lambertian surfaces, reflecting light non-directionally; 3. transmitted radiation penetrates further into the canopy as diffuse radiation.

Environment for the model consists of a point source of light simulating the sun, which may be at any elevation above the horizon, and a hemispherical sky. The variables used are

1. solar elevation (or zenith angle),
2. solar intensity,
3. brightness of diffuse radiation.

Azimuth angle is not necessary since the leaves are assumed to be randomly dispersed and are given uniform directional orientation. Skylight is assumed to come from a sphere of uniform brightness.

The treatment is in two parts. The penetration of the direct beam may be considered as a function of the area of the leaves, their angle, and of the solar elevation. The assumption of random distribution allows the use of the Poisson distribution equation to estimate the probability

of penetration by rays of light.

Using the theory developed by Reeve (1960) for inclined point quadrats and the F'/F ratio developed by Wilson (1960) which, in this context, is the ratio between the shadow cast by a leaf on a plane normal to the sun's rays F' and the actual area of the leaf F Duncan et al. (1967) arrive at

$$S(z) = S(h).\ \exp\left[-(F'/F)_{jm} / \sin m.\ F_c\right], \qquad (15)$$

where $(F'/F)_{jm}$ is the Wilson-Reeve F'/F ratio for the leaf angle j and sun angle m; F_c is the cumulative leaf-area-index; and sin m is the sine of the angle of the sun above the horizon. Expressed in terms of solar zenith angle, ζ, Eq. 15 becomes

$$S(z) = S(h).\ \exp\left[-(F'/F)_{jm}.\ \sec\zeta\ .\ Fc\right]. \qquad (16)$$

This is a form of the Beer-Lambert law as used by Monsi and Saeki (Eq. 10) with $(F'/F)_{jm}.\ \sec\zeta$ equivalent to their k. In this case instead of a constant depletion coefficient the rate of depletion is controlled by leaf area and angle and by solar angle.

The treatment of diffuse skylight follows the method of Hanau (1967) which enables illumination of either or both surfaces of a leaf of any angle, from any zone of the hemispherical sky to be calculated. An equation of the same form as Eq. 15 is obtained for each zone, solved, and the total value of skylight in the middle of each foliage layer computed as the sum of the values of S calculated for radiation from each sky zone.

This method is clearly a considerable improvement over the simple

relationship given in Eq. 10. The major problems are the complexity of the variables and the difficulty in obtaining representative values for each.

In all the models discussed so far a source of error is neglect of the changing spectral composition of radiation, selectively depleted of wavelengths used for photosynthesis as it proceeds downwards. This means that k will decrease with increasing leaf area. This was confirmed by Allen and Brown (1965) and by Gates, Keegan, Schleter and Weidner (1965). They found two distinct regions of the solar spectrum as far as gross optical properties of the canopy are concerned. Their data showed that the average percent transmission at the ground level was of the order of 5 - 10% in the 0.4 to 0.7 μm region whereas it was 30 - 40% in the 0.7 to 1.0 μm range. This supports the view that the short-wave radiation characteristics throughout a plant community should be considered in two parts, visible and near infrared.

To describe changes in intensity and quality of the radiation penetrating a crop with leaf-area-index F, Monteith (1965b) proposed dividing the foliage into F horizontal layers each of unit leaf-area-index. He further specified average arrangement and orientation of the leaves by a parameter, s, which is the fraction of incident radiation that passes through a layer without being interrupted. This imposes the limiting conditions of $s = 0$ for a horizontal sheet of foliage and $s = 1$ for leaves parallel to a collimated beam of radiation. In practice, according to Monteith, s will be the fractional area of sunflecks below the first leaf layer.

Following Monteith (1965b), if τ_λ is the mean fractional trans-

mission and S_λ is the corresponding radiation intensity in the part of the spectrum between λ and $\lambda + d\lambda$, the effective transmission coefficient over a spectral range is

$$\tau = \int S_\lambda \tau_\lambda d_\lambda \; / \; \int S_\lambda d_\lambda . \tag{17}$$

The fraction of radiation transmitted through F leaves is then

$$\tau^F = \int S_\lambda \tau_\lambda{}^F d_\lambda \; / / \int S_\lambda d_\lambda \; . \tag{18}$$

Measuring downwards from the top of the crop canopy, the radiation below the first leaf layer is

$$S_{(1)} = [s + (1 - s)\tau] \; . \; S_{(h)} . \tag{19}$$

Because of the assumption that there is no leaf overlap in unit layer, then after F layers have been penetrated the intensity is

$$S_{(F)} = [s + (1 - s)\tau]^F \; . \; S_{(h)} . \tag{20}$$

In the expansion of the binomial, any term of the form τ^n is given by Eq. 18 with $1 \leqslant n \leqslant F$. The form of the expansion is given by Fig. 6 for F = 3. The flux of radiation after n layers has n + 1 components. The first (s^n) is the fractional area of the uninterrupted beam; the second ($ns^{n-1}(1-s)\tau$) is the fractional area of radiation suffering one interception and so on. By integration over all the leaf layers the total leaf area receiving radiation after interception by n higher layers is found by summing the coefficients of τ^n.

Monteith (1965b) plots curves from his own measurements on barley and kale at Rothamsted and fits data from Brougham (1958) and Stern and

FIG. 6. *TRANSMISSION AND INTERCEPTION OF RADIATION IN A CROP WITH THREE LEAF LAYERS (after Monteith, 1965 b)*

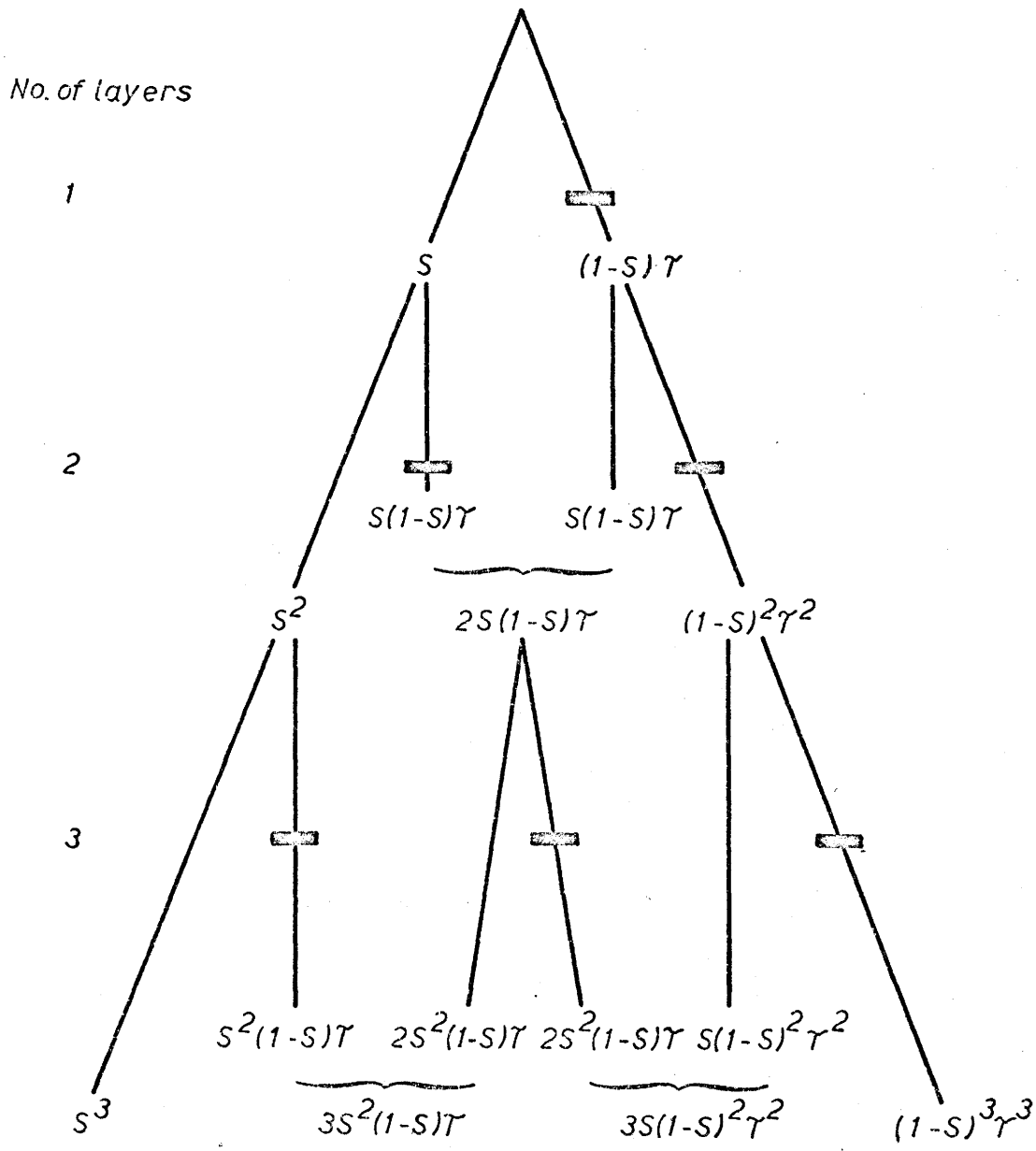

Donald (1962) for grass and clover swards to support his claim that by specifying the average arrangement and orientation of the leaves by the parameter s, the fraction passing through unintercepted, good agreement can be obtained between measured and theoretical profiles. The major problem in this approach is to find appropriate values of s for different types of crops and to justify the assumption that s is constant with depth in the canopy. This does not seem to be the case and any assumption that s is independent of leaf-area-index is not strongly supported by observations.

3. Net radiation profiles

The prediction of net radiation successfully in the plant canopy is a much more difficult task because the presence of the crop elements contributes to the sources and sinks of long-wave radiation. However, it has been found that the decline of net radiation in the canopy can be closely approximated by an exponential relationship similar to that used for short-wave radiation depletion. Brown and Covey (1966) noted that the exponential equation only approximates the data points, whereas an upward concave curve fits them better (Fig. 7). This is in agreement with findings by Isobe (1962) in a theoretical study of relations between short-wave radiation and cumulative leaf-area-index. From his calculations he also concluded that the semi-log plot of extinction dependence on leaf area demonstrated an upward concave relationship. Clearly common factors are operating in both cases.

Maharaj Singh, Peters and Pendleton (1968), working with soybeans, also plot net radiation as a function of height and hence of leaf area,

FIG. 7. *RELATIONSHIP BETWEEN NET RADIATION TRANSMISSION AND LEAF-AREA-INDEX IN A CORN CROP (after Brown & Covey, 1966)*

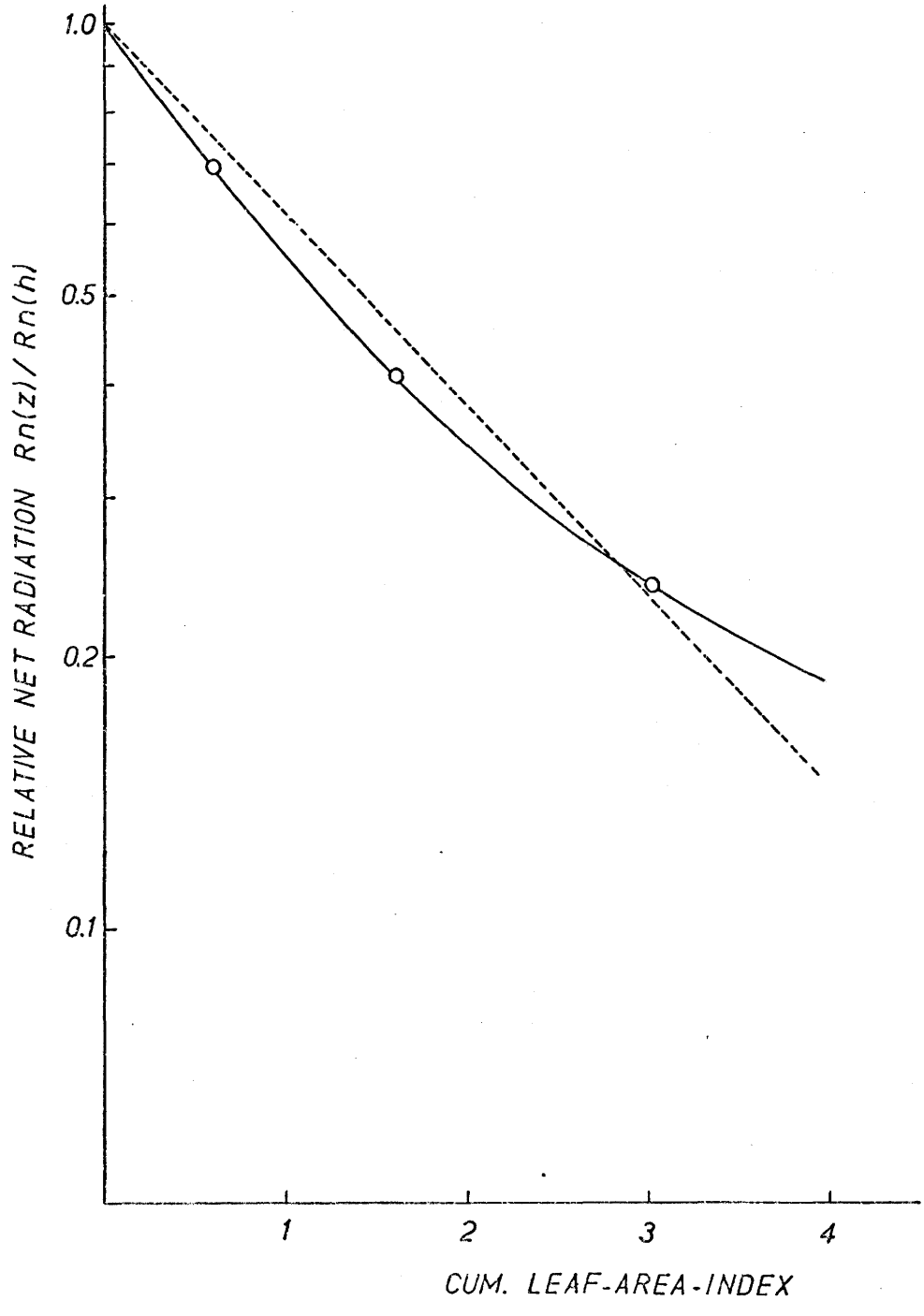

to simulate how closely net radiation can be represented by Beer's Law absorption. Strong deviations were shown in the bottom quarter of the canopy, where leaf density began to decline and where the net radiation becomes strongly influenced by soil characteristics. The shape of their extinction curves however, closely approximates the computed shape for horizontal leaves due to Cowan (1966). This might be expected with a low crop with predominantly horizontal leaves such as soybeans.

Usually net radiation prediction has been used to determine the energy available for sensible and latent heat in energy balance studies. On a daily basis, mean profiles of net radiation derived from the exponential model have been used with a considerable success by Allen, Yocum and Lemon (1964) Brown and Covey (1966) and others. These workers noted that the mean daily profile was at best a close approximation and pointed out the daily variation in the extinction coefficient which is closely linked with solar angle and crop structure.

Until more is learned concerning the many factors likely to control flux divergence of net radiation in the canopy the exponential model allows a straightforward approximation which appears to be adequate for energy budget studies on a daily basis. However, if insight is to be gained into the controlling mechanisms a more rigourous treatment of individual fluxes, temperature profiles and canopy structure is needed.

CHAPTER III

CONSTRUCTION AND EVALUATION OF LINEAR RADIATION SENSORS

1. Theory

In principle, the measurement of net radiation is relatively simple. A thermopile is placed in the radiational field and the temperature difference is measured electrically. The principle involved is that the temperature difference between two blackened elements is directly proportional to the difference in radiation received. If such a thermopile is mounted above a surface so that one element faces upwards and one faces downwards, the temperature difference $(T_t - T_b)$ is proportional to the net all-wave radiation:

$$Rn = C\,(T_t - T_b). \tag{21}$$

The constant of proportionality, C, depends on the physical properties of the sensor, and the free air windspeed. Convection is the most important error term.

Following Tanner (1963) the relation between net radiation and temperature can be expressed as:

$$Rn = C(2K_p/\varepsilon A + K_a/\varepsilon A + 4\sigma T_m^3)\,(T_t - T_b) - 2\delta(T_m - T_a)/\varepsilon A, \tag{22}$$

where $T_m = (T_t + T_b)/2$ is the mean temperature of the plate; T_t, T_b, and T_a are the temperature of the top and bottom surfaces of the plate, and the air temperature respectively; $K_a = (K_{at} + K_{ab})/2$ is the mean transmission coefficient from the plate to the air at the top and bottom faces and $\delta = (K_{at} - K_{ab})/2$. In order to use a measurement of $(T_t - T_b)$ to give net radiation (Eq. 22) δ must be zero ($K_{at} = K_{ab}$) and the sum of terms associated with $(T_t - T_b)$ should be constant. The $2K_p/\varepsilon A$ term is a property of the construction material and is constant and usually large compared with $4\sigma T_m^3$. The major problem is in keeping K_a constant and/or small compared with K_p. This may either be done by force-ventilating the surface or by shielding it from variable ventilation by natural winds.

With ventilated net radiometers such as that designed by Gier and Dunkle (1951) major problems arise in attempting to swamp natural winds so that convective loss (K_a, Eq. 22) does not vary. Difficulty is also encountered in achieving equal forced ventilation above and below the plate ($\delta = 0$). Alternatively the flux plate can be covered with a shield which is transparent to radiation and which protects the plate from natural wind so that K_a is defined and δ can be made zero by proper attention to symmetry. This arrangement is satisfactory if T_t and T_b are not too different and if T_m is close to T_a (Eq. 22). K_a will then not be affected by convection within the shield and the changes in K_a with temperature are of the same magnitude as molecular heat diffusion in air. This effect can be further minimised if K_p is large compared to K_a, when the changes in K_a with temperature can be neglected. A complete analysis of shielded radiometers is given by Funk (1962).

In designing a net radiometer to measure relative intensities below the canopy top there are a number of important considerations. Of prime importance is the sampling area. In any plant community, and particularly a row crop, the horizontal distribution of radiation is often irregular. To measure mean intensity in a meaningful way the instrument should either be small enough for easy movement among the plants, or should be large enough to sample a representative area from a fixed position.

For a net pyranometer to be used among plants Monteith (1959b) lists the main design criteria as:

a) linearity of response; the instrument depends on the equilibrium temperature of a horizontal surface gaining heat by short-wave radiation and losing it by conduction, convection, and long-wave radiation to the surroundings. Linearity is governed by the temperature dependence of the transfer coefficients and on the magnitude of the temperature difference between the sensing surface and its environment.

b) zero constancy; this means that there must be no long-wave exchange within the instrument which could initiate a temperature gradient in the thermopile even when no short-wave radiation is incident upon it.

c) cosine and azimuth response; the response of a pyranometer to a beam of radiation of constant intensity should be proportional to the cosine of the angle of incidence of the radiation on the sensing surface but independent of its azimuth.

d) spectral response; the ideal sensor is a thermopile, uniformly sensitive over the whole solar spectrum. Among plants this is very important because visible radiation is selectively absorbed by green leaves.

e) response time; this should not exceed the maximum lag error acceptable in the study when radiation is changing rapidly in the absence of cloud.

In addition Fritschen (1963) referring to net radiometers,cites symmetry as a necessary consideration in instrumental design. Symmetry is especially important in the correct functioning of net radiation instruments since they are constructed of thermo-junctions in series with opposed polarity. Ideally output from each side of the sensor should be identical under conditions of equal radiation incident on both.

In order to sample a representative area without much replication use can be made of linear sensors which employ a thermopile unit inside a glass (Szeicz, Monteith and Dos Santos, 1964) or polyethylene tube (Denmead, 1967). Both instruments are intended to measure, in foliage, the average net radiation along a horizontal plane. Linear sensors are potentially the most useful for radiation work in plant canopies because they can be constructed large enough to sample a representative area, and lend themselves suitable for recording. To accomodate the desirable design features already noted the construction and design of linear sensors must be such that errors arising due to these causes is minimised.

2. Design and construction

The basic design of the sensor is similar to that described by Denmead (1967), versions of which are available commercially (Swissteco Pty. Ltd., Melbourne, Australia). The instrument is an extended thermopile, 1 metre long, encased in either a polyethylene, for net all-wave radiation, or a glass tube, for net short-wave radiation.

The sensing element of the radiometer consists of two sections of

plexiglas, 102 cm long, 2 cm wide, and 0.7 cm thick, bonded, after insertion of a signal lead, by polyester resin to form a "sandwich" 1.7 cm thick. The edges of the former are slightly chamfered to prevent damage to the wire, and, after sanding, they are marked to show the subsequent position of the thermocouples (Fig. 8). This former is wound with about 280 turns of 30 a.w.g. bare constantan wire. One half of the element is masked to ensure that it remains unplated. Masking tape and nail polish were found to be adequate for this task. The whole unit is cleaned with carbon tetrachloride before immersion in a standard copper sulphate plating bath. To ensure uniform copper deposit the cathode lead takes the form of a bare copper wire laid lengthwise along the centre of the former and secured at each end. The current is restricted to 15 ma cm^{-2} hr^{-1} to avoid overplating with a brittle deposit of copper.

Once plated the element is cleaned in acetone and the masking tape removed carefully, avoiding damage to the thermopile. The thermopile is then connected to the signal leads. A thin layer of polyester resin is applied to the upper and lower sensing surfaces to protect the junctions. When dry, one metre long brass shim stock (1.9 cm wide, 4 thou. thick) strips are bonded to the element with epoxy resin. These are painted with Parson's optical black (undercoat and lacquer), a matt black paint with an absorbtivity > 0.985 for all wavelengths (Eppley Laboratory Inc., Newport, RI, USA).

The remote end of the sensor is then bonded to the remote end-plug. This plug is made of plexiglas machined as in Fig. 8a. It contains an external levelling platform in the plane of the thermopile. In the case of the net pyranometer draught excluder strip is placed along

FIG. 8. *THERMOPILE FOR LINEAR NET RADIOMETER*

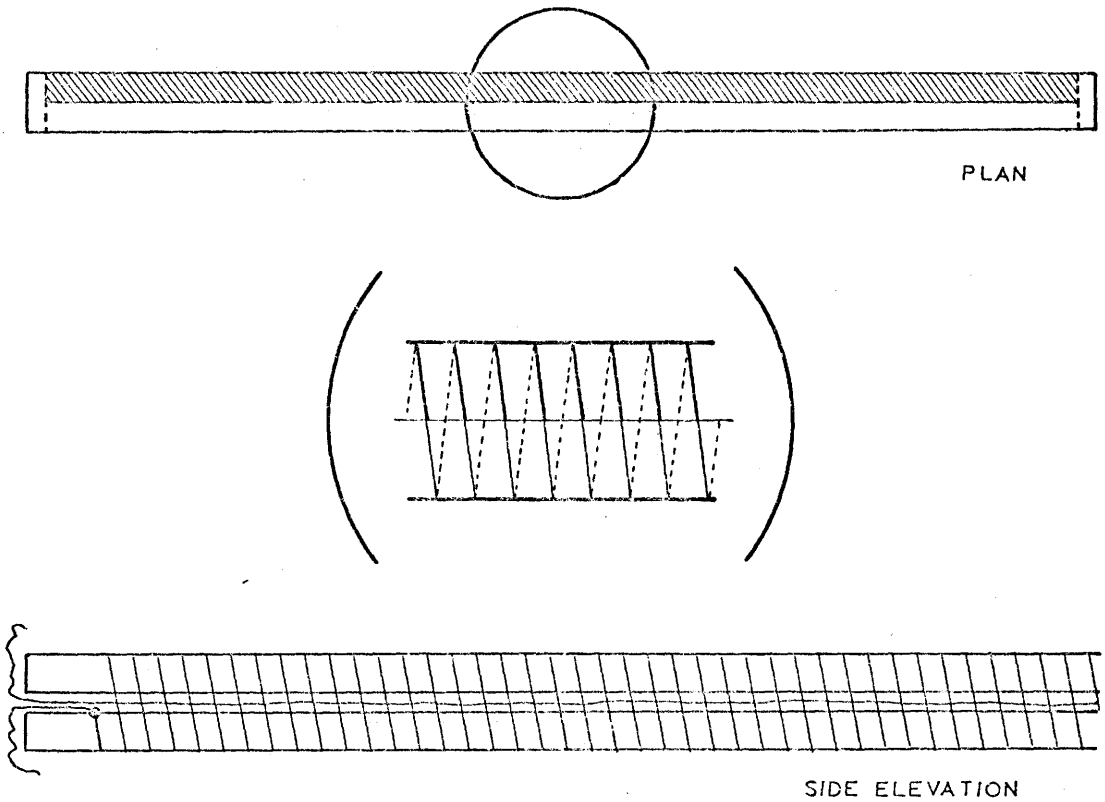

(a) REMOTE END PLUG
(b) CROSS SECTION OF ASSEMBLED SENSOR
(c) TERMINAL END PLUG

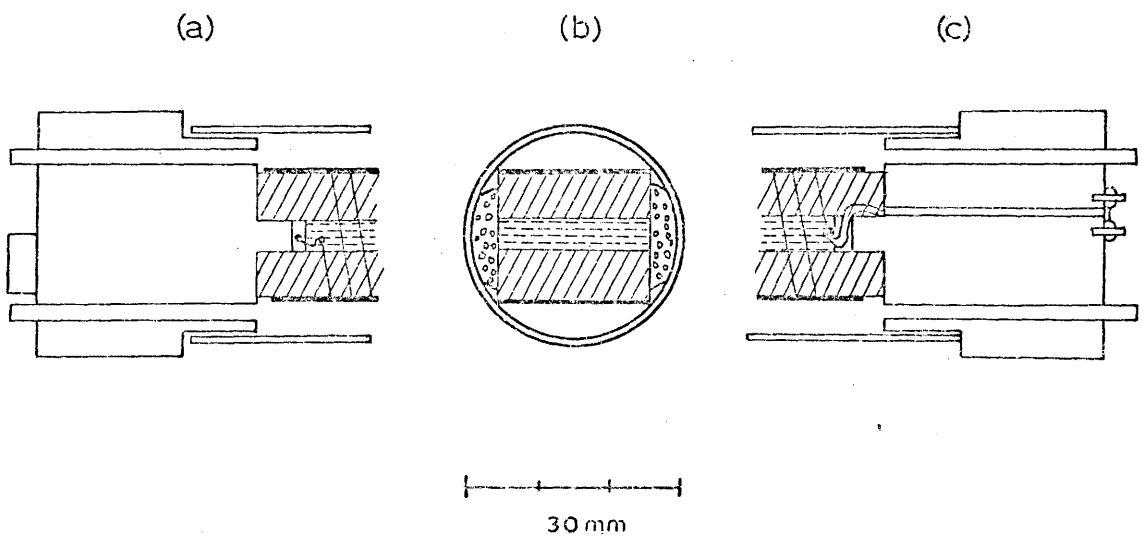

each side of the element to prevent convective exchange between top and bottom sensing surface. The glass tube (30 mm O.D.) is slipped over the element (Fig. 8b) until it rests on the shoulder of the remote end-plug. Finally the terminal end-plug (Fig. 8c) is connected, with the signal leads in place, and both ends are sealed to the glass with silicone compound. For the net radiometer, 4 mil polyethylene tube is placed over the element and held in place by two thin plexiglas strips (1 m x 1.1 cm x 0.3 cm) along the sides. These are located by five 2/56 brass machine screws. The terminal end-plug is then joined and the unit sealed as before. In both cases ventilation is achieved by tubes inserted in the end-plugs as shown in Fig. 8a and c.

3. Performance and evaluation

In August 1970 similar instruments were exposed on a rack (Plate 1) one metre above a bare soil surface. A standard net radiometer (Swissteco Pty. Ltd., Melbourne, Australia) calibrated by the Canadian Department of Transport, Met. Branch was used for comparison of sensitivities. Two net pyranometers (S 001 and S 002) were exposed initially, one oriented with its long axis north-south, the other east-west.

Comparison with the Swissteco showed that the sensitivity of the units was fairly similar, about 0.053 mV / W m^{-2} for sensor S 001 and about 0.058 mV / W m^{-2} for sensor S 002, under cloudy sky conditions. With cloudy skies the response of the two units was very similar with no orientation effect apparent (Fig. 9). Under clear skies sensitivity was markedly azimuth dependent; it was higher when the sun was at right-angle to the long axis of the instrument than when the sensor was pointing towards the sun (Fig. 10). The scatter of the data in the afternoon can

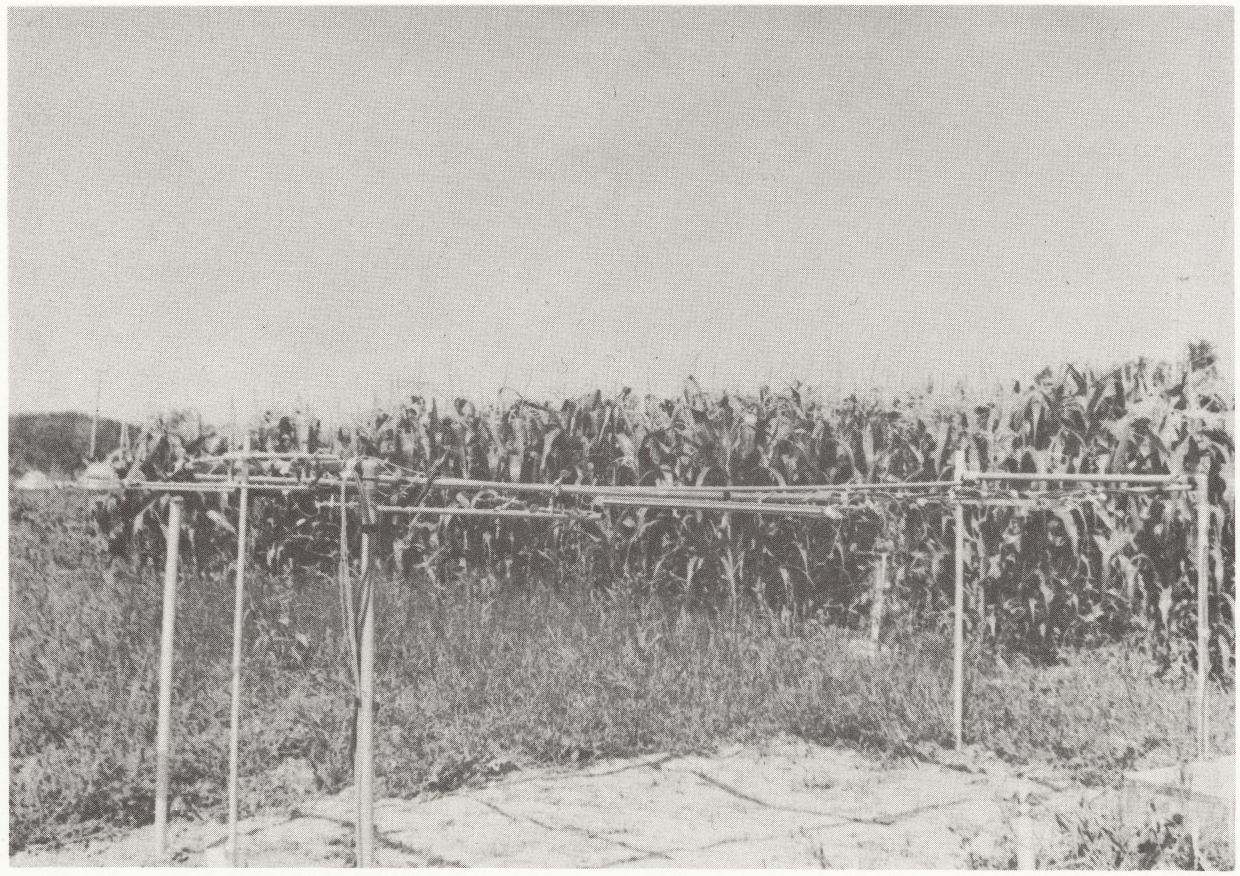

Plate 1. Linear radiometer evaluation rack.

FIG. 9. *THE EFFECT OF LINEAR SENSOR ORIENTATION ON SENSITIVITY TO SHORT-WAVE RADIATION (cloudy skies)*

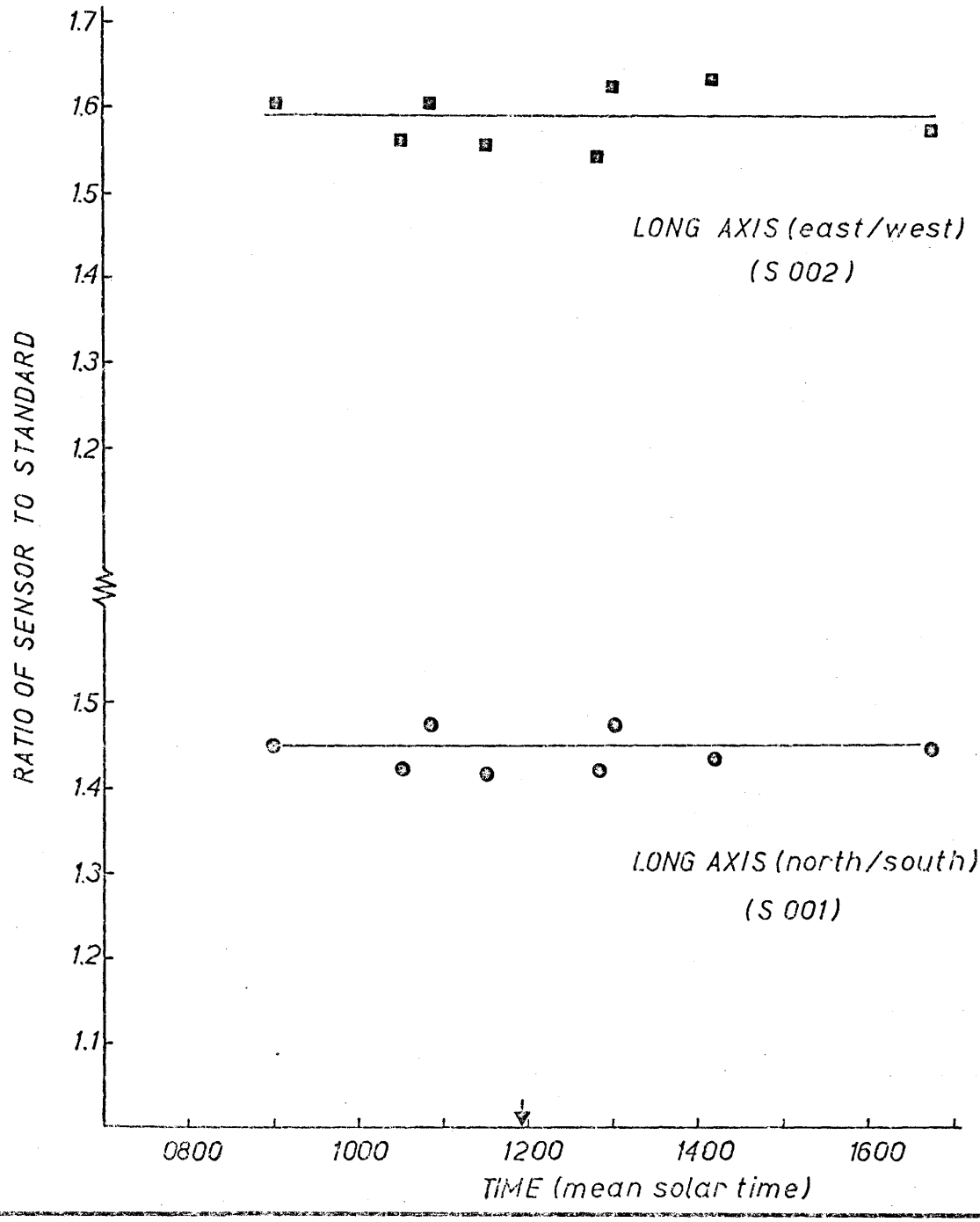

FIG. 10. *THE EFFECT OF LINEAR SENSOR ORIENTATION ON SENSITIVITY TO SHORT-WAVE RADIATION (clear skies)*

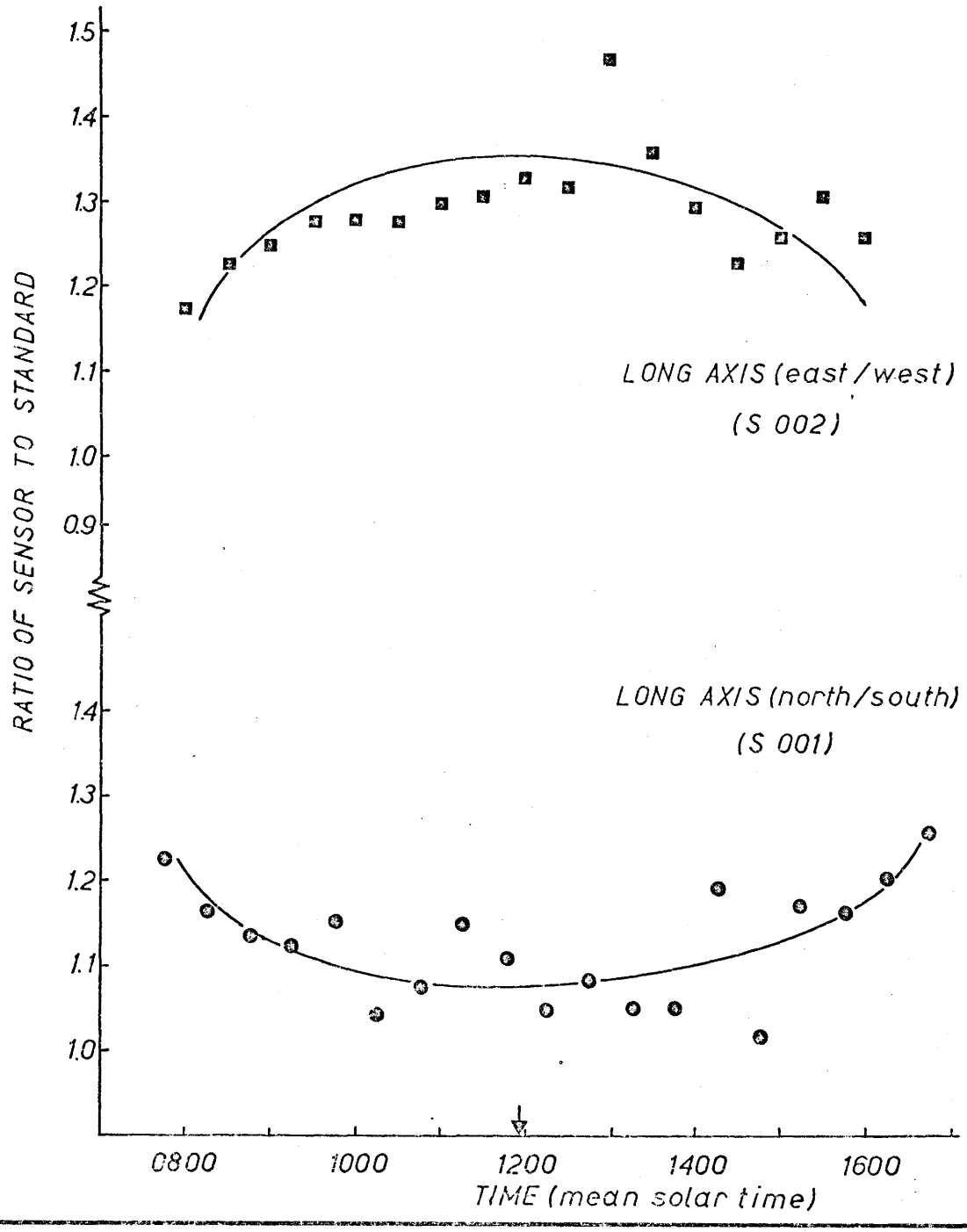

be accounted for by increased cloudiness from 1100 onward. The performance of the east-west tube was superior under clear skies because the loss of sensitivity occurred when the intensity of direct beam solar radiation was small, early in the morning, and in the evening. Comparison of Fig. 9 and 10 also reveals that the sensitivity of the instruments was higher under diffuse radiation conditions than when direct beam radiation was predominant. Evidently part of the incoming radiation was lost to the sensor by reflection of the direct beam from the glass tube thus lowering the sensitivity of the instrument. This reflected component was larger at high zenith angles when the tube was east-west oriented, or at low zenith angles when the tube was north-south oriented. When using linear sensors it seems that they should be positioned with the long axis east-west so that decrease in sensitivity occurs when intensities of direct beam radiation are low. Further investigations of the effect of solar angle on the sensitivity of the sensors with both short-wave and all-wave instruments oriented with their long axes east-west were carried out.

In Fig. 11 sensitivity is plotted against solar azimuth relative to south. Hence at an azimuth angle of 0^{o} the sun is at right angles to the tube. For azimuth angles larger than 60^{o} (early morning and late afternoon) sensitivity declines as reflection from the tube increases. This trend is somewhat obscured in the afternoon by cloudiness. For angles less than 60^{o} sensitivity is virtually constant with variations of only $\pm$ 4.6% for the short-wave, and $\pm$ 4.2% for the all-wave instrument. This response agrees well with the figures quoted by Szeicz et al. (1964) and is adequate for an instrument designed primarily to measure radiation

FIG. 11. *THE EFFECT OF AZIMUTH ANGLE ON THE SENSITIVITY OF LINEAR RADIOMETERS*

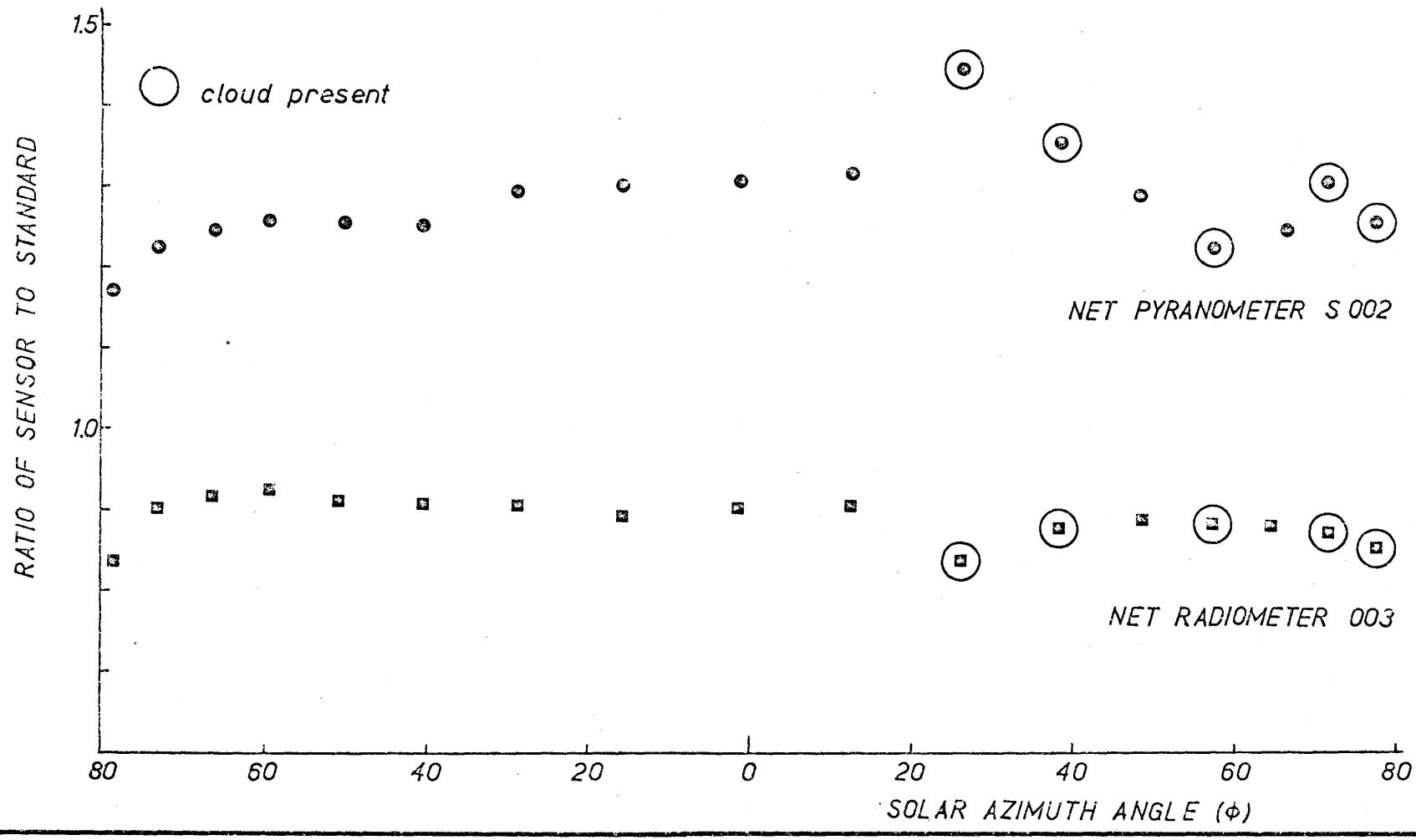

among foliage.

Since changes in instrument sensitivity may also be accounted for by variations in the zenith angle of the sun, sensitivities were plotted against solar zenith angle. Fig. 12 shows clearly the decrease in sensitivity at high zenith angles beyond 50°. At zenith angles less than 50° the variation in sensitivity is small, about 5% for both sensors. It seems that changes in instrument sensitivity can adequately accounted for using either azimuth or zenith angle although they obviously involve a combination of the two parameters.

For measurements of relative intensities of radiation below a canopy these variations are unlikely to cause problems if the radiation is largely diffuse. This is likely to be the case with a fairly dense, uniform foliage cover. However, for calibration of the sensor, necessarily done in the open, and for work in crops with an incomplete canopy structure the effect of the angle of incidence of the radiation falling on the sensor is of considerable importance.

FIG. 12. *THE EFFECT OF ZENITH ANGLE ON THE SENSITIVITY OF LINEAR RADIOMETERS*

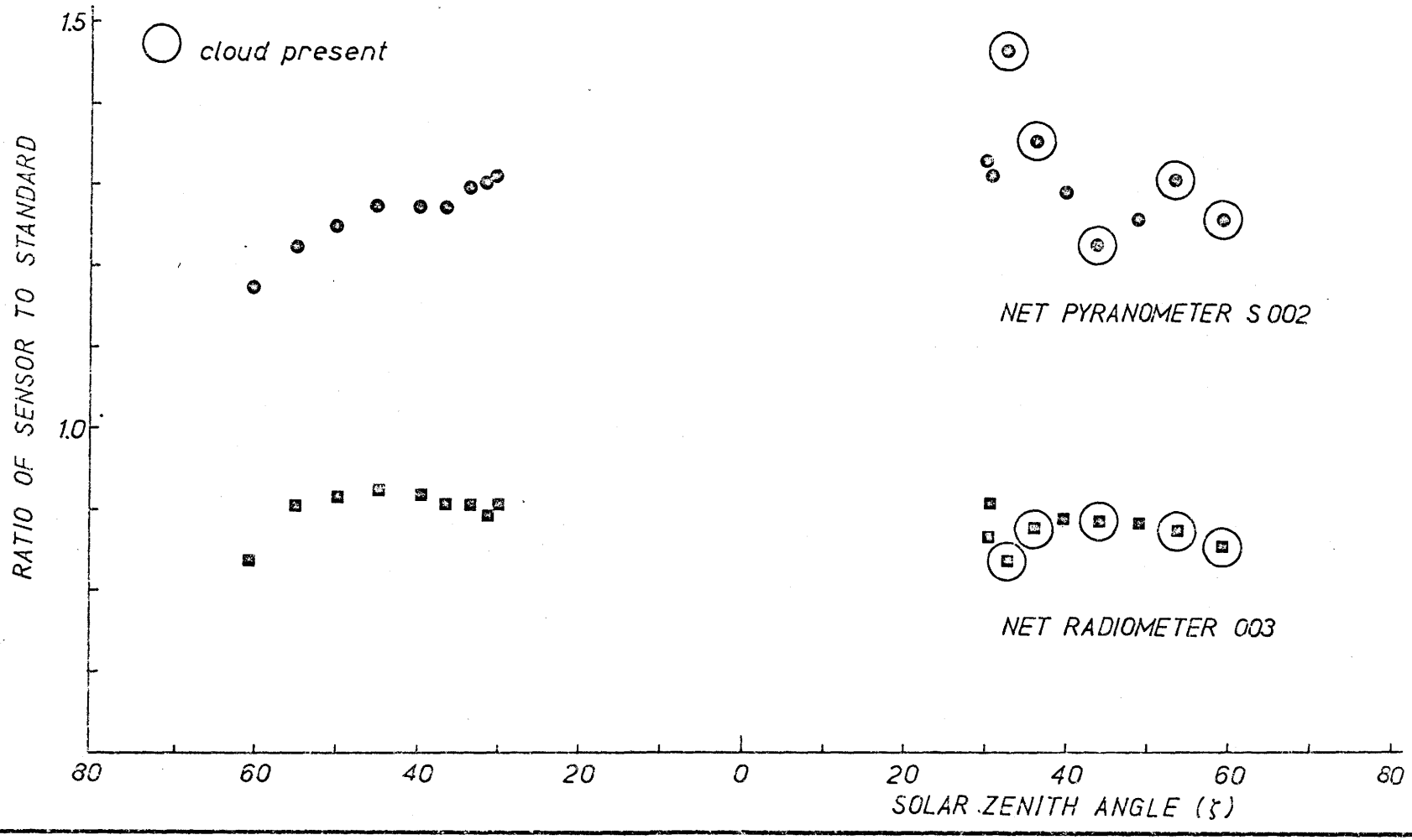

CHAPTER IV

SITE AND INSTRUMENTATION

1. Measurement site

1. Area of study

The study was carried out at the Ontario Horticultural Experiment Station near Simcoe in southern Ontario (42°51' N, 80°16' W) about 15km north-west of Lake Erie (Fig. 13). Apart from occasional trees the site was fairly open and subject to prevailing south-westerly winds. The soil was a light sandy loam (Fox sandy loam) offering good drainage, although during intense summer storms surface runoff was very noticeable. In the late morning and afternoon the area was characterised by a marked build-up of cumulus cloud associated with a lake breeze from Lake Erie. The experiment was conducted in the months of August and September, 1970.

The instrument site (Fig. 14) was a 15 x 15 m plot of corn (Zea mays, var. Seneca Chief) planted in north-south rows, 90 cm apart at a density of 54,000 plants per hectare, across which linear radiometers were placed. A field laboratory in which a data logger and recorders were housed was located to the north-east of the plot.

2. Crop characteristics

The corn was planted unusually late for the area due to unforeseen circumstances. After planting in early July the corn increased in height,

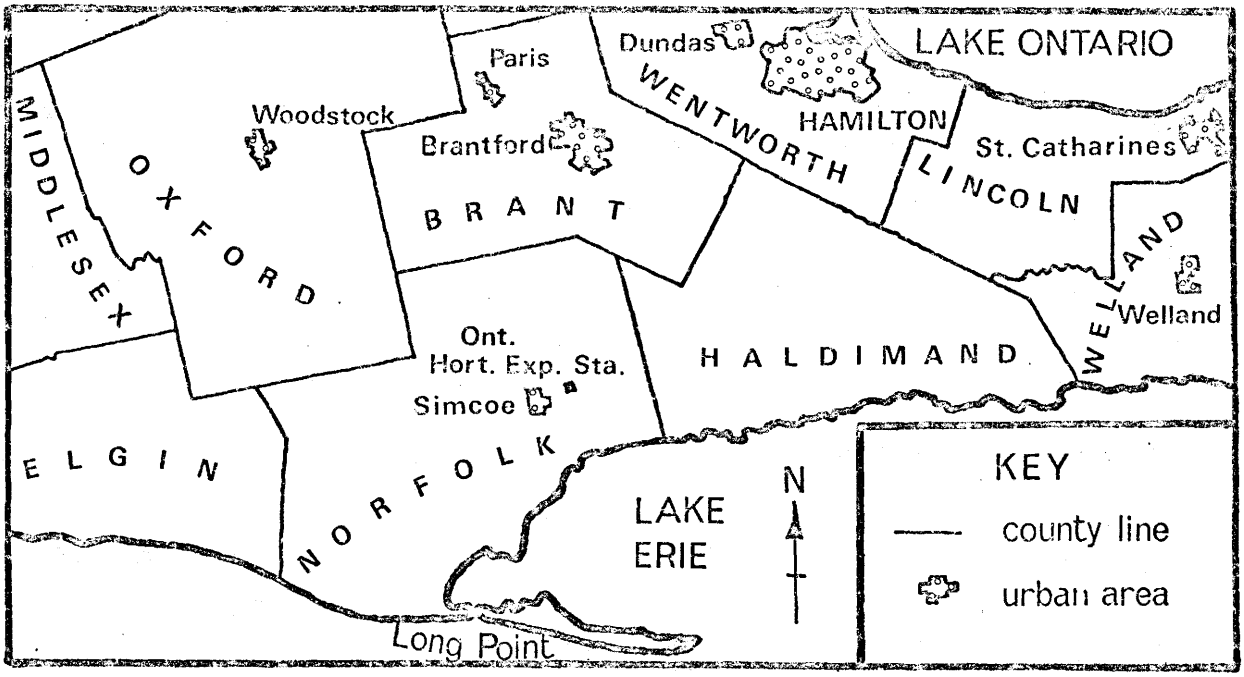

FIGURE 13 STUDY AREA AT SIMCOE, SOUTHERN ONTARIO.

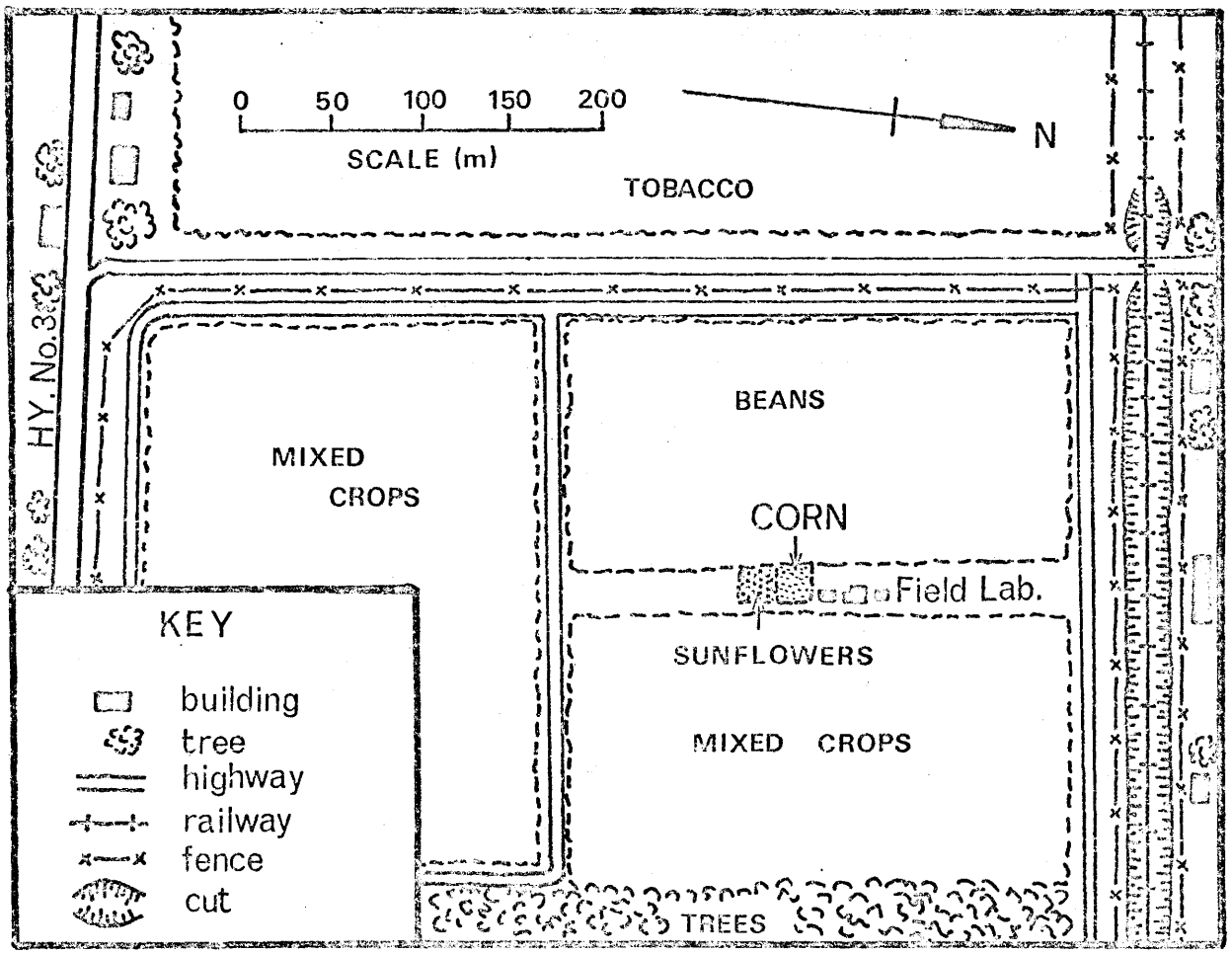

FIGURE 14

MEASUREMENT SITE

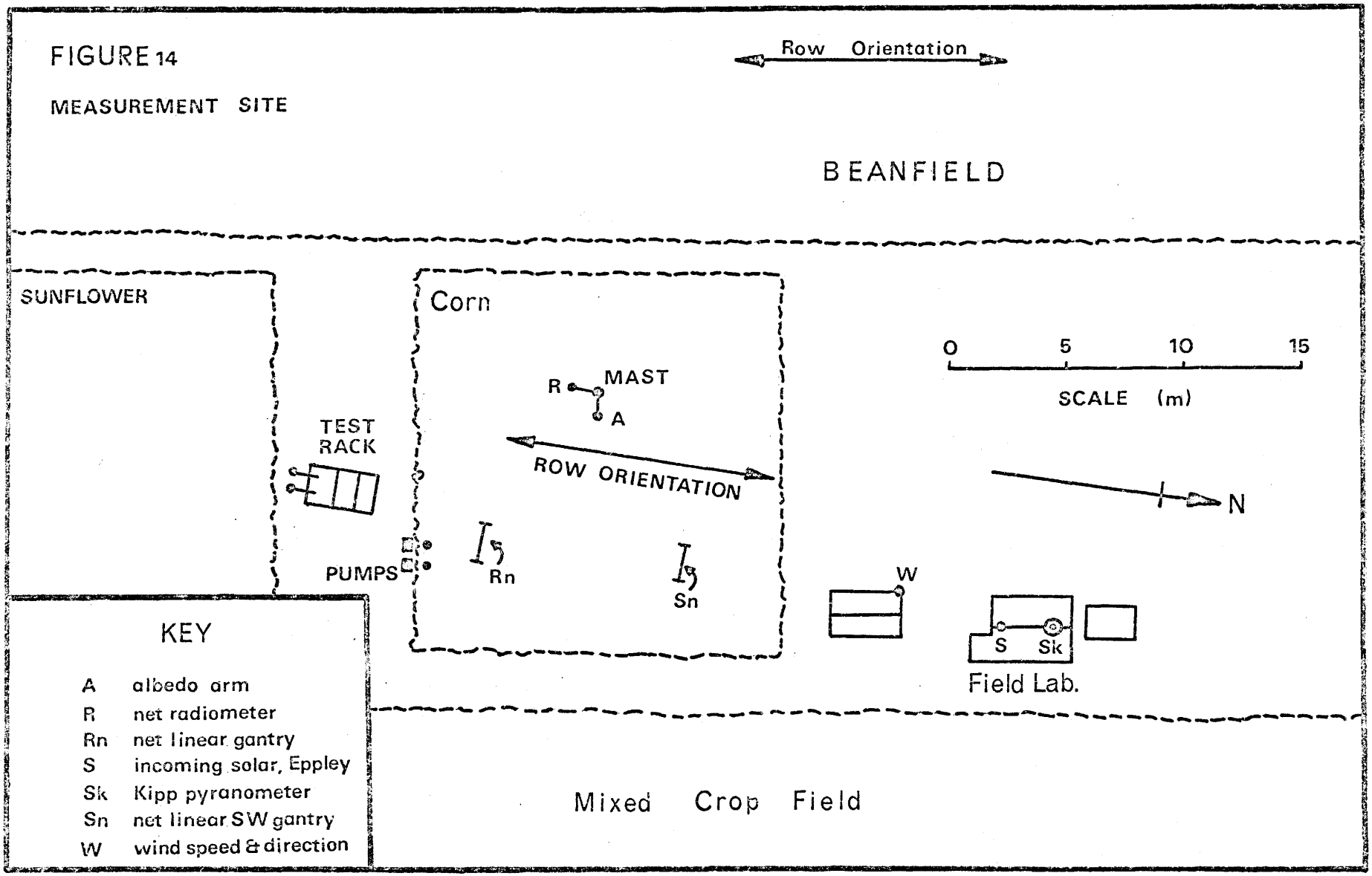

Plate 2. Measurement site.

reaching a maximum in mid-August and ripening afterward. The data were obtained during this period so the crop remained essentially constant in height and the only changes were in internal structure. Mean values of crop height were measured (each mean consisting of 25 samples) at intervals during the growing period to obtain the growth curve shown in Fig. 15. Emergence was slow and terminal height was lower than in previous studies due to inadvertant use of Eptam, a pre-emergent herbicide.

Crop structure, as defined by leaf-area-index, the ratio of leaf surface area (one side only) to the area of the underlying ground (Watson, 1947), was also measured during the experimental period. These showed (Fig. 16) that the structure of the canopy changed slightly during the collection of data as the upper leaves accumulated more dry matter. The overall height of the plants was almost constant. When measurements were taken the canopy was closed and horizontally uniform up to 120 cm above the ground.

2. Instrumentation

1. Short-wave radiation

Measurements of incoming and reflected short-wave radiation (direct and diffuse) were obtained using Eppley pyranometers (Eppley Laboratory Inc., Newport, RI, USA). The latter measurements were obtained by siting a pyranometer in an inverted position on a horizontal cross-arm attached to a mast (Plates 5 and 6), the former by a roof-mounted instrument (Plates 3 and 4). The albedo arm attachment was very satisfactory. However, the height of the down-facing instrument was a compromise between the need to view the whole canopy satisfactorily and the

FIG. 15. GROWTH CURVE FOR CORN, 1970 SEASON

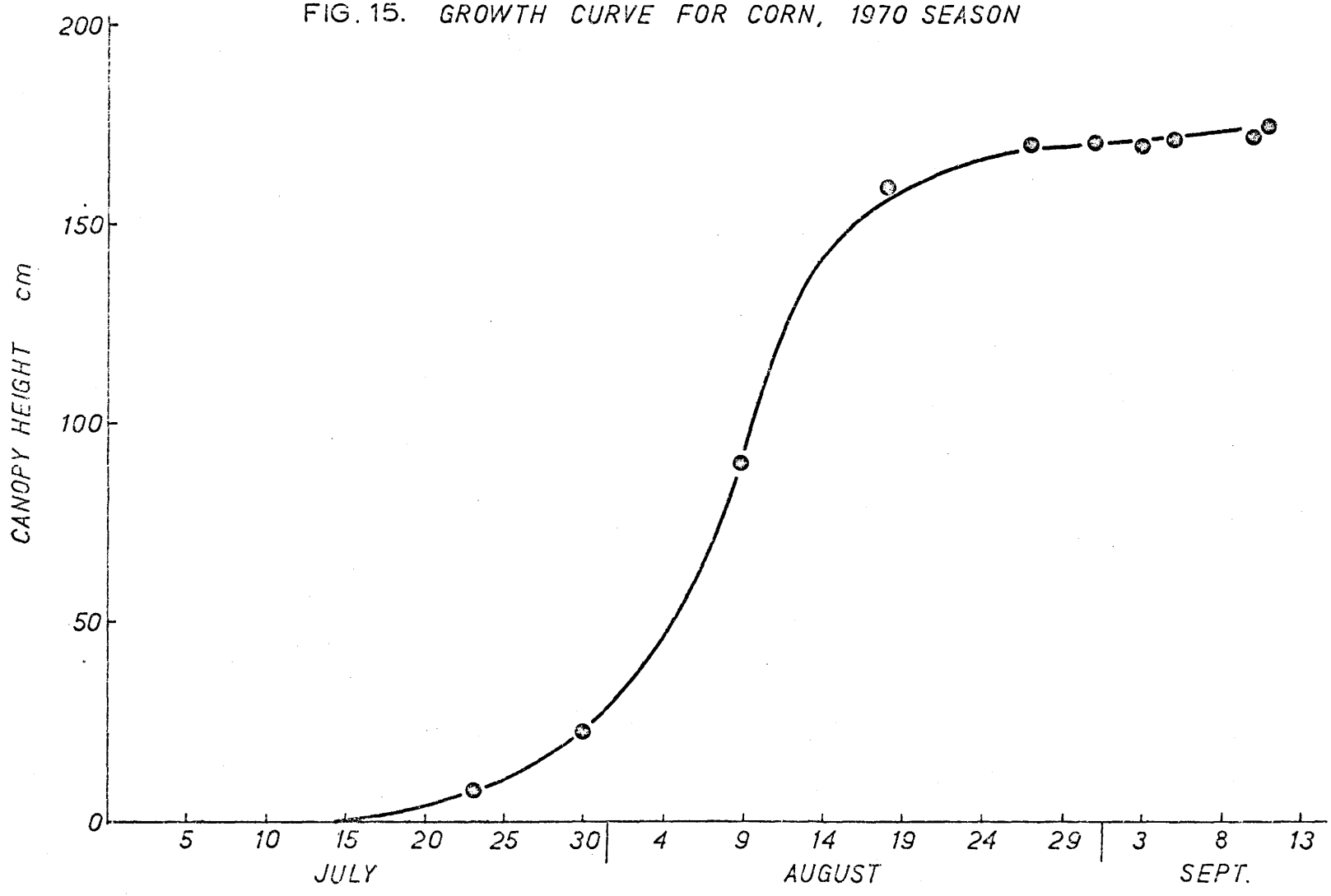

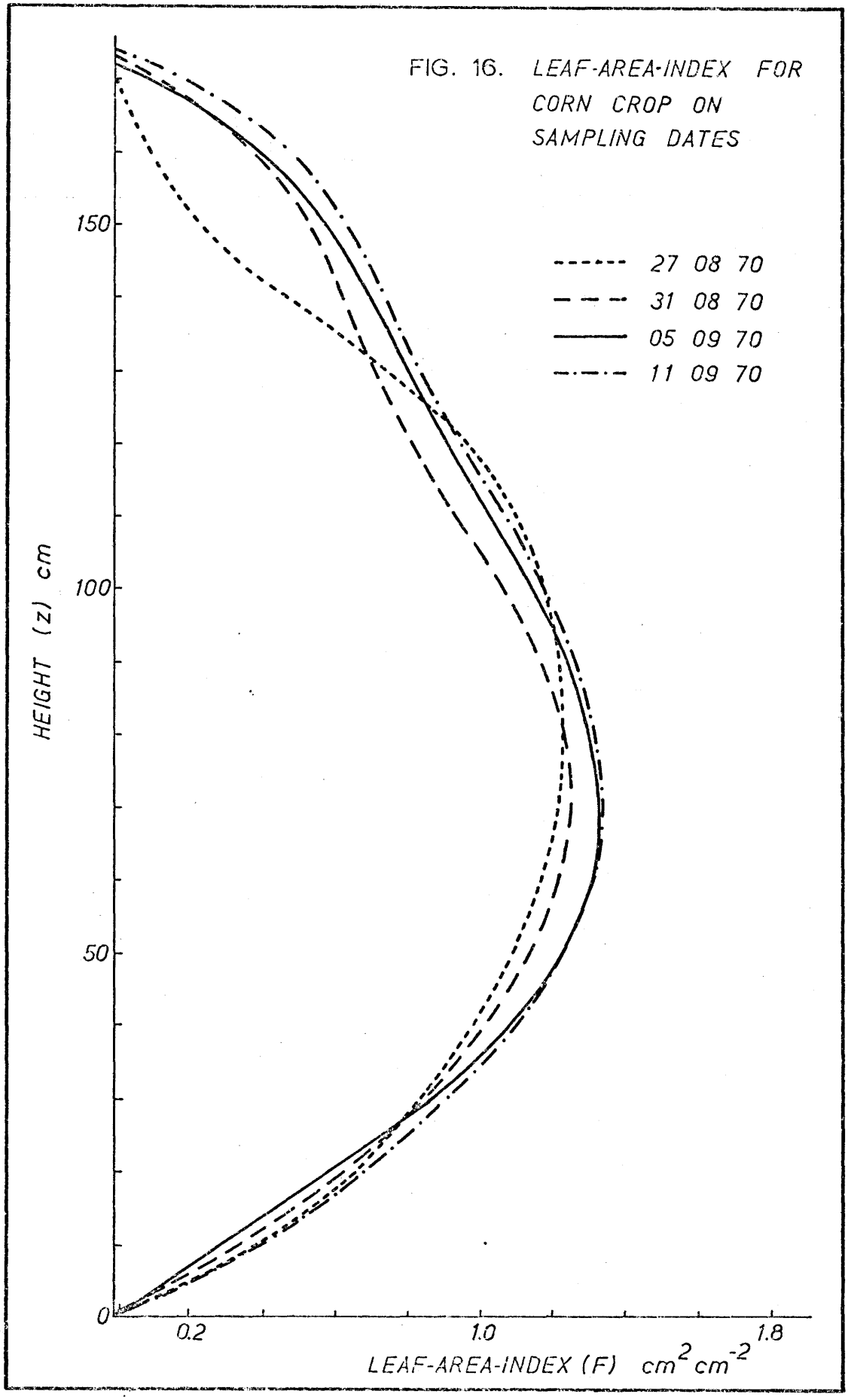
FIG. 16. LEAF-AREA-INDEX FOR CORN CROP ON SAMPLING DATES
27 08 70
31 08 70
05 09 70
11 09 70
HEIGHT (z) cm
150
100
50
0
0.2
1.0
1.8
LEAF-AREA-INDEX (F) cm² cm⁻²

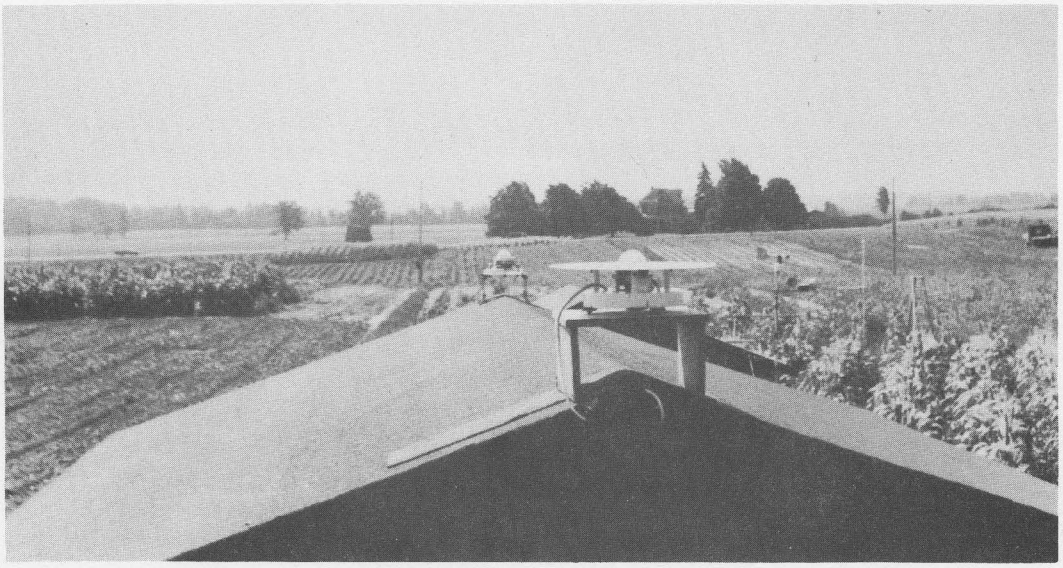

Plate 3. Kipp and Eppley pyranometers for measurement of global radiation.

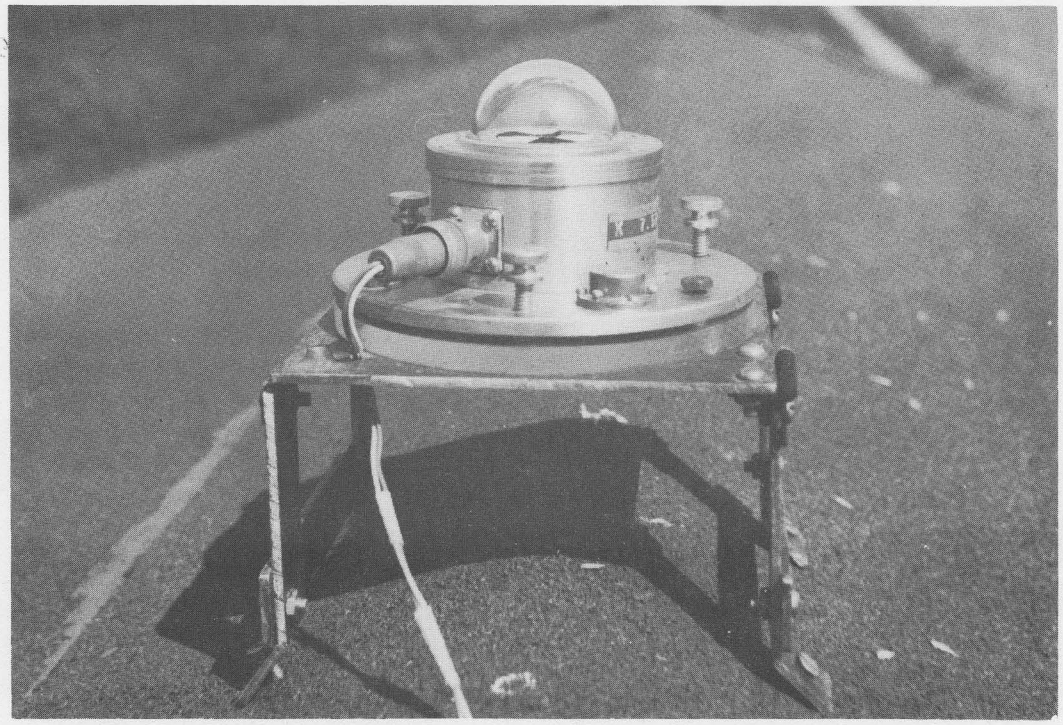

Plate 4. Eppley pyranometer on roof of the field laboratory.

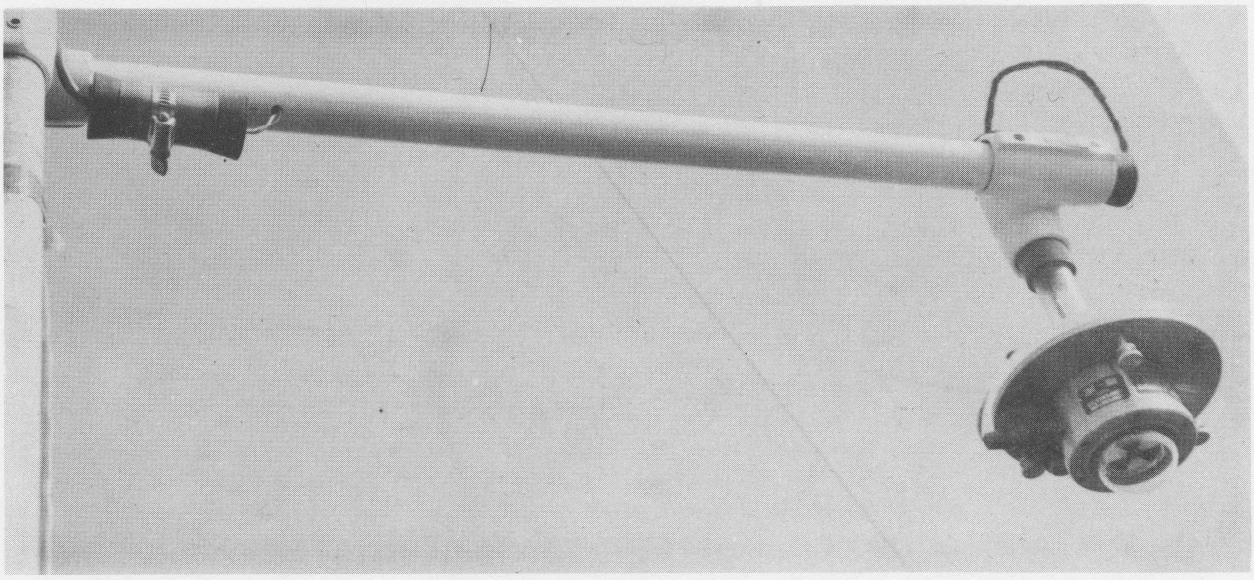

Plate 5. (above)

Eppley albedo arm.

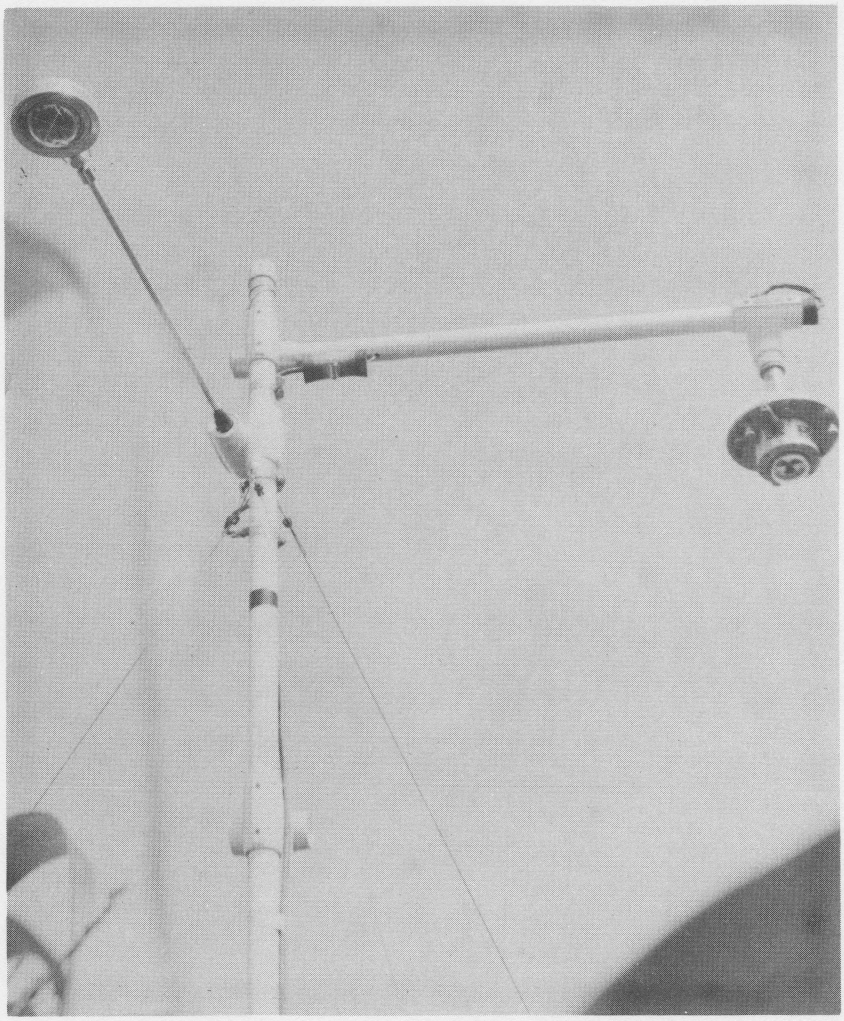

Plate 6. (left)

Radiometer mast with albedo arm and Swissteco net radiometer.

need to minimise direct receipt of incoming radiation at high zenith angles, (Brown, Rosenberg and Doraiswamy, 1970). The height was set at 1 metre above the crop. Interpretation of albedo values at high zenith angles in subsequent analysis was approached cautiously with these facts in mind.

Net short-wave radiation was also measured at three levels within the canopy, 40, 80, and 130 cm with linear net pyranometers (Swissteco Pty. Ltd., Melbourne, Australia) as illustrated in Plate 7. Linear sensors were used to satisfy the requirement for reasonable horizontal spatial sampling. The pyranometers were positioned in east-west alignment across the rows and care was exercised to ensure the instruments were level at all times. This is very important since their shape produces considerable azimuth sensitivity (Anderson, 1969a). The sensors were sited on racks sloping at 60° to the horizontal to avoid the possibility of mutual shading of instruments positioned at the three levels.

2. All-wave radiation

In addition to net short-wave radiation data, measurements are required of net all-wave radiation in order to assess the radiation balance of the cropped surface, the net long-wave radiation being obtained by residual. Above the canopy the net all-wave radiation was measured using a Swissteco net radiometer (Type S1), essentially the same as that described by Funk (1959) (Plate 8). The instrument was mounted on a mast above the canopy with the support arm pointing south (Plate 6). Hence the sensor received minimal interference from shadows cast by the mast.

Net all-wave radiation in the canopy was measured at the same levels as net short-wave radiation. The 1 metre long linear net radio-

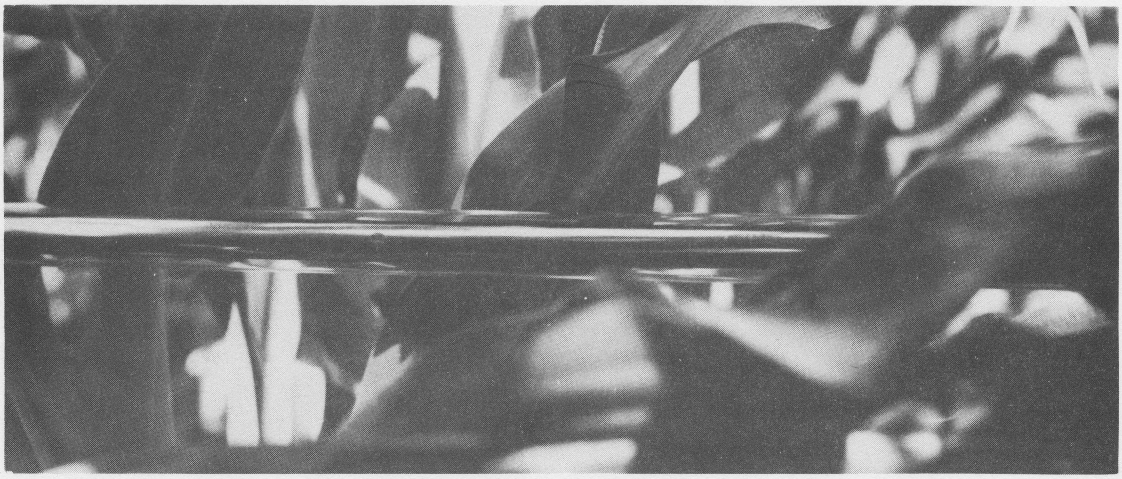

Plate 7. Swissteco linear net pyranometer.

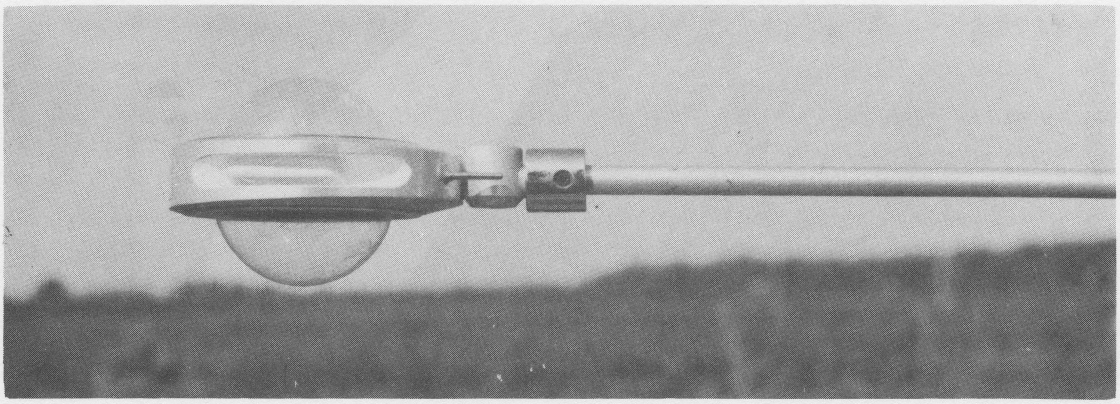

Plate 8. Swissteco net radiometer (Funk type).

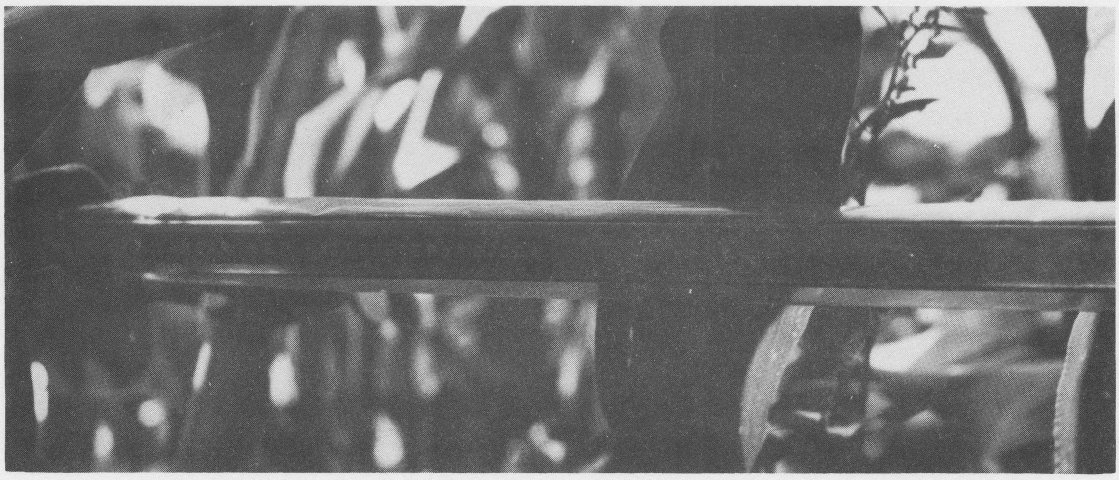

Plate 9. Kyle linear net radiometer.

meters constructed as described in Chapter Three were used (Plate 9). As before the instruments were mounted horizontally on a sloping rack, whose vertical supports were on the north side to lessen shadow effects, with their long axes aligned east-west.

3. Additional instrumentation and systems

Incoming solar radiation was continuously monitored with a pyranometer (Kipp and Zonen, Delft, Holland) mounted on the field laboratory roof, (Plate 3). The signal was recorded on a strip-chart recorder (Toa Electronics, Tokyo, Japan). This gave a day-to-day permanent record of solar radiation used mainly to classify data during analysis. Wind speed and direction were also recorded visually at half-hourly intervals during field measurements.

Ventilation systems necessary for the net radiation instruments were sited on the south side of the experimental plot (Plate 10). These consisted of individual aquarium pumps serving each instrument, housed in groups in plexiglas cases. The air supply from the pumps was dried by passage through containers of dessicant (silica gel) and led to the instruments in teflon tubing.

4. Instrument calibration

The Eppley pyranometers were calibrated a short time prior to the study. All other instruments were calibrated from field comparisons with a conventional Swissteco net radiometer (Model S1). This instrument was calibrated by the Meteorological Branch, Canadian Department of Transport under controlled conditions. All calibrations were achieved by exposing the instruments and the standard at a constant height above the ground.

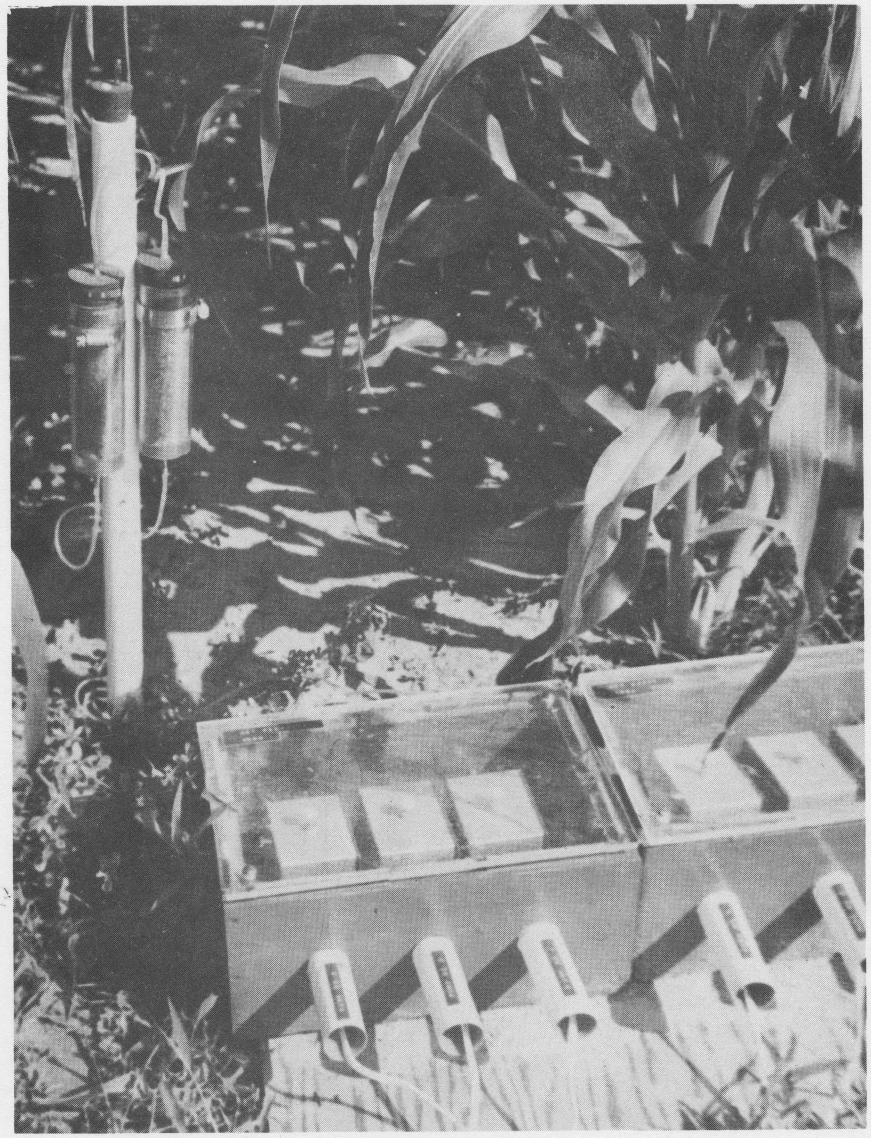

Plate 10. Pump/dessicant system.

Simultaneous measurements of the outputs of the sensors were recorded over a period of a few hours when the radiation conditions were fairly constant (clear sky conditions). This is important since the time constants of the instruments may vary. The ratios of the outputs were calculated and used to determine the calibration coefficient for each instrument.

Throughout the comparison period the ratio of the output of the net radiometer No. 6683 to the standard radiometer was fairly constant ($< 1\%$). A mean calibration constant was calculated and used throughout the study. The sensitivity of the linear radiometers varied, being lower in the morning and late afternoon than during the mid-day period, (Fig. 17). Clearly, as outlined in Chapter Three, the linear sensors exhibit a variation in sensitivity with solar angle. During the three hours either side of solar noon this effect is not very marked ($< 5\%$), and for use in canopies a constant calibration coefficient is acceptable. However, outside this time period instrument sensitivity drops markedly and a calibration is desirable which depends on solar angle (azimuth and/or zenith.

A second order polynomial expression was fitted to the data with considerable success. This revealed that azimuth angle was not such a good predictor of sensitivity as zenith angle, particularly for the linear all-wave instruments.

FIG. 17. SWISSTECO LINEAR NET PYRANOMETER SENSITIVITY AS A FUNCTION OF MEAN SOLAR TIME

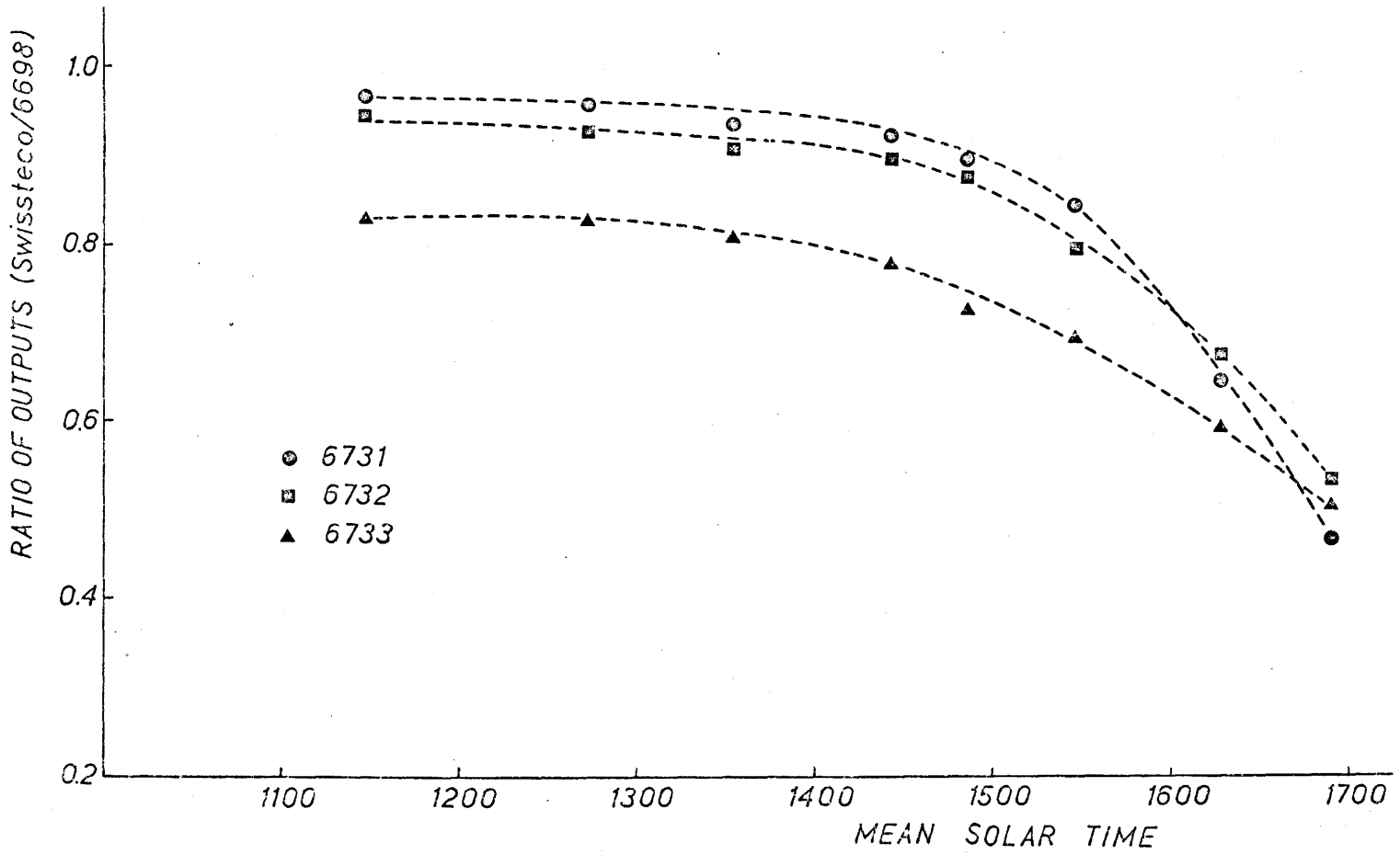

TABLE TWO

MULTIPLE CORRELATION COEFFICIENTS

FOR SECOND ORDER POLYNOMIALS

SENSOR	DEPENDENCE OF CALIBRATION FUNCTION		
	AZIMUTH	ZENITH	COS Z
S 6731	0.963	0.995	0.998
S 6732	0.974	0.997	0.998
S 6733	0.991	0.998	0.998
K 002	0.946	0.998	0.998
K 004	0.931	0.966	0.962
K 006	0.911	0.991	0.996

Table two gives the multiple correlation coefficients for all six sensors. A calibration of the form $y = a + b(\cos Z) + c(\cos Z^2)$ where a, b, and c are determined empirically was eventually chosen although Table two shows that cos Z and zenith angle are equally good predictors. The former expression was used since it relates the sensitivity of the instrument to a beam orthogonal to the sensor at maximum zenith angle, i.e., solar noon. Fig. 18 and 19 show two calibration curves obtained using this empirically determined relationship, the former for a short-wave sensor and the latter for an all-wave sensor. The greater decline in sensitivity of the all-wave instrument is probably a function of its greater length, 1 m, as compared with 53 cm for the short-wave sensor.

FIG. 18. *SWISSTECO LINEAR NET PYRANOMETER CALIBRATION (No. 6732)*

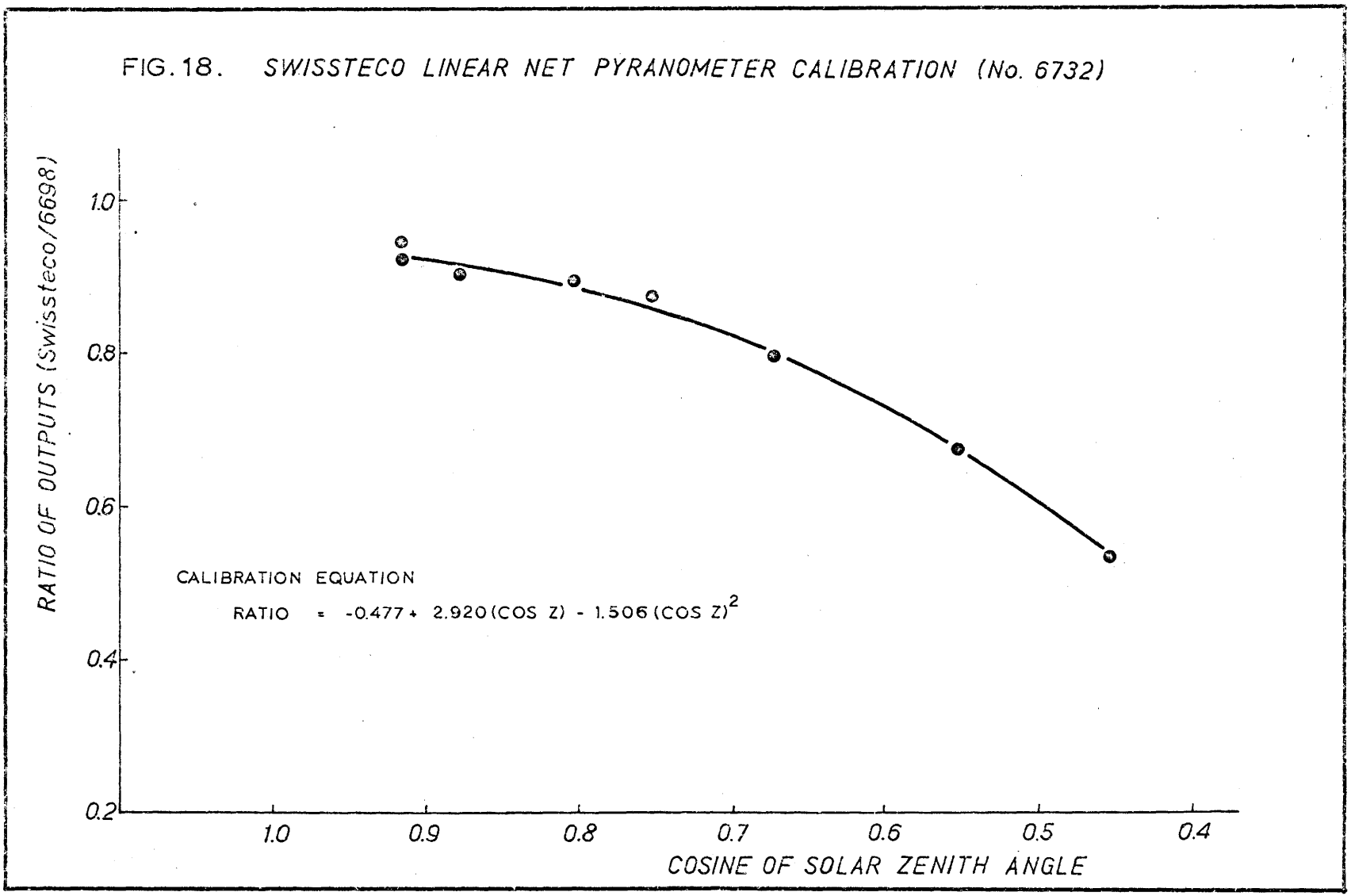

FIG. 19. KYLE LINEAR NET RADIOMETER CALIBRATION (No. K002)

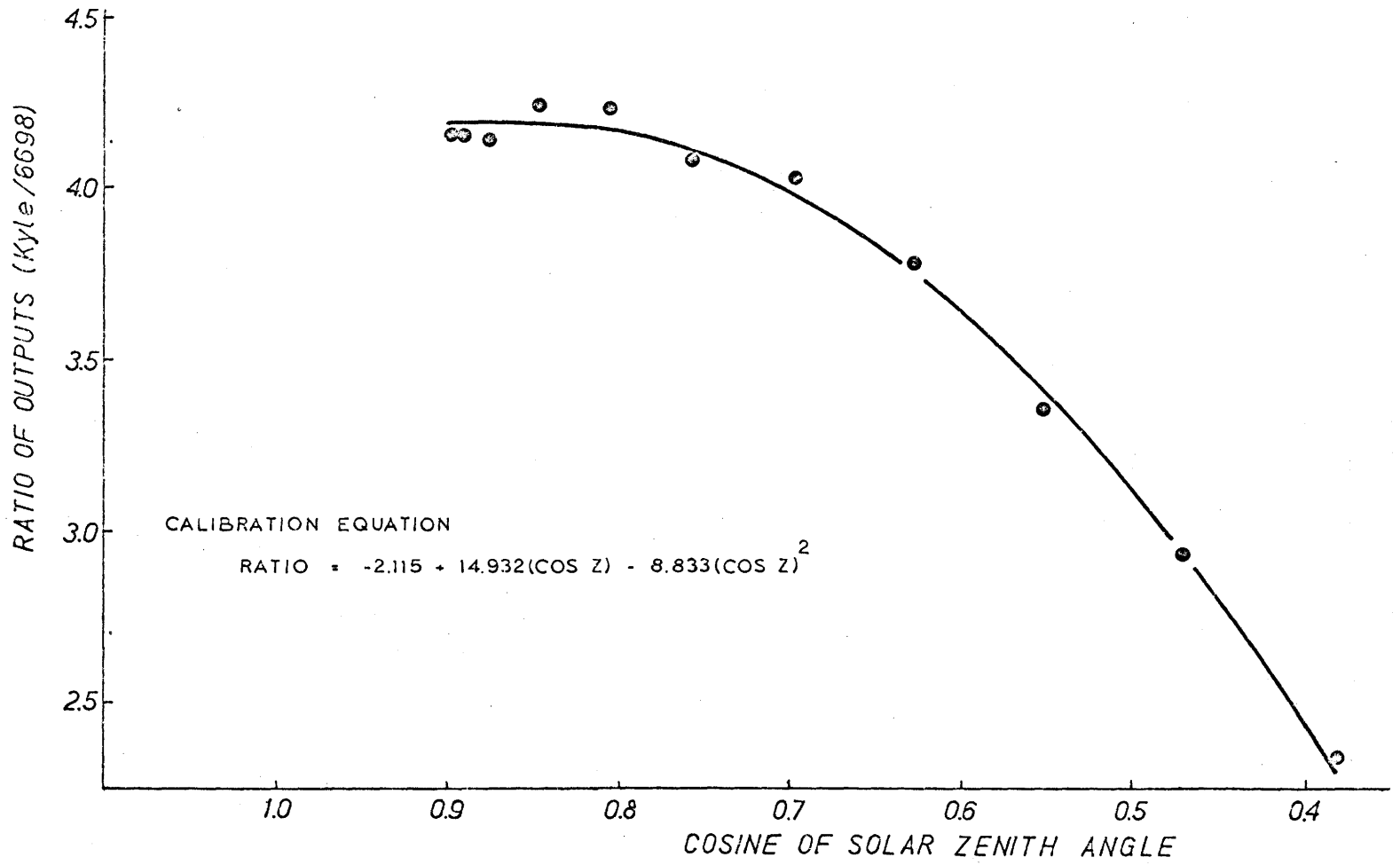

The major problem in the use of zenith angle dependent calibration coefficients for crop canopy studies is the decreasing fraction of direct-beam radiation with penetration into the canopy. This fraction could not be determined in this study. The zenith angle dependent calibration produces an over-estimation of radiation within the canopy since the calibration equation under-predicts the instrument sensitivity. Although undesirable this is better than using a constant calibration factor which is likely to under-estimate radiation intensity in the upper canopy layers at high zenith angles. The zenith angle dependent calibration will produce increasing relative error with increasing depth in the canopy but absolute errors incurred will be very small because of low radiation levels. These errors are much smaller than those encountered by using a calibration constant at the top of the canopy where zenith angle variation is significant. This is illustrated graphically for high zenith angles in Fig. 20 where curves are drawn representing a constant calibration factor (Case 1) and a zenith angle dependent calibration coefficient (Case 2). In Fig. 20a the predicted sensitivity differs by 20%. In Fig. 20b the true radiation profile is given by the curve PQ with a radiation intensity of 350 W m^{-2} at P and 50 W m^{-2} at Q. At W the radiation is assumed to be completely diffuse and between S and W there is a decreasing proportion of direct beam radiation. In Case 1, radiation intensity is under-estimated by 20%, corresponding to a flux of 70 W m^{-2}, at the top of the canopy. The error decreases as the fraction of direct beam radiation decreases with depth, until, at the depth W the profiles merge to give the profile RQ. In Case 2 the resulting profile is PT. The radiation intensity is predicted correctly near the top of the canopy but

FIG. 20. *THEORETICAL EFFECT OF CALIBRATION ON THE MEASURED FLUX WITHIN A PLANT CANOPY*

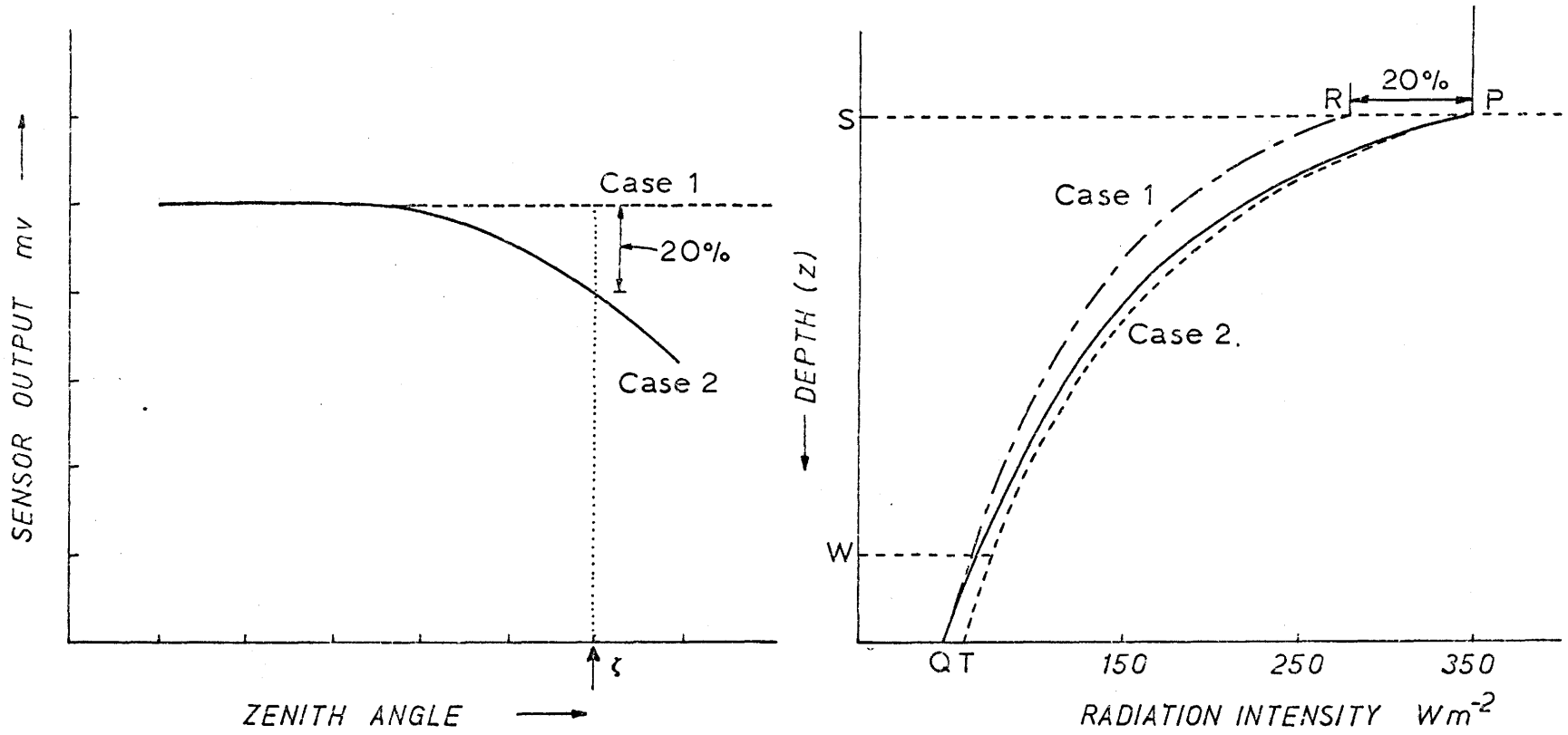

as the fraction of diffuse radiation increases radiation intensities are increasingly over-estimated. At the bottom of the canopy the over-estimation reaches 20% (10 W m^{-2}). Hence, the use of zenith angle dependent calibration coefficients is recommended. These correct for decreased sensitivity of the instrument in the early morning and late afternoon, when losses occur due to reflection from the shielding material, even though the intensity of direct beam radiation at high zenith angles is low.

5. Data acquisition system

All signals from the experimental site were led to the field laboratory by means of shielded cables, in an effort to reduce external electrical noise, where they were connected to a data logger (Solartron Electronic Group, Farnborough, United Kingdom). The system consisted of a scanner and digital voltmeter unit connected to a teleprinter output device. Digital clock control allowed all outputs to be scanned at one minute intervals and printed out on the teleprinter. A patchboard on the rear of the data logger permitted signals to be connected to the appropriate range and multiplier for the output of the instrument. With this system all signals could be scanned at the rate of 0.6 channels per second for each one minute interval throughout the sampling period, every scan taking 15 seconds.

3. Observations and procedure

1. Radiation data

The instrumentation gave observations of net all-wave and net short-wave radiation above and at three levels within the canopy. Before

each run a consistent procedure was adopted to check the instruments, particularly those in the more adverse canopy environment (Anderson, 1969a). Each morning the sensors were uncovered and the shields dried and cleaned to remove dew and/or plant debris which may have accumulated. The cleaning materials supplied by the manufacturer were used in each case. The instruments were then checked carefully for levelness since this is critical, particularly with the known sensitivity of linear sensors to solar angle. Adjustments were carried out if necessary. After checking all electrical connections to ensure that they remained water-tight, the system was started and ran for ten minutes as a final check. It was found that by this means it was possible to find any signal anomalies indicating malfunction. On completion of this checkout procedure, sampling commenced. At the end of the sample period the instruments were again covered to protect the shields from damp and possible damage from rain.

2. Crop parameters

At intervals throughout the study leaf-area-index determinations were obtained. A sample plot of known ground area was selected in the canopy. All the plants in the plot were removed and divided into layers corresponding to the heights of the sensors above the ground: top of the canopy to 130 cm, 130 cm to 80 cm, 80 cm to 40 cm, and 40 cm to the ground. The leaf-area-index was determined on the same plants by measuring the length and width of the leaves in each layer and multiplying their product by the factor 0.75 (Brown and Covey, 1966). This factor gave good agreement ($\pm$ 2%) with leaf area determined on the same samples with

a planimeter (Table three). Where leaves protruded from one layer into the next they were also cut and the areas of the pieces added to the area of the appropriate layer. Leaf-area-index was then calculated for each layer as leaf area per unit ground area. Cumulative leaf area index was obtained by summing the layer leaf-area-indexes from the top of the canopy to the ground. Leaf-area-density defined as leaf area per unit crop volume was also calculated by dividing the layer leaf-area-index by the depth of the layer. In this study where the crop layers under consideration were not equal in depth this parameter may provide a more realistic guide to the canopy architecture than leaf-area-index.

TABLE THREE

LEAF AREA DETERMINATIONS BY PLANIMETER

AND USING LEAF DIMENSIONS

SAMPLE	PLANIMETER L A (cm^2)	0.75 FACTOR L A (cm^2)	% DIFFERENCE
1	438.15	439.65	0.34
2	1,550.22	1,545.86	-0.28
3	1.628.16	1,599.11	-1.78
4	852.98	859.13	0.72

Fig. 16, 21, and 22 give leaf-area-index, cumulative leaf-area-index, and leaf-area-density for the crop on four sample days. Since all measurements were taken after the crop had achieved its maximum height

FIG. 21. DOWNWARD CUMULATIVE LEAF AREA INDEX FOR CORN CROP ON SAMPLING DATES

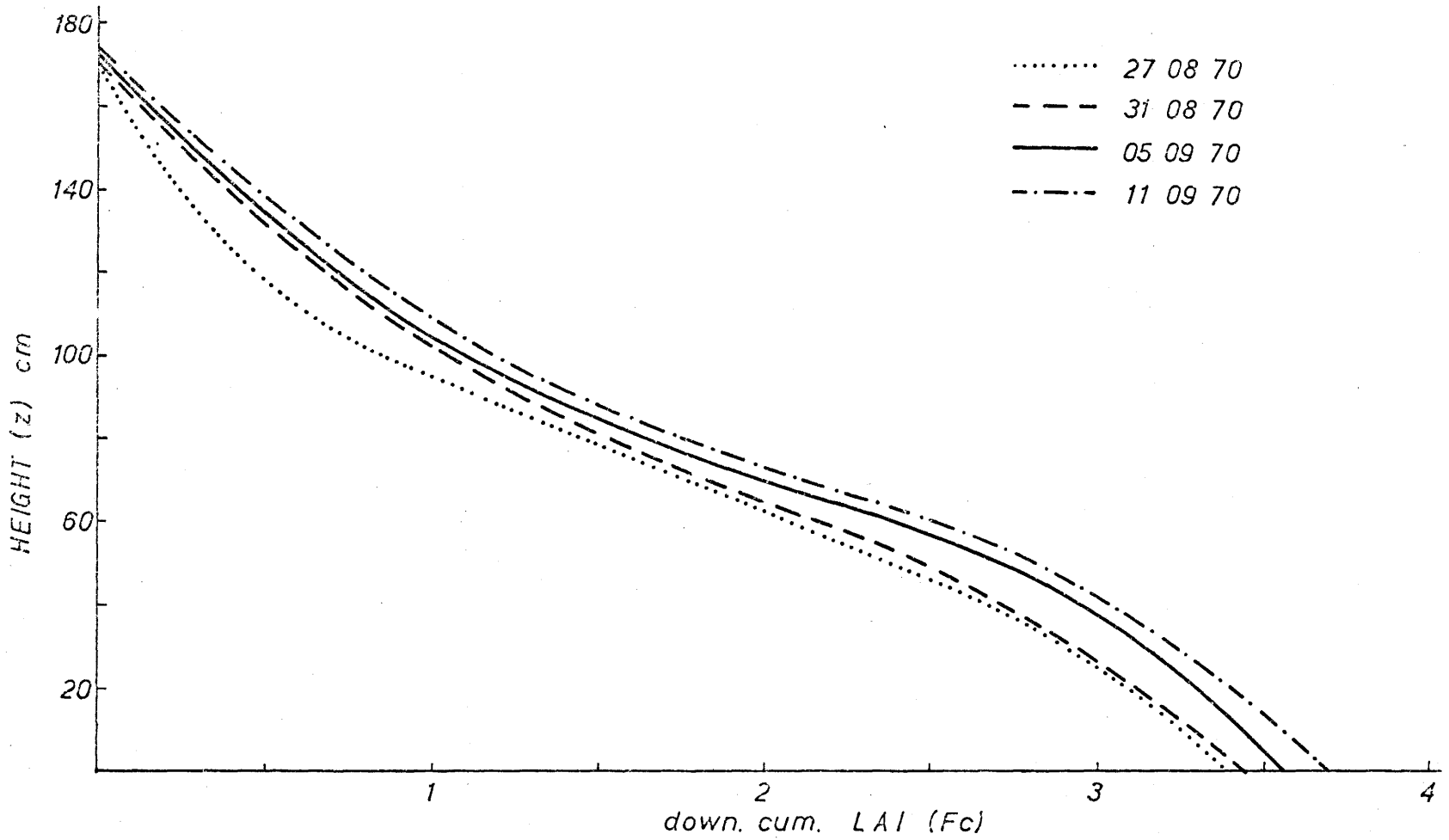

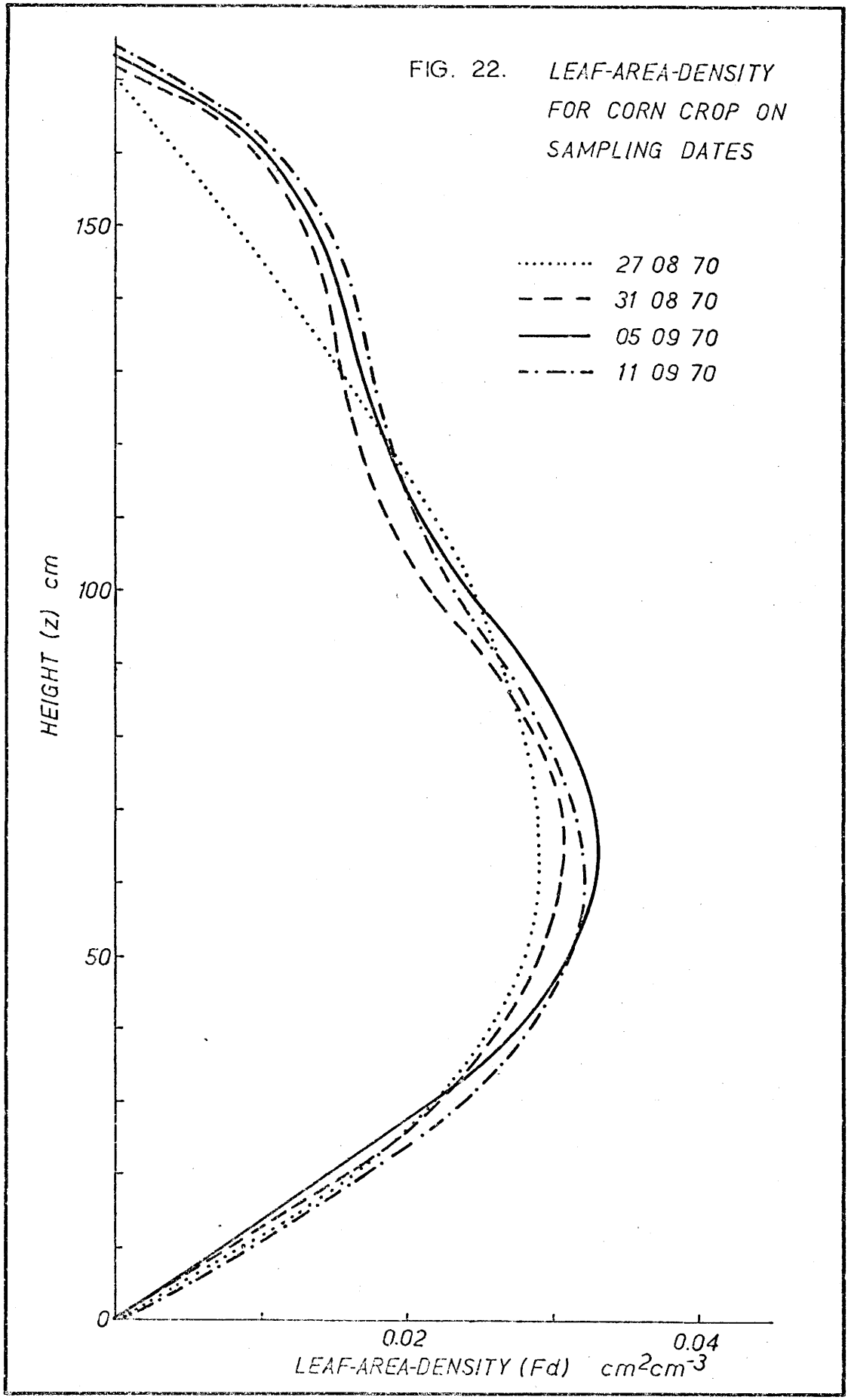
FIG. 22. LEAF-AREA-DENSITY FOR CORN CROP ON SAMPLING DATES
27 08 70
31 08 70
05 09 70
11 09 70
HEIGHT (z) cm
150
100
50
0
0.02
0.04
LEAF-AREA-DENSITY (Fd) cm2cm-3

they all have a very similar form. Total leaf area did not change very much although its distribution in the canopy varied as can be seen from the leaf-area-density curves in Fig. 22.

4. Summary of data obtained

The observations provided simultaneous measurements of net radiation (all-wave and short-wave) above the canopy and at heights of 40 cm, 80 cm, and 130 cm above the ground, and of incoming (global) and reflected short-wave radiation over the crop for 1 minute intervals during each sampling period. Table four gives an overall statement of the measurements taken, although it should be pointed out that malfunctioning instruments sometimes reduced the number of observations.

TABLE FOUR

MEASUREMENTS MADE AT VARIOUS HEIGHTS

IN THE CORN CROP

HEIGHT	INCOMING SHORTWAVE	REFLECTED SHORTWAVE	NET SHORTWAVE	NET ALLWAVE
300	x	x	x	x
130	-	-	x	x
80	-	-	x	x
40	-	-	x	x

Most of the runs were taken under cloudy-bright day-time conditions. Some profiles of net long-wave radiation were also obtained after

nightfall when short-wave radiation was absent. The data for each run were converted to half-hourly means and then stored on computer cards. The first stage of the analysis involved the selection of suitable data for the purposes of the investigation.

CHAPTER V

RADIATION REGIME ABOVE THE CANOPY

1. Radiation balance

The components of the radiation balance over the corn crop were calculated for every half-hourly period. Sky conditions varied considerably and produced markedly different diurnal radiation distributions. These distributions, particularly those for global radiation, were used to classify sky conditions.

The diurnal variation in radiation components for the day with least cloud amount is shown in Fig. 23. Global, net global and net all-wave radiation are all measured quantities. Net long-wave radiation was calculated from Eq. 5 as a residual and therefore exhibits more irregularities than the other components. Short periods of cloud occurred around noon and before 1400 thus reducing the magnitude of the fluxes. General trends are similar to those in many published studies. Under cloudless conditions the net long-wave flux should show a diurnal variation with largest negative values near solar noon (Monteith and Szeicz, 1961; Idso, Baker and Blad, 1969; Impens and Lemeur, 1969a; and others). The absence of a diurnal trend in Fig. 23 could be due to changes in either the atmospheric emissivity or the effective radiative temperature of the atmosphere, both of which would affect the downward long-wave radiation flux or to irregular changes in surface heating during the day.

FIG. 23. *DIURNAL VARIATION OF RADIATION BALANCE COMPONENTS OVER CORN*

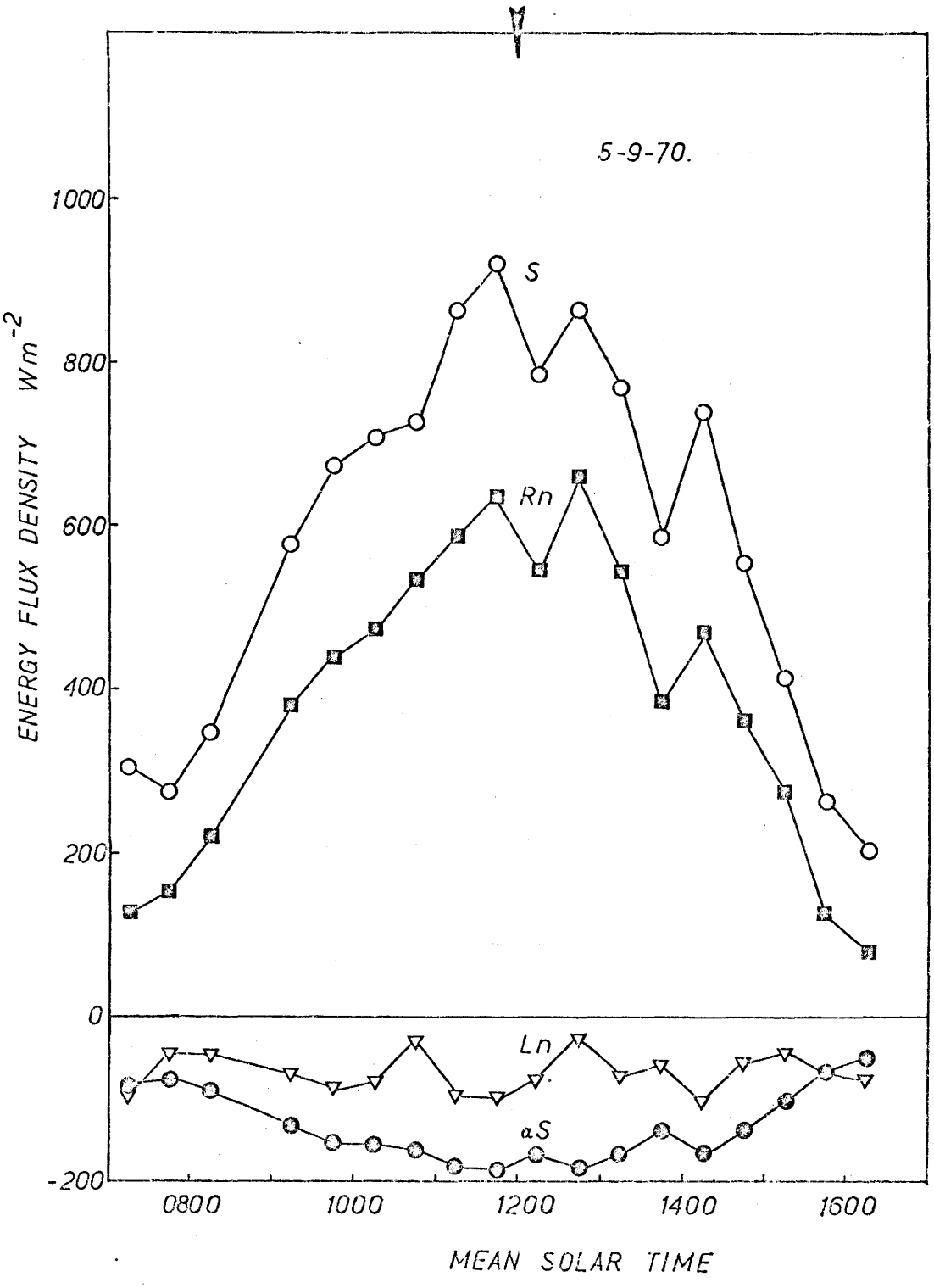

Linear correlations were obtained between solar and net radiation for all days. Analyses were performed using both net global and global radiation as independent variables (Eq. 6 and 9). Fig. 24a and b show excellent correlation and it is noteworthy that the inclusion of the reflected term (Fig. 24b) did not significantly improve the correlation (Student's test, t = 0.0113 with 63 degrees of freedom). This agrees with previous Simcoe findings (Davies and Buttimor, 1969) and with results elsewhere (Davies, 1967; Fritschen, 1967). It is also apparent that the correlation coefficient remains very high even with variable cloud amount. Regression and correlation parameters and the standard error of the estimate are listed in Table five. Values of the standard error of the estimate are slightly larger than listed by previous workers (eg. Fritschen, 1967, 14 - 21 W m^{-2}), probably because they refer to cloudy conditions.

Values of the heating coefficient calculated from the data on clear days are lower than those quoted by Monteith and Szeicz (1962) for Britain (0.10 - 0.29), and also much lower than those reported previously at Simcoe, (0.17 - 0.31, around a mean value of 0.26). On days with cloud present, values fall within the range given by Monteith and Szeicz. Negative values such as those obtained by Ekern (1965), Stanhill et al. (1966) and Idso (1968) were not observed.

Monteith and Szeicz (1961) found marked hysteresis loops in plots of Rn against $(1 - \alpha)S$, with net radiation always smaller in the afternoon than in the morning, which they attributed to greater Ln in the afternoon due to higher surface temperatures. This was not found in the present investigation.

FIG. 24. *RELATIONSHIP BETWEEN NET AND GLOBAL (a) RADIATION, AND BETWEEN NET AND NET GLOBAL (b) RADIATION OVER CORN*

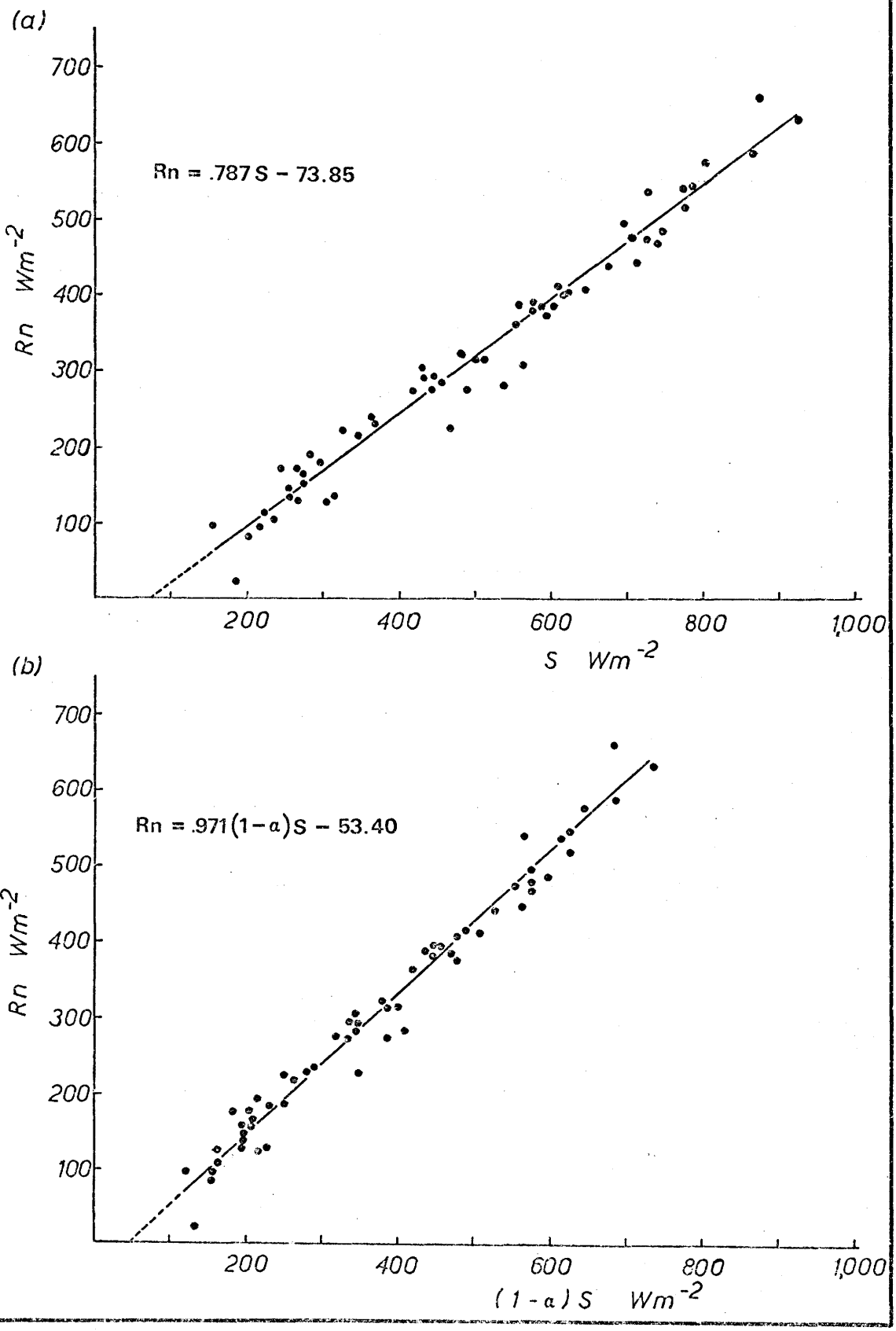

TABLE FIVE

REGRESSION AND CORRELATION PARAMETERS

SKY CONDITION	PERIOD	REGRESSION	a	b	r	s.e. ($W\ m^{-2}$)
clear	5.9.70	Rn/S	0.787	-73.85	0.993	21.5
clear and cloudy	2-10.9.70	Rn/S	0.744	-52.75	0.985	26.9
clear	5.9.70	Rn/Sn	0.971	-53.40	0.992	23.4
clear and cloudy	2-10.9.70	Rn/Sn	0.923	-39.45	0.987	25.0

Stanhill et al. (1966) suggested that this effect should be most marked for surfaces with small or negative heating coefficients. Further data from Idso, Baker and Blad (1969) revealed various cycles of Rn against $(1 - \alpha)S$ including values of higher Rn in the afternoon and cycles with crossovers at varying times. They found no evidence to support the view of Stanhill et al. that such effects were due to small or negative heating coefficients. An apparent anomaly was found. They discovered net radiation to be greater in the afternoon than in the morning, in seeming contradiction to the higher surface temperatures expected in the afternoon. Long-wave thermal radiation was measured as a check and surface fluxes were indeed much larger after noon owing to higher surface temperatures. However, atmospheric emission was not constant and they suggested that the β values appear to be more intimately connected with atmospheric rather than surface conditions.

If this is the case, and it is the atmospheric emission which determines the gross nature of the daily cycles then some correlation may be expected between this parameter and the value of β. Variations in β (Table 7 and Fig. 25) point to a marked dependence of the heating coefficient on prevailing weather conditions, possibly through the mechanisms outlined above.

Values of β were consistently higher on cloudy days than on days with little cloud. Subjective examinations revealed that the magnitude of β may be correlated with cloud amounts and thus indirectly with atmospheric emission. However the variations in atmospheric emission are unpredictable, and these combined with surface factors such as sensible and latent heat exchanges at the crop surface all appear to govern β

FIG. 25. *VARIATION OF β OVER CORN DURING MEASUREMENT PERIOD*

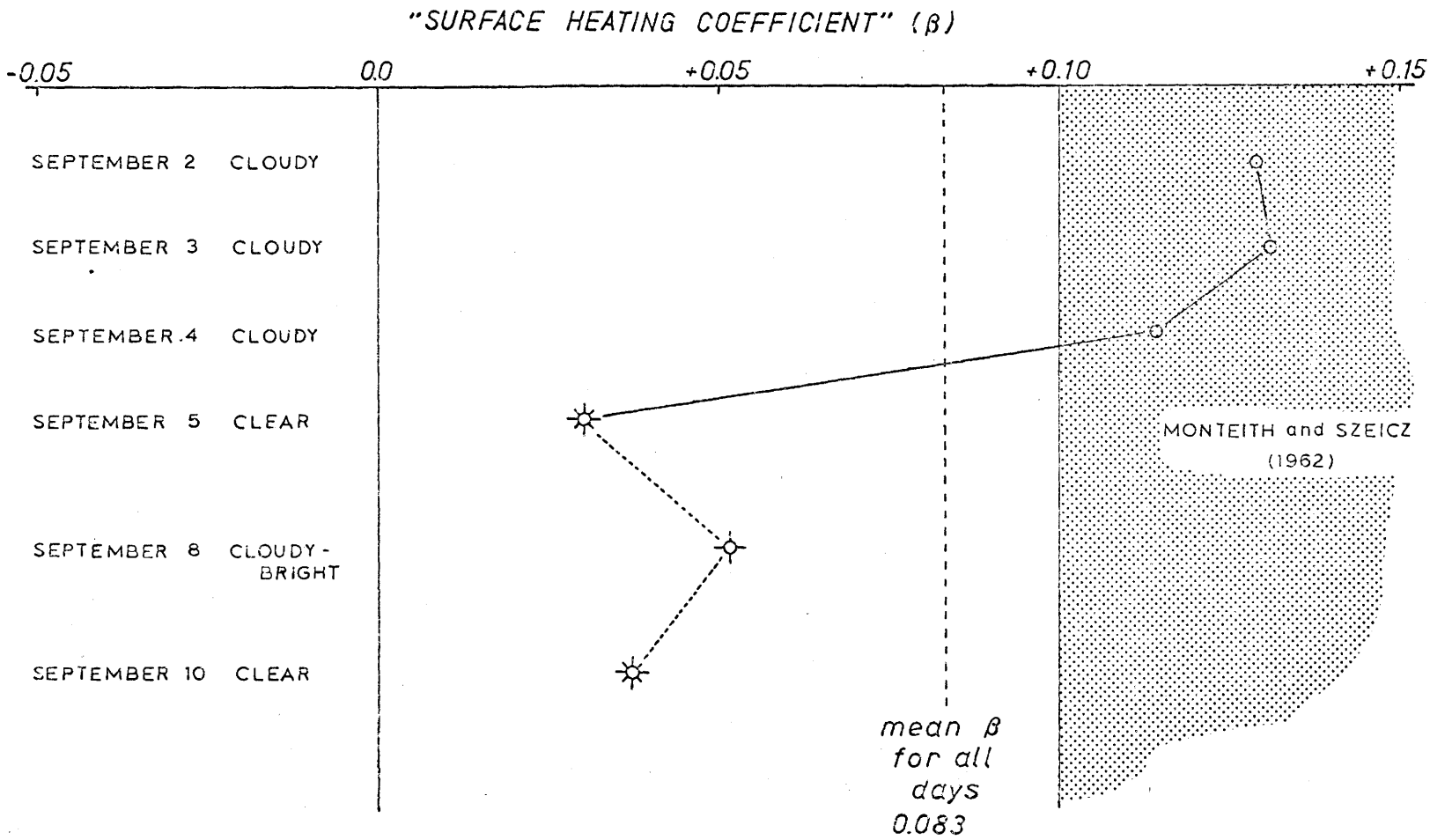

and make it seem unlikely that a representative value of this parameter can be used.

The data also indicate that the proportion of the incoming short-wave radiation that appears as net radiation is nearly the same for clear and cloudy conditions on a daily basis (Table six). The mean value for all the data is 0.63 which compares favourably with the value of 0.67 given by Decker (1964) for irrigated corn in Missouri.

On a half-hourly basis (Fig. 26) the Rn/S ratio exhibits a diurnal variation reaching a maximum around mid-day and decreasing to zero as the turnover points of net radiation are approached. During the greater part of the day the ratio is high and fairly constant between 0.60 and 0.70, clear days appearing to give a higher ratio than cloudy days. The slightly lower mean value obtained for all days of 0.63 (cf. Decker (1964) 0.67) may be due to the predominance of cloudy conditions.

The intercept of the linear regression of net radiation on net global radiation is sometimes interpreted as the long-wave balance when global radiation is zero (Eq. 8). Daily values are listed in Table 6. However, these values may not represent the entire nocturnal flux but only the flux balance at sunrise and sunset. According to Monteith and Szeicz (1961) Lo over-estimated the measured night-time loss for grass surfaces. The only data available in this investigation gave a night-time flux between sunset and midnight of -70.62 Wm^{-2} compared with the intercept value of -79.08 Wm^{-2}. This tends to support previous findings and it seems that Eq. 8 can only refer to periods of positive global radiation.

These results and previous Simcoe work (Davies and Buttimor,

TABLE SIX

HEATING COEFFICIENT, RATIO OF NET RADIATION TO TOTAL RADIATION, LONG-WAVE BALANCE AT ZERO GLOBAL RADIATION (Wm^{-2}), AND REFLECTION COEFFICIENT ON A DAILY BASIS

DATE	SKY CONDITION	β	Rn/S	α (slope)	α (mean)	Lo
2.9.70	cloudy	.129	.61	.204	.221	-36.40
3.9.70	cloudy	.130	.65	.210	.221	-10.21
4.9.70	cloudy	.114	.61	.217	.240	-19.76
8.9.70	cloudy-bright	.052	.62	.208	.230	-41.45
5.9.70	clear	.030	.64	.191	.226	-53.40
10.9.70	clear	.037	.62	.169	.213	-79.08
MEAN	-	.083	.63	.194	.224	-39.45

FIG. 26. *VARIATION OF Rn/S FOR HALF-HOURLY INTERVALS DURING MEASUREMENT PERIOD*

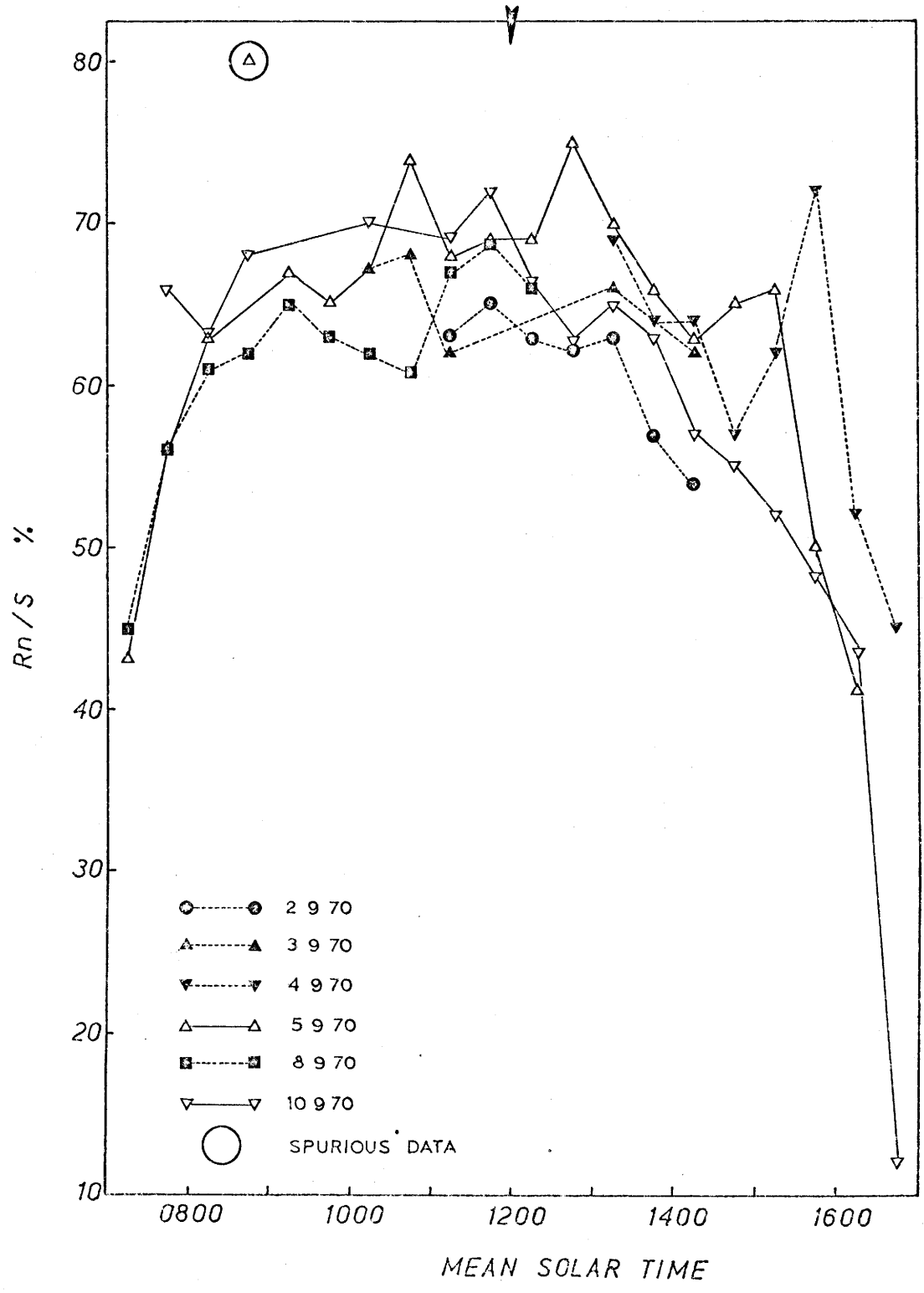

1969) suggest that β is not a surface parameter but is a parameter which accounts for interaction between surface and atmosphere (Stanhill et al., 1966). However, the results of this study appear to be the first to show a dependence of β upon cloud amount. It seems that β is too variable on a day-to-day basis to be useful in predicting Rn for individual days, certainly for days with cloud cover present. The evidence also points to the redundancy of α in the linear relationship, and indicates that Rn is a conservative linear function of S.

2. Reflection coefficient

1. Diurnal variation

The mean reflection coefficient for different ranges of solar zenith angles is shown in Fig. 27. A diurnal variation is evident, with smallest values occurring at mid-day, increasing almost linearly with zenith angle (at least up until 70°). Over the full range of zenith angles the changes in α are very large as noted by Impens and Lemeur (1969a), Davies and Buttimor (1969) and others. However, the higher values of α at large zenith angles have little influence on net global radiation because S is small.

The mean value of the reflection coefficient was obtained for each date of measurement as the slope of the linear regression equation relating reflected short-wave radiation to the global radiation. Greater curvature and larger displacements from the origin were found on clear days when variation in the reflection coefficient was greatest. The method, according to Stanhill et al., (1966), effectively weighted the measurements according to the intensity of global radiation thus minimis-

FIG. 27. DIURNAL VARIATION OF REFLECTION COEFFICIENT

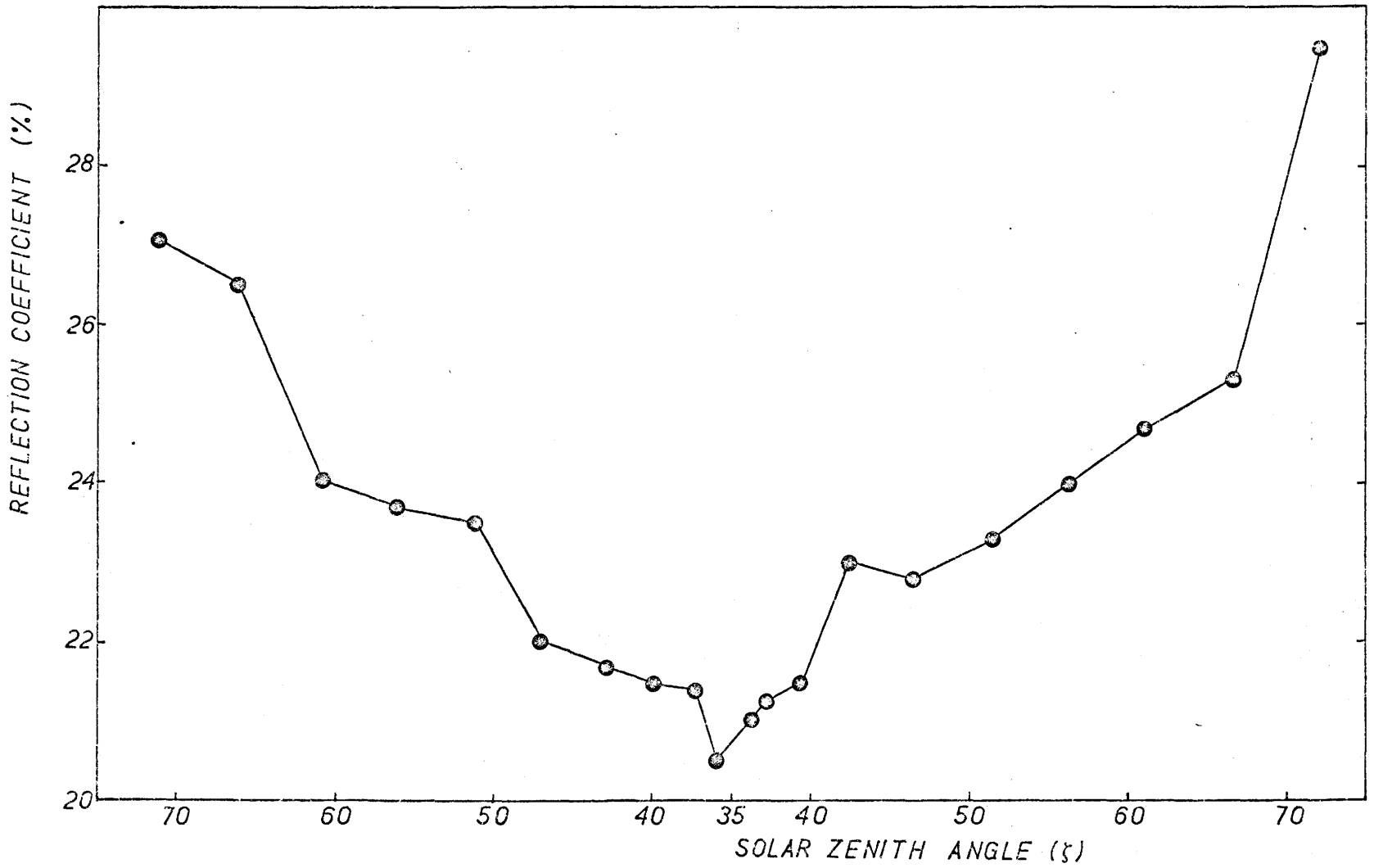

ing possible erroneous values of the reflection coefficient at low radiation intensities. In Table 6 the value of α obtained by this method was 0.194. For clear days only the value was 0.18. This method is clearly unsuitable in this case since the resulting average reflection coefficient is lower than all of the hourly values shown in Fig. 27. The method used by Monteith and Szeicz (1961) and Fritschen (1967) whereby the ratios of daily totals of reflected and incoming radiation are calculated gave an average reflection coefficient for all days of 0.224 and for cloudless days of 0.213. The mean values of α obtained from the slope of the regression are generally lower than those previously reported for this site but fall within the range of values (0.12 - 0.21) observed by Graham and King (1961) at Guelph in S. Ontario. Values obtained by the latter method agree well with previous Simcoe values for corn (0.22).

2. Dependence on solar zenith angle

An almost linear decrease ($r > 0.9$) of reflection with decreasing solar zenith angle less than 70^{o} was found. Poorer correlations were obtained under cloudy-bright conditions than under clear skies. The decrease in reflection coefficient for various solar zenith angles on a clear day is shown in Fig. 28 ($r = 0.98$, s.e. $= 0.004$). A similar plot under cloudy conditions is also shown.

In general under cloudy-bright conditions the dependence on zenith angle was less, as indicated by the lower slope of the regression line, and the scatter was considerably greater. This is to be expected since higher amounts of diffuse radiation with irregular temporal distribution are present, and is consistent with data published by Impens and Lemeur

FIG. 28. *DEPENDENCE OF REFLECTION COEFFICIENT ON SOLAR ZENITH ANGLE*

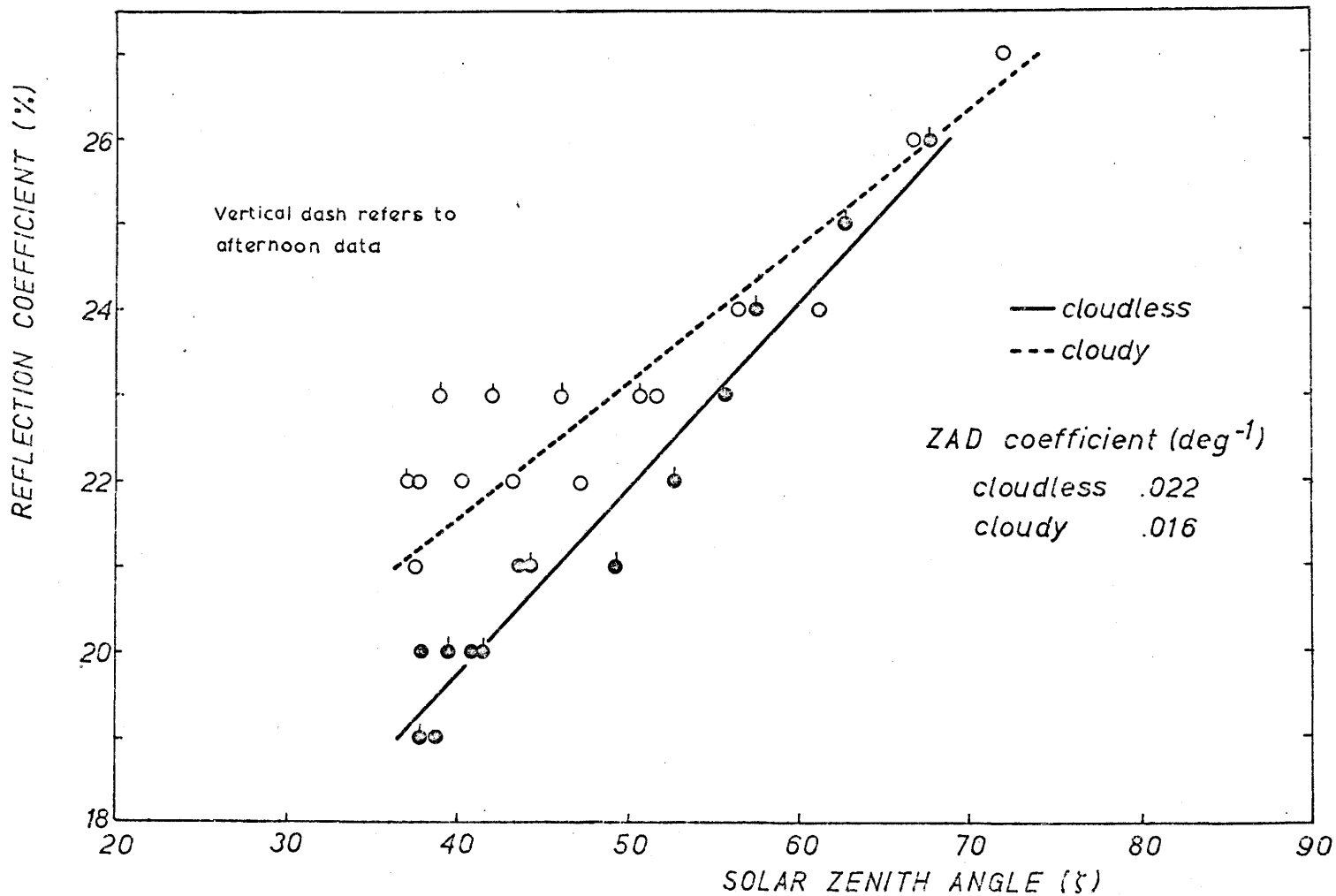

(1969a).

The slope of the line relating reflection coefficient and zenith angle has been termed the ZAD coefficient (for zenith angle dependence), which is the change in reflection coefficient per unit change in solar zenith angle, with units of degree^{-1}. It is suggested that when further data are accumulated it may be possible to obtain characteristic values for the ZAD coefficient on clear days for different surfaces. Further studies are needed to evaluate the effect of cloud amount on this parameter so that a correction can be applied to the clear day value to accomodate this additional term.

CHAPTER VI

RADIATION REGIMES IN THE CANOPY

1. Radiation profiles

From data collected over a six day period, two days, considered representative of clear-sky and cloudy-bright conditions, were selected for the study of canopy profiles. These two days were used exclusively to test the various models of canopy radiation.

Typical profiles of net short-wave radiation under cloudless skies are illustrated in Fig. 29. The decline of short-wave radiation within the plant canopy is considerable. The depletion profiles exhibit a diurnal variation in response to solar angle, although at lower levels within the crop this variation is small. The form of the profiles is non-linear with height, the greatest depletion occurring in the top 60% of the canopy.

Fig. 30 shows the vertical divergence ($\partial Sn/\partial z$) calculated by finite differences (Δ Sn/ Δ z) for a constant Δ z(20cm). The presence of two distinct zones in the canopy is immediately apparent. In the corn crop the height at which the leaves of adjacent plants overlapped was approximately 110 - 120 cm above the ground. This will be termed the transition zone. Below the transition height the canopy was complete and relatively uniform. In the complete canopy region depletion is an inverse function of cumulative leaf-area-index.

FIG. 29. *NET SHORT-WAVE PROFILES IN CORN CANOPY (clear day)*

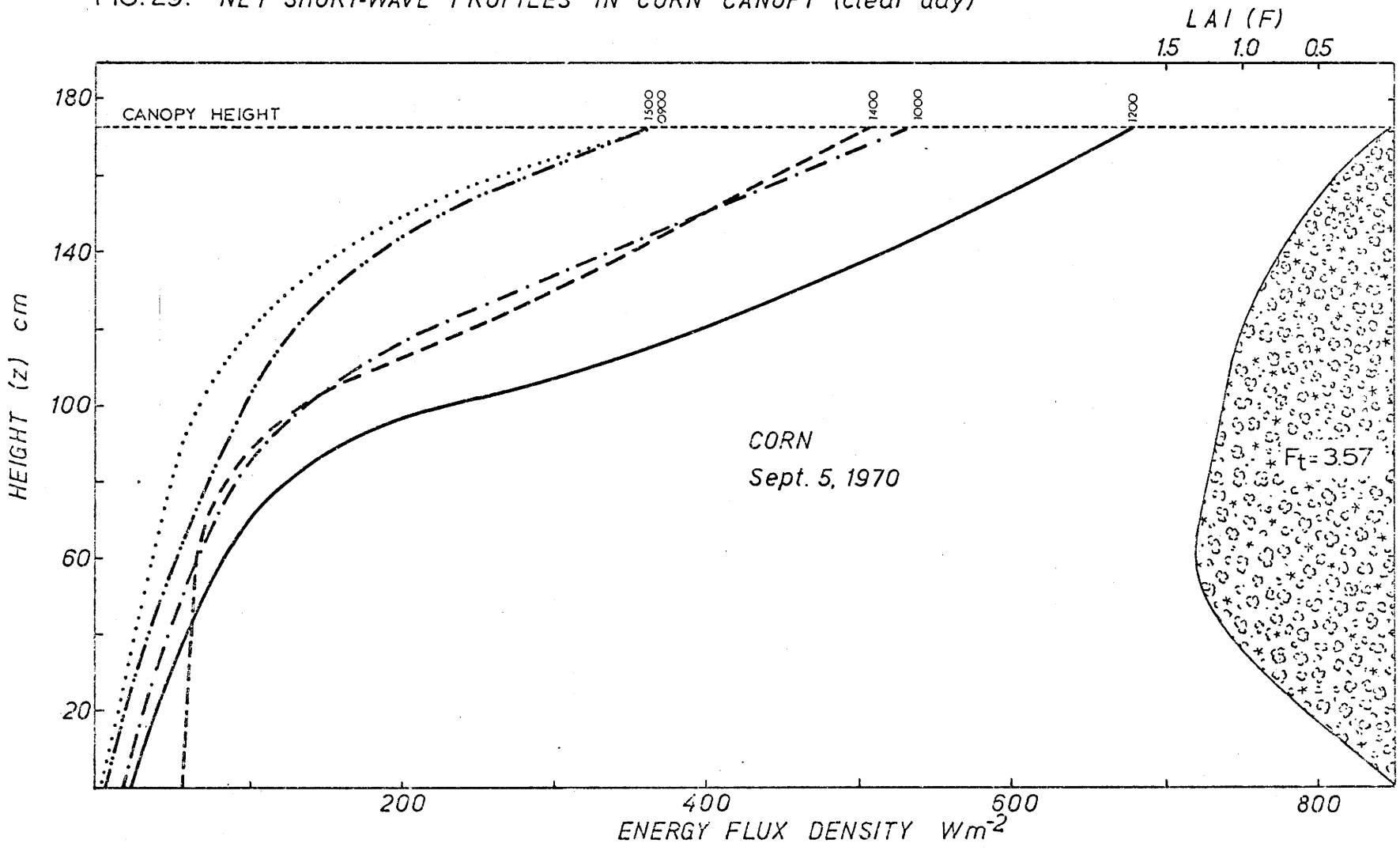

FIG. 30. *VERTICAL DIVERGENCE OF NET SHORT-WAVE RADIATION (∂Sn/∂Z) IN CORN CANOPY*

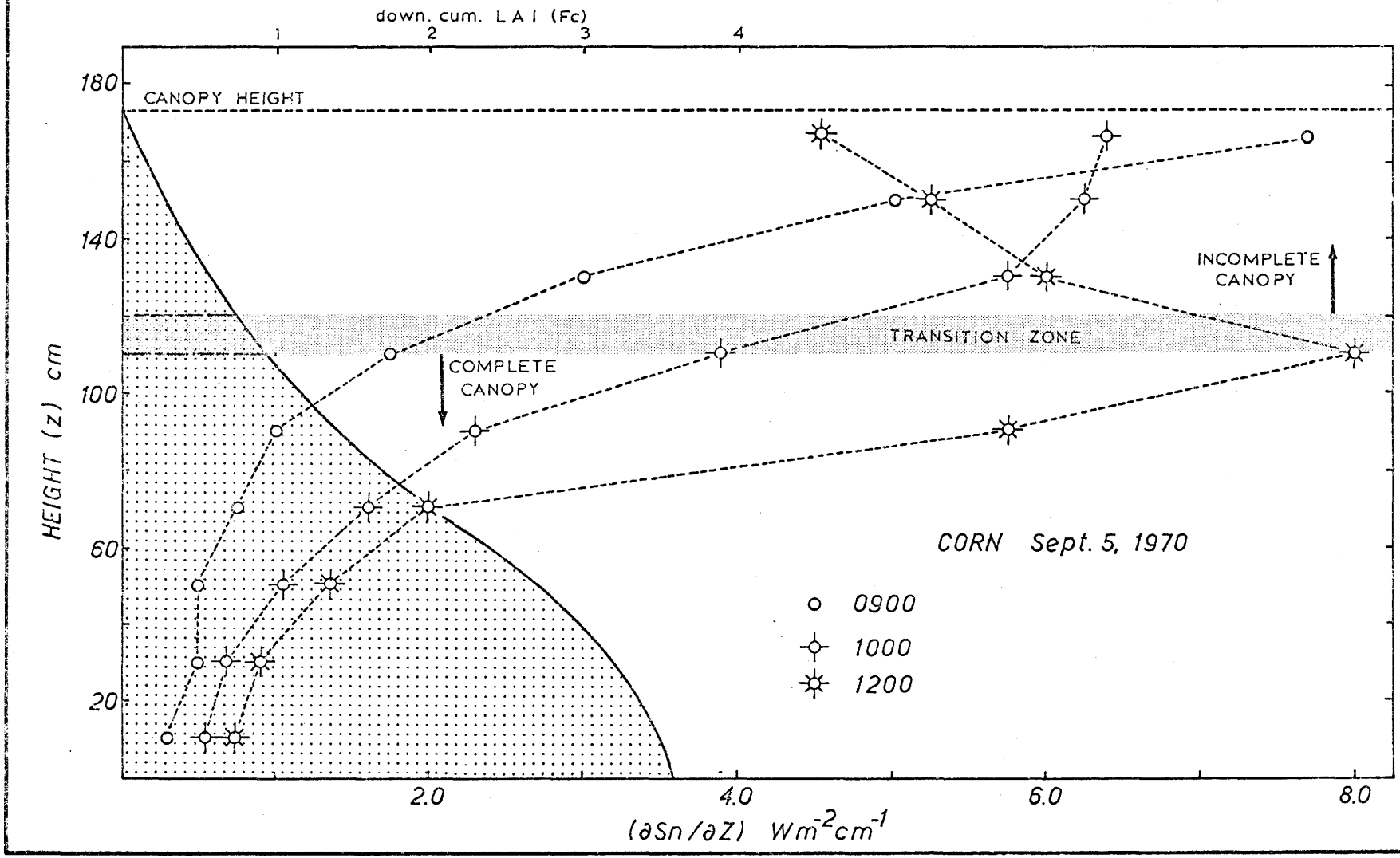

Above the transition zone the "density" of leaves between adjacent rows and between adjacent plants within rows decreases as the top of the canopy is approached. In this incomplete canopy region the rate of depletion, particularly at the higher levels, is strongly dependent on the position of the sun, (Fig. 31). At noon the depletion rate is minimum in the highest zone of the canopy. This may be attributed to the effect of row orientation, since the azimuth angle of the sun relative to the rows is zero (Fig. 31b). In effect the sun is shining down the rows. Multiple reflection of the incident beam along the rows almost certainly contributes to the decrease in depletion rate in this situation. In addition, at noon, the sun is closest to the zenith and the effective path length of the solar beam through the crop foliage is minimum (Fig. 31a). These effects become less marked with increasing depth in the canopy and as solar azimuth and zenith angles increase.

In general the trends are similar on the cloudy day, (Fig. 32). The total depletion is less, as might be expected when the diffuse component constitutes a larger proportion of the global radiation. The profile at 0900 is similar to the profile for 0900 on the clear day because cloud did not develop until later in the morning. Hence this profile and that for 0800 are representative of clear sky conditions. The other profiles, typical of cloudy skies, are independent of zenith angle. This emphasises the need for separate treatments of direct and diffuse radiation depletions in crop canopies.

The net radiation profiles under a clear sky are shown in Fig. 33. These are different from the net short-wave radiation profiles since they have a sigmoid shape. The greatest depletion occurs between the second

FIG. 31. *VERTICAL DIVERGENCE IN THE INCOMPLETE CANOPY REGION*

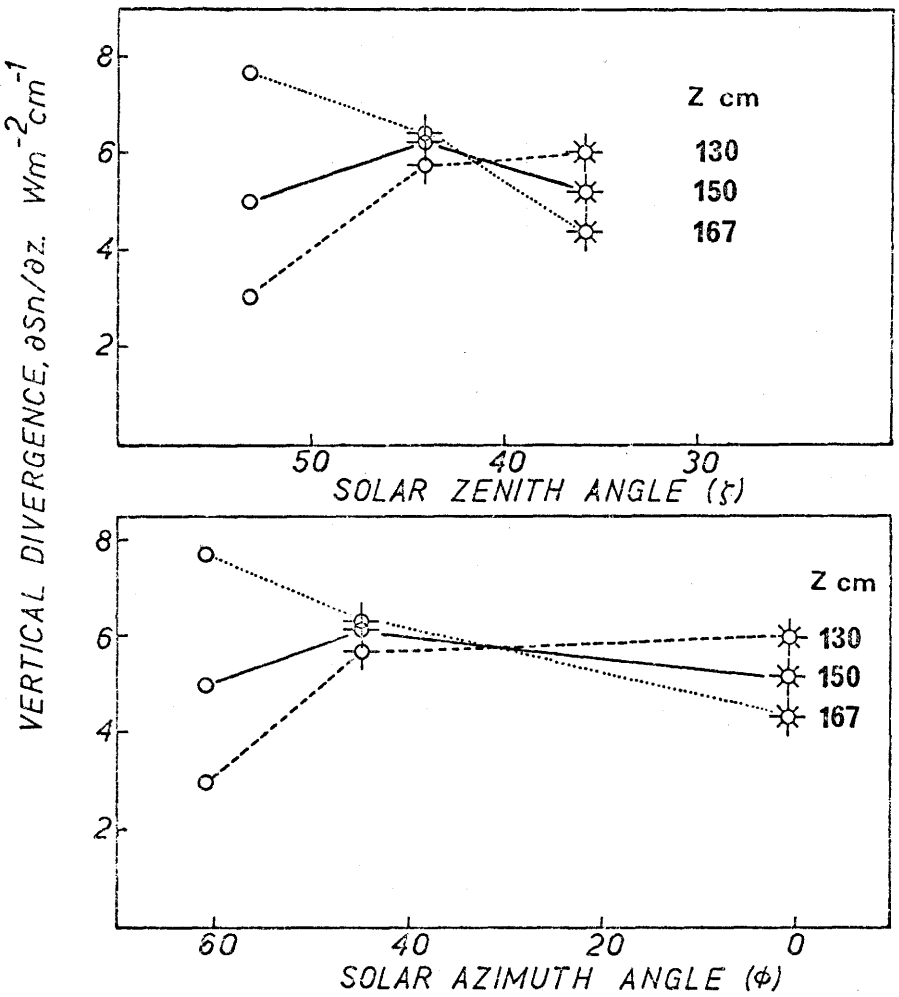

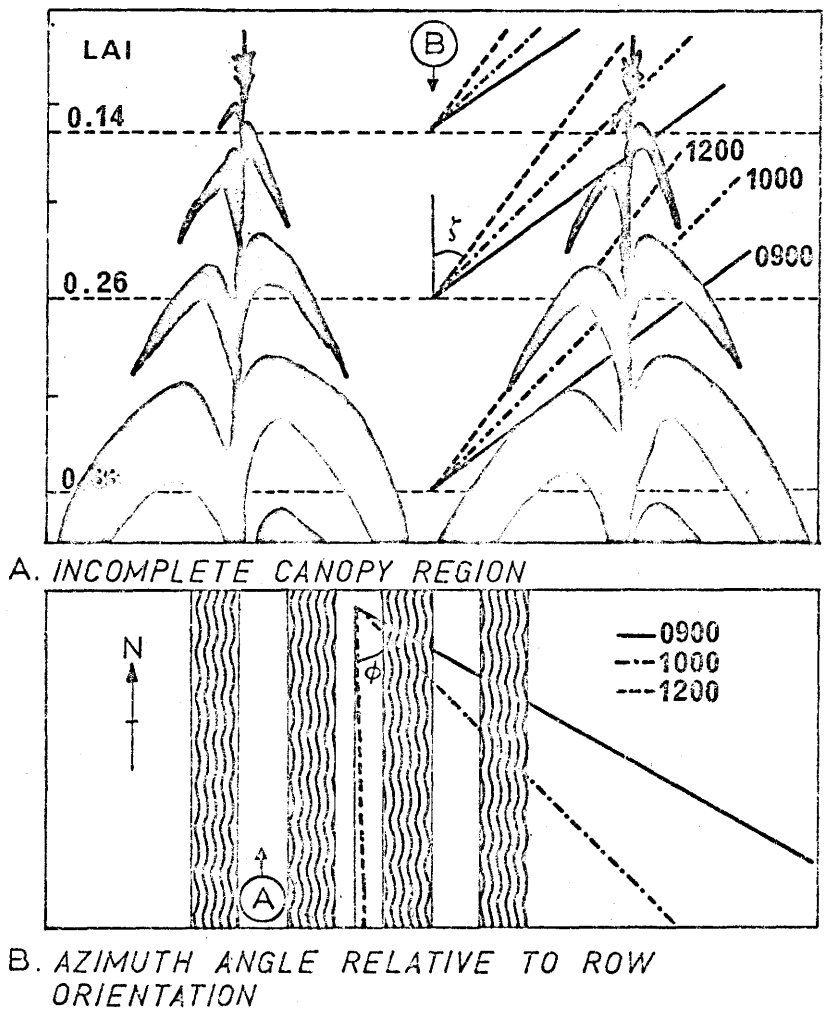

FIG. 32. *NET SHORT-WAVE PROFILES IN CORN CANOPY (cloudy day)*

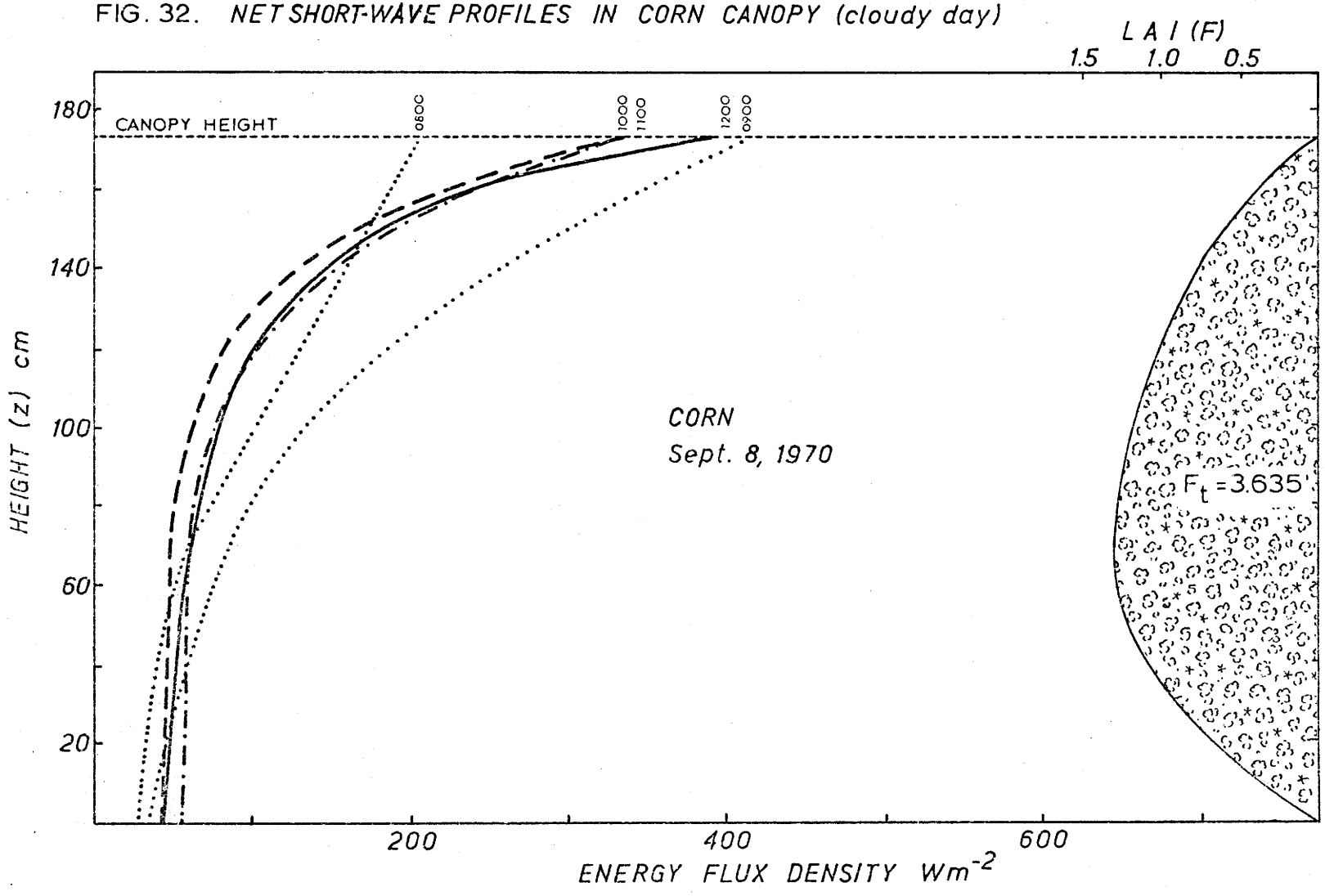

and third level in the canopy between 0930 and 1430. At other times (early morning and late afternoon) the radiation regime is changing from positive to negative and the effect of solar radiation is diminishing rapidly. Hence, the profile at 0730 consists of almost uniform, but small values of net radiation at each height. Since this study is concerned with daytime conditions the nocturnal regime and transition periods are ignored.

Vertical flux divergence ($\partial R/\partial z$) was calculated in the same manner as for net solar divergence. These are shown in Fig. 34. The maximum divergence increases in magnitude from 0900 to 1200. In addition the depth where the maximum depletion rate occurs also increases. This change in position of the maximum Rn depletion rate is most likely related to the long-wave balance. With increasing solar zenith angle, global radiation penetrates to greater depths in the canopy and is potentially available to increase the temperature of the crop elements. Such a temperature increase would result in a larger outgoing long-wave radiation flux thereby effectively increasing the net radiation depletion rate in the layers immediately above the source of thermal radiation. To test this hypothesis depletion rates of thermal radiation were calculated from profiles constructed as the residual in

$$Ln\ (z) \quad = \quad Sn\ (z) \quad - \quad Rn\ (z). \tag{23}$$

These are shown in Fig. 35. The sources of thermal radiation reveal considerable consistency with the observed maxima of Rn depletion rates. To be certain that this is not a direct consequence of the residual method of obtaining the thermal radiation profiles an independ-

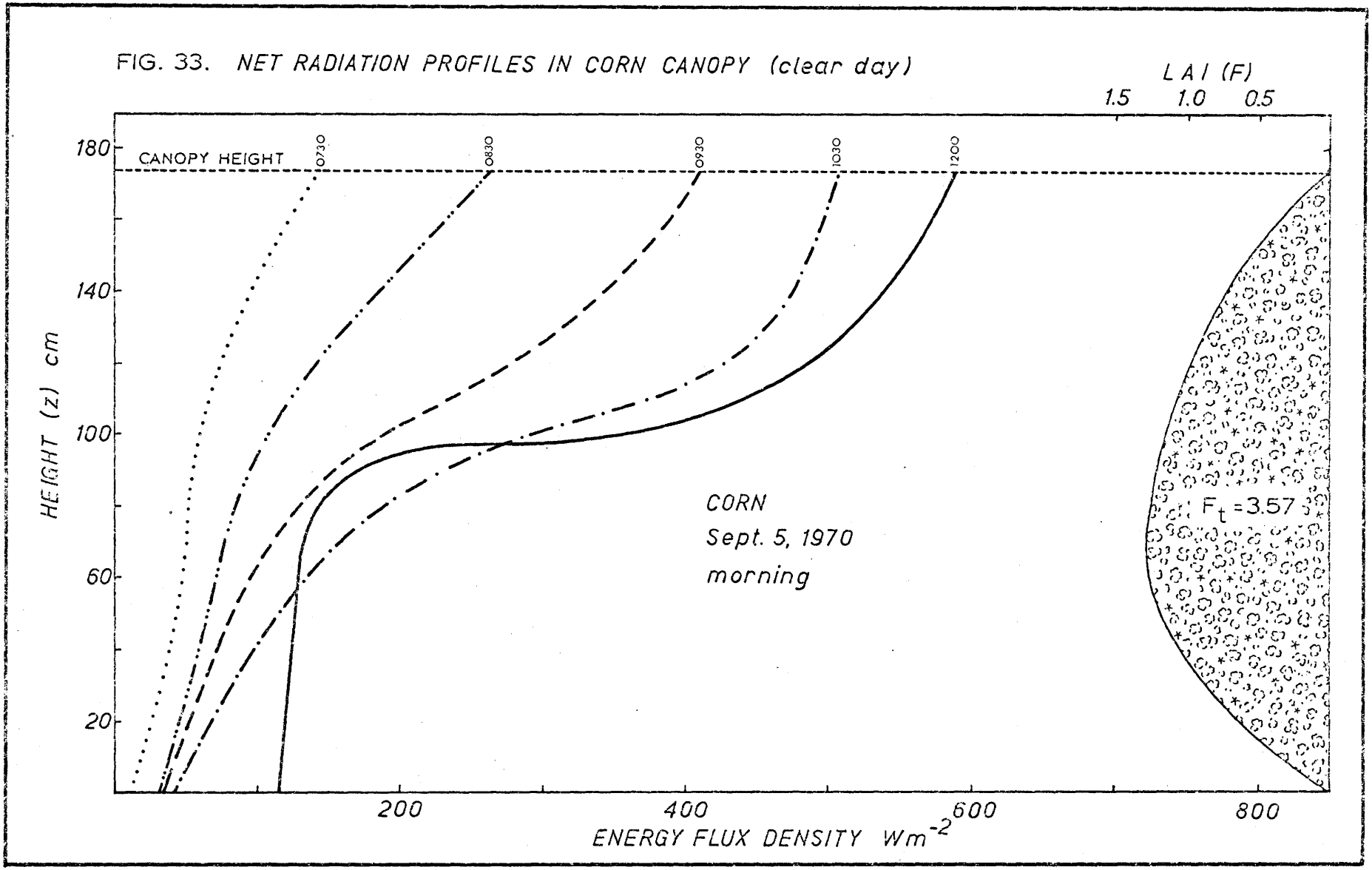
FIG. 33. NET RADIATION PROFILES IN CORN CANOPY (clear day)
LAI (F)
1.5
1.0
0.5
180
140
100
60
20
CANOPY HEIGHT
0730
0830
0930
1030
1200
HEIGHT (z) cm
CORN
Sept. 5, 1970
morning
F_t = 3.57
200
400
600
800
ENERGY FLUX DENSITY Wm^{-2}

FIG. 34. *VERTICAL DIVERGENCE OF NET RADIATION (∂Rn/∂Z) IN CORN CANOPY*

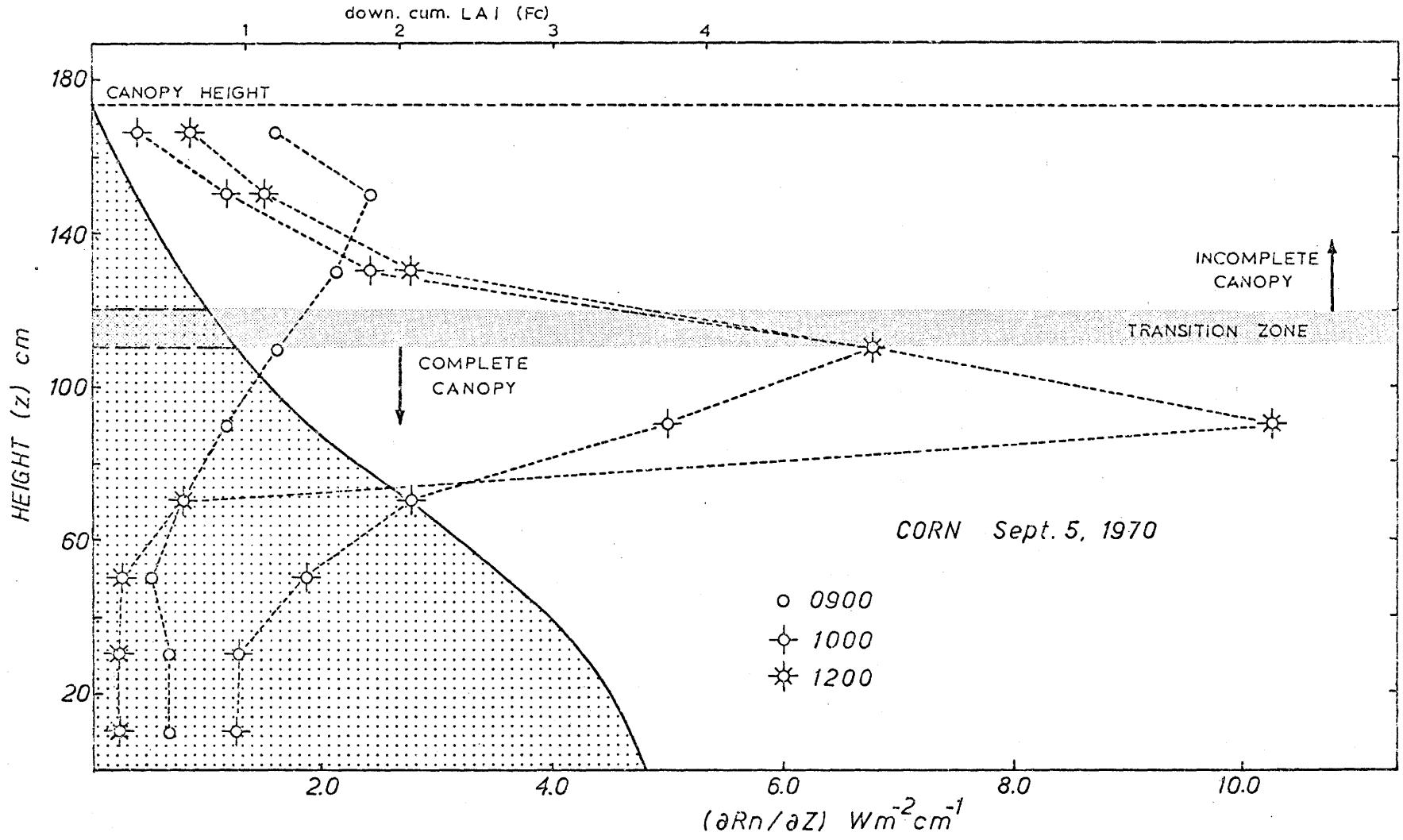

FIG. 35. *VERTICAL DIVERGENCE OF NET THERMAL RADIATION (∂Ln/∂Z) IN CORN CANOPY*

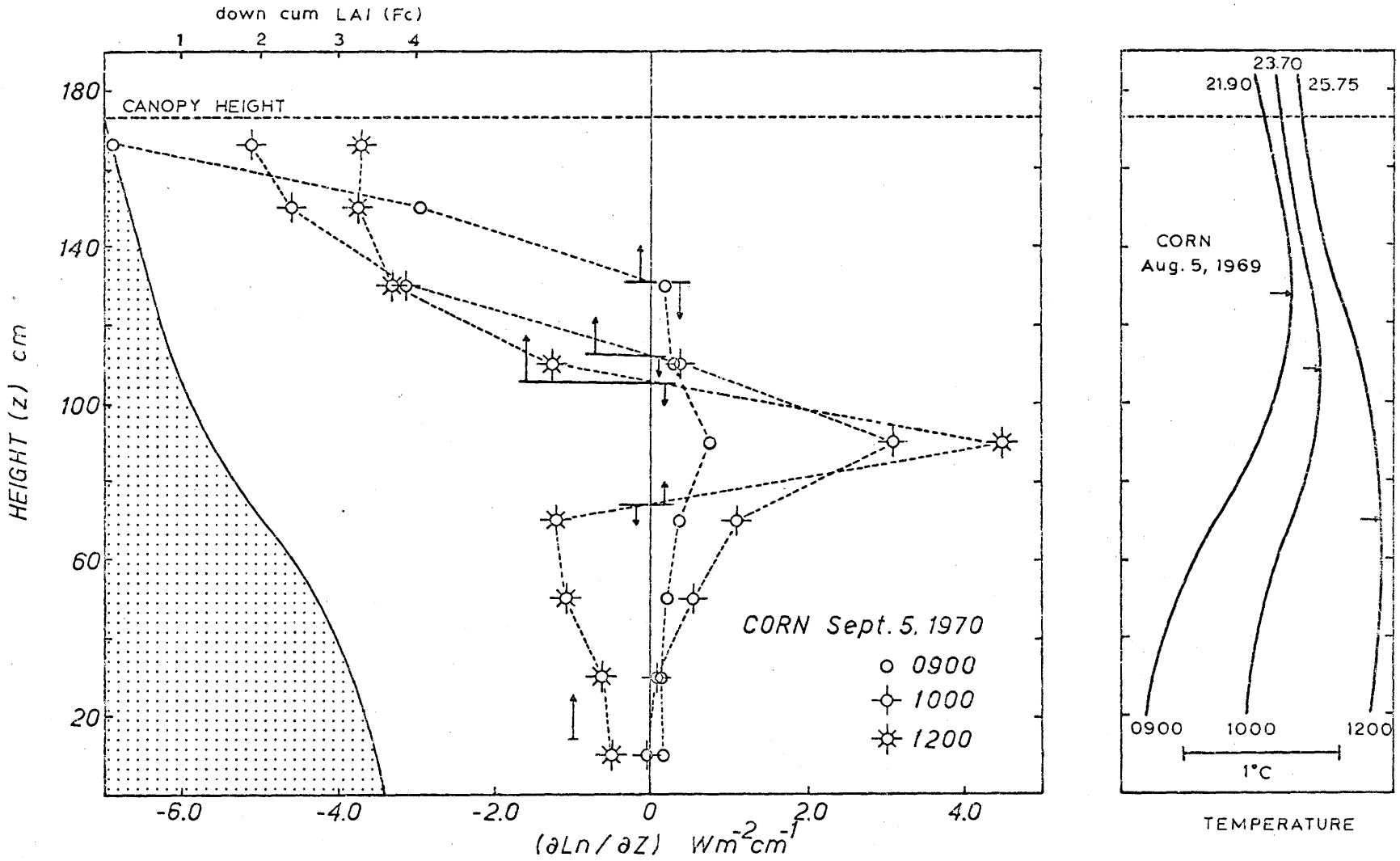

ent assessment of the validity of the Ln profiles is required. Unfortunately, no temperature data were available during the investigation. However, temperature profiles obtained under similar conditions in corn at Simcoe (McCaughey, unpublished data) are likely to be representative. These were obtained when the crop geometry, as measured by leaf-area-index and leaf-area-distribution, was very similar to that in this investigation. Prevailing radiation conditions were also markedly similar. In Fig. 35 temperature profiles for August 5, 1969 are plotted on the same height axis as the vertical divergence. Observed temperature maxima (as shown by arrows) correspond very closely with the calculated sources of thermal radiation. The noon situation is more complex due to the row effects outlined previously. The influence of soil characteristics is most noticeable at this time since global radiation penetrates to the soil surface. Soil temperatures are therefore likely to be higher thus creating a strong thermal radiation source at ground level.

Under cloudy conditions similar profiles to those with clear skies are obtained (Fig. 36). The major difference is the proportionally lower flux intensities. As global radiation is the ultimate source of net radiation this reflects the decrease in incoming short-wave radiation fluxes under cloudy skies.

2. Short-wave profile models

Several models were tested using the measured short-wave profile data for the same two days.

1. The exponential model

Values of the extinction coefficient, k, in the exponential model

FIG.36. *NET RADIATION PROFILES IN CORN CANOPY (cloudy day)*

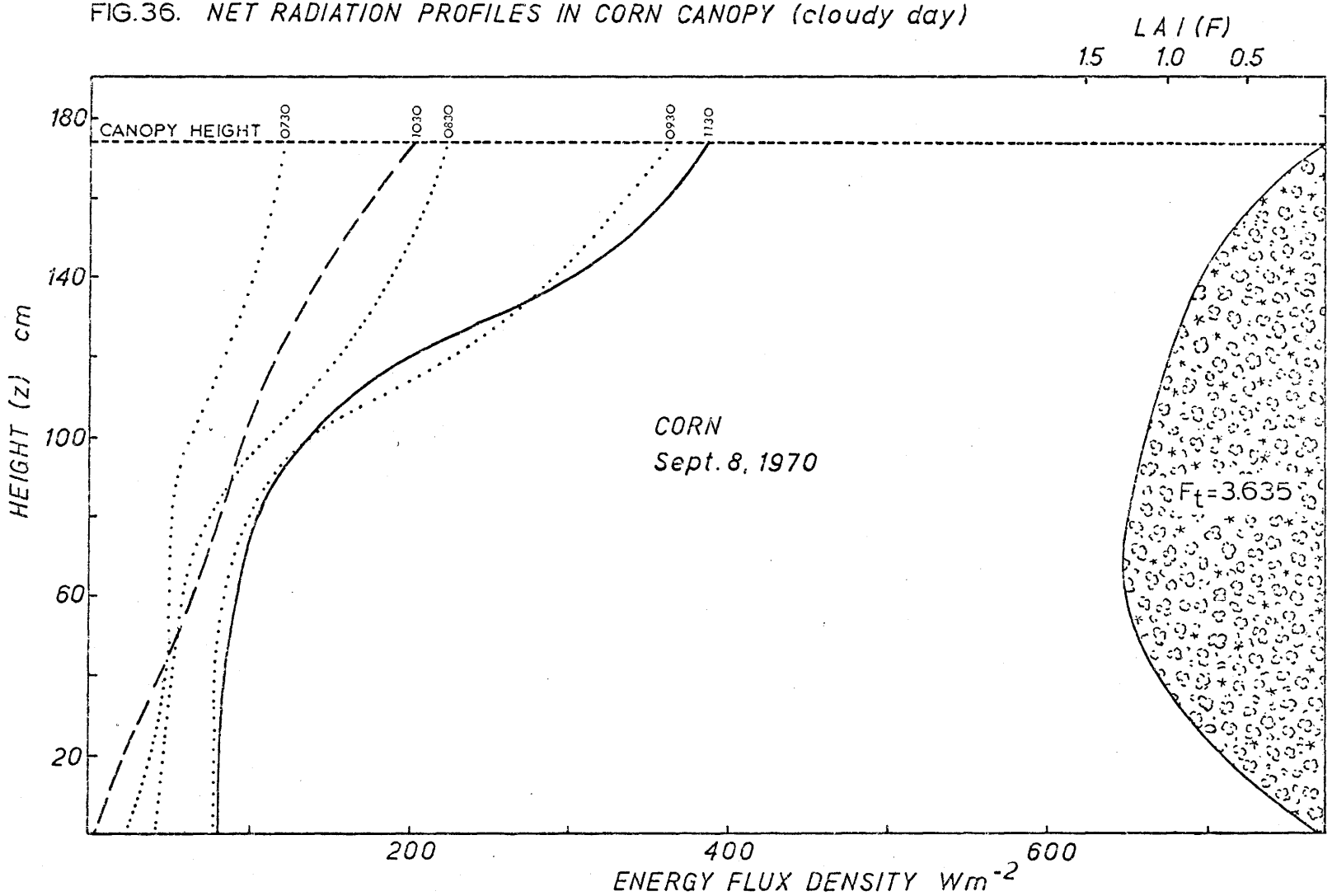

of Monsi and Saeki (1953) were calculated for the profiles of net short-wave radiation on clear and cloudy days. The mean extinction profiles for both days are shown in Fig. 37 and 38. The extinction coefficients vary markedly, with the lower value obtained for the cloudy day. This is consistent with the higher proportions of diffuse radiation present. As noted by previous workers (Isobe, 1962; Anderson, 1966) the semi-log plot of extinction dependence on leaf area demonstrates an upward concave curve. The exponential approximation performs considerably better on clear days with more regular radiation distributions. The evidence supports previous findings that even on a daily basis the exponential model does not provide a sufficiently powerful method for dealing with the variables controlling divergence of flux in plant canopies.

On an hourly basis, the model performs much less satisfactorily. Fig. 39 and 40 show the measured profiles for the morning on the same two days. Under clear skies the model over-predicts net short-wave radiation in the greater part of the canopy. The under-prediction in the top level of the canopy may be too high due to an effect of N-S row planting. The solar beam was then aligned along the row and the net pyranometer was relatively unshaded by leaves. On the cloudy day the model consistently over-predicted radiation levels in the canopy. The error increased as the quantity of diffuse in the global radiation increased between 0900 and 1200 to as much as 50% in the middle canopy layers.

The individual extinction coefficients under clear skies showed a marked diurnal trend (Fig. 41). Assymetry in the curve can be attributed to small cloud amounts present at 1400. Extinction coefficients on cloudy

FIG. 37. *MEAN SHORT-WAVE EXTINCTION PROFILE (clear day)*

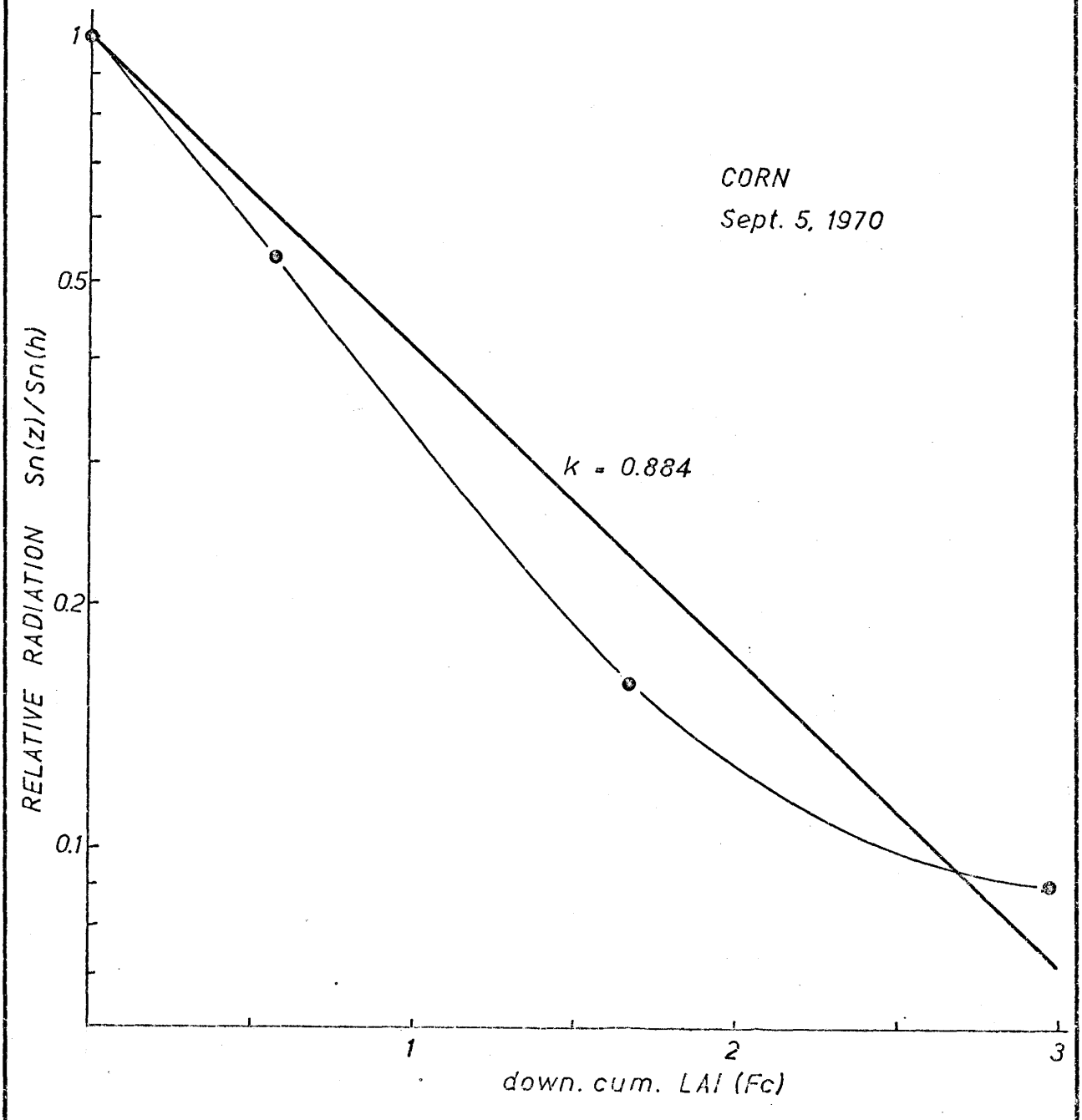

FIG. 38. *MEAN SHORT-WAVE EXTINCTION PROFILE (cloudy day)*

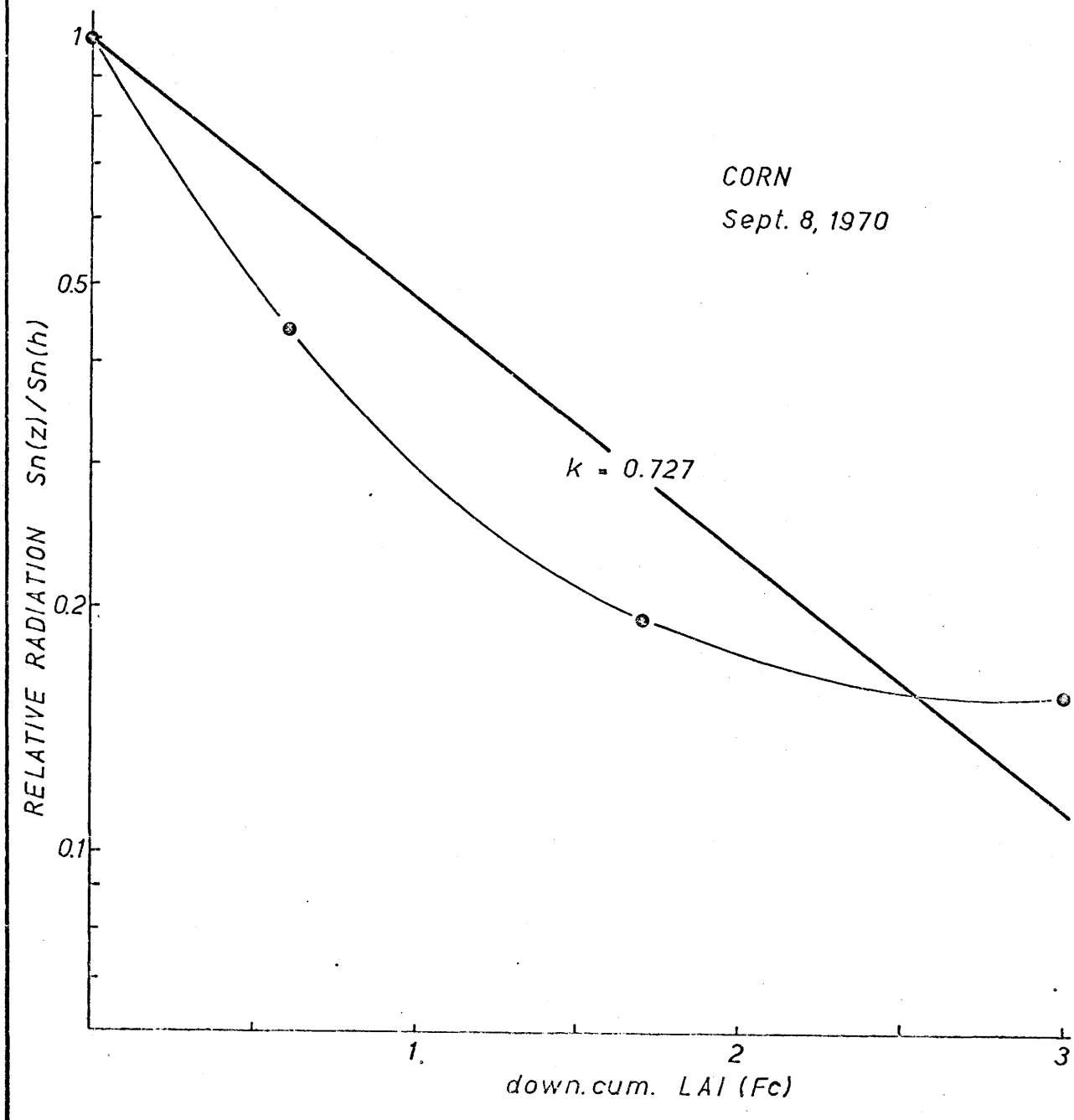

FIG. 39. *EXPONENTIAL MODEL FOR NET SHORT-WAVE RADIATION (clear day)*

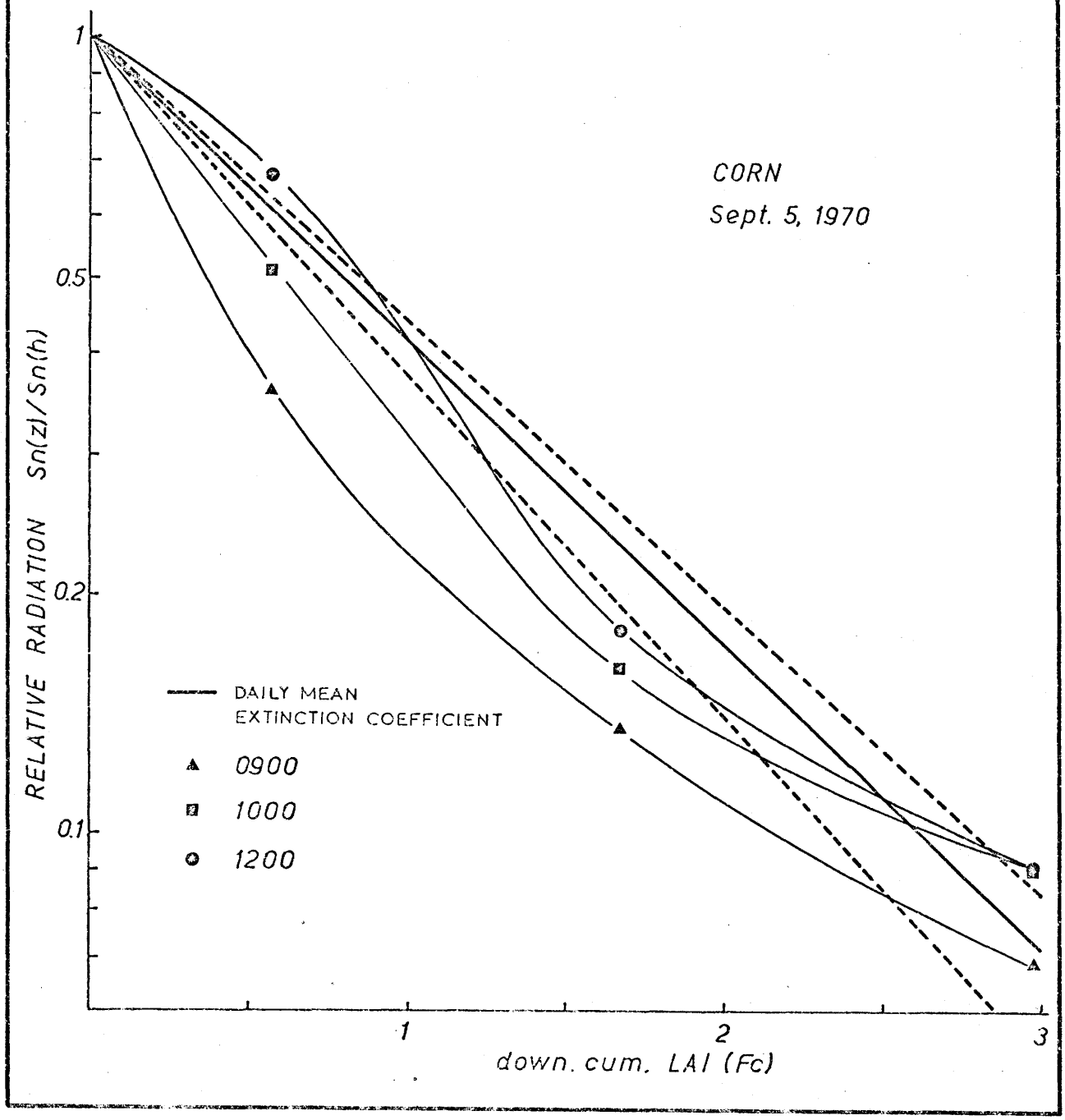

FIG. 40. *EXPONENTIAL MODEL FOR NET SHORT-WAVE RADIATION (cloudy day)*

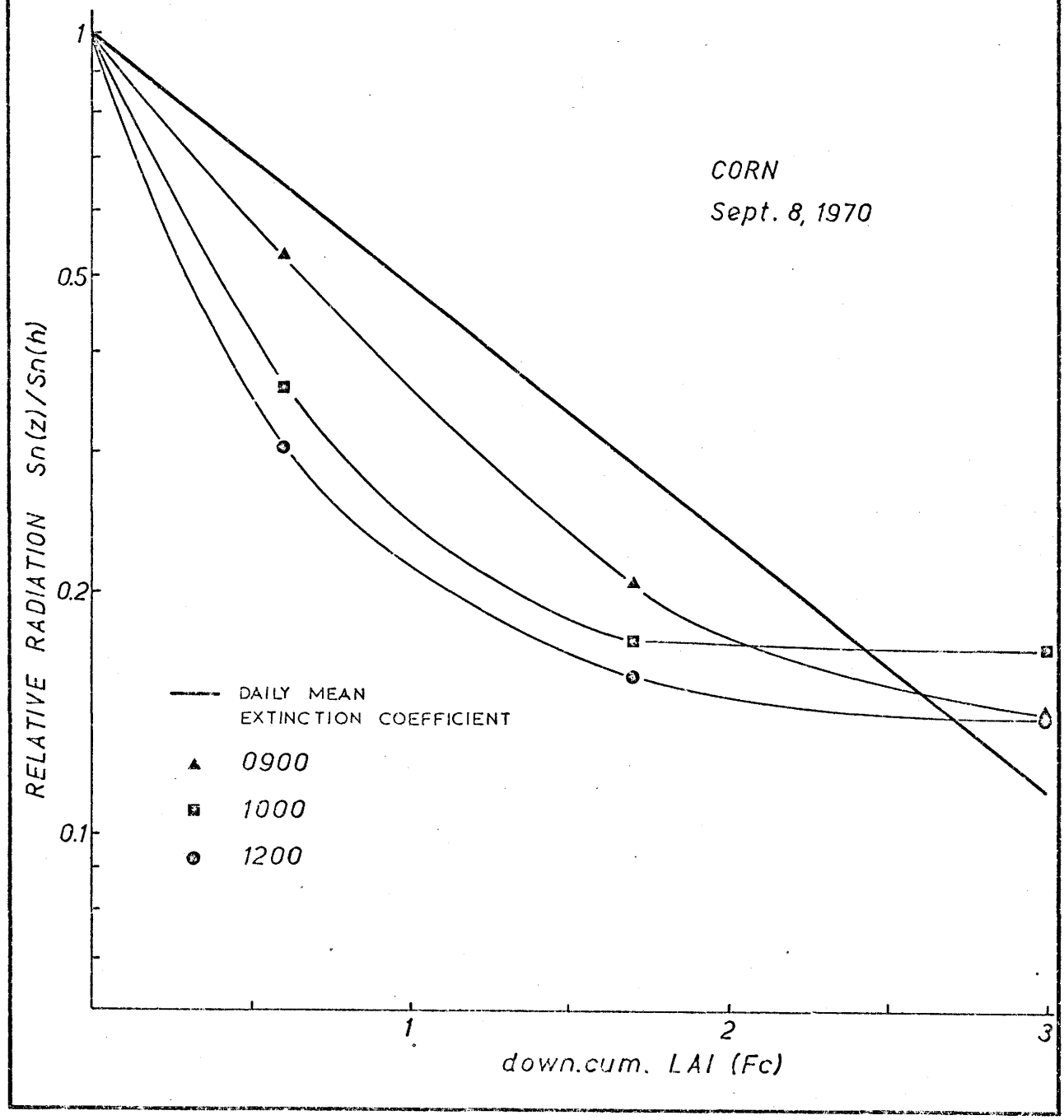

FIG. 41. VARIATION OF SHORT-WAVE EXTINCTION COEFFICIENT WITH SOLAR AZIMUTH ANGLE

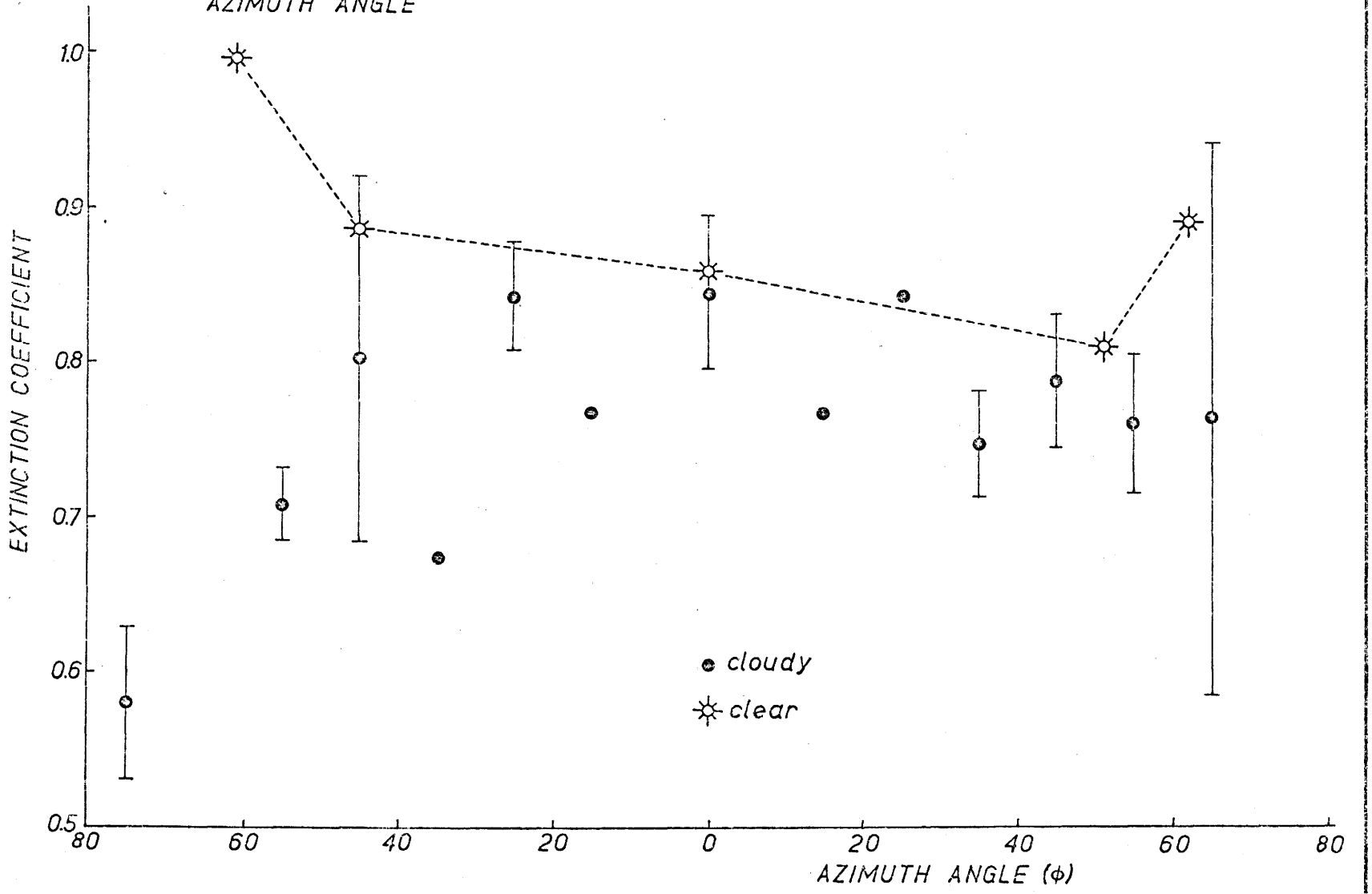

days were consistently lower indicating a lower depletion rate for diffuse radiation. No apparent trend was found although the great variability in values of k suggests that the extinction coefficient is sensitive to the relative proportions of direct and diffuse in the incident global radiation.

The evidence points to the inadequacy of the exponential model to successfully predict the flux of net short-wave radiation at any level in the canopy. Apart from previous criticisms of the model by Anderson (1966), substantiated in this study, that the model does not account for leaf angle and sun angle changes, it also appears that the proportions of direct and diffuse radiation in the incident beam, not accomodated in the model, have an important bearing on the rate of depletion. This is shown by the considerable variations in k when cloudy conditions are predominant.

2. Modified exponential models

Various modifications of the exponential model have been suggested by Anderson (1966), Duncan et al., (1967), Cowan (1968) and others in an effort to obtain a better prediction of short-wave radiation in the canopy. Basically these modifications consist of attempts to account for variations in leaf inclination and posture and changes in the position of the sun relative to the canopy. To evaluate the usefulness of these suggestions the profiles for the morning on the clear day were chosen.

Initial calculations were made to evaluate the expression

$$Sn\,(z) = Sn\,(h).\ \exp\left[-(F'/F.\sec\zeta\ .Fc\right], \qquad (23)$$

where F'/F is the Wilson-Reeve ratio for a leaf angle of 45^{o} and a solar

altitude equal to ($\pi/2 - \zeta$), and Fc is the downward cumulative L.A.I. The sec ζ term in the exponent is analagous to the optical air mass used in atmospheric studies and will therefore be termed "foliage mass". It corrects the leaf-area-index for increases in path length when the sun is low in the sky.

The prediction as formulated in Eq. 23 is shown in Fig. 42. Since the F'/F ratio is fairly conservative for a leaf angle of 45° (0.565 to 0.465 between 0900 and 1200) the zenith angle of the sun has the greatest effect on model values. Least depletion occurs at noon when the sun is nearest the zenith and sec ζ is minimum. Throughout the profile the model very markedly over-predicts radiation fluxes. Greatest errors occur in the middle canopy layers particularly around noon where the prediction over-estimates by 40%. Clearly leaf angle and solar angle are not the only parameters which must be considered. The changing nature of the direct beam as it is scattered down into the canopy must play an important role in the shape of the resulting profile.

With increasing depth in the canopy the ratio of diffuse to direct beam radiation changes markedly. The depletion of diffuse radiation is different from that of the direct beam. In particular, diffuse radiation in the deeper canopy layers will not exhibit a dependence on solar zenith angle since radiation is scattered in all directions by crop elements.

An empirical approach, to correct for this effect, is to allow (F'/F.sec ζ) to vary with depth in the canopy. This may be accomplished by an expression of the form

$$Sn\ (z) = Sn\ (h).\ \exp\ \left[-(F'/F.\sec\zeta)^{\frac{h-z}{z}}.\ Fc\right], \qquad (24)$$

FIG. 42. *MODIFIED EXPONENTIAL MODEL (clear day)*

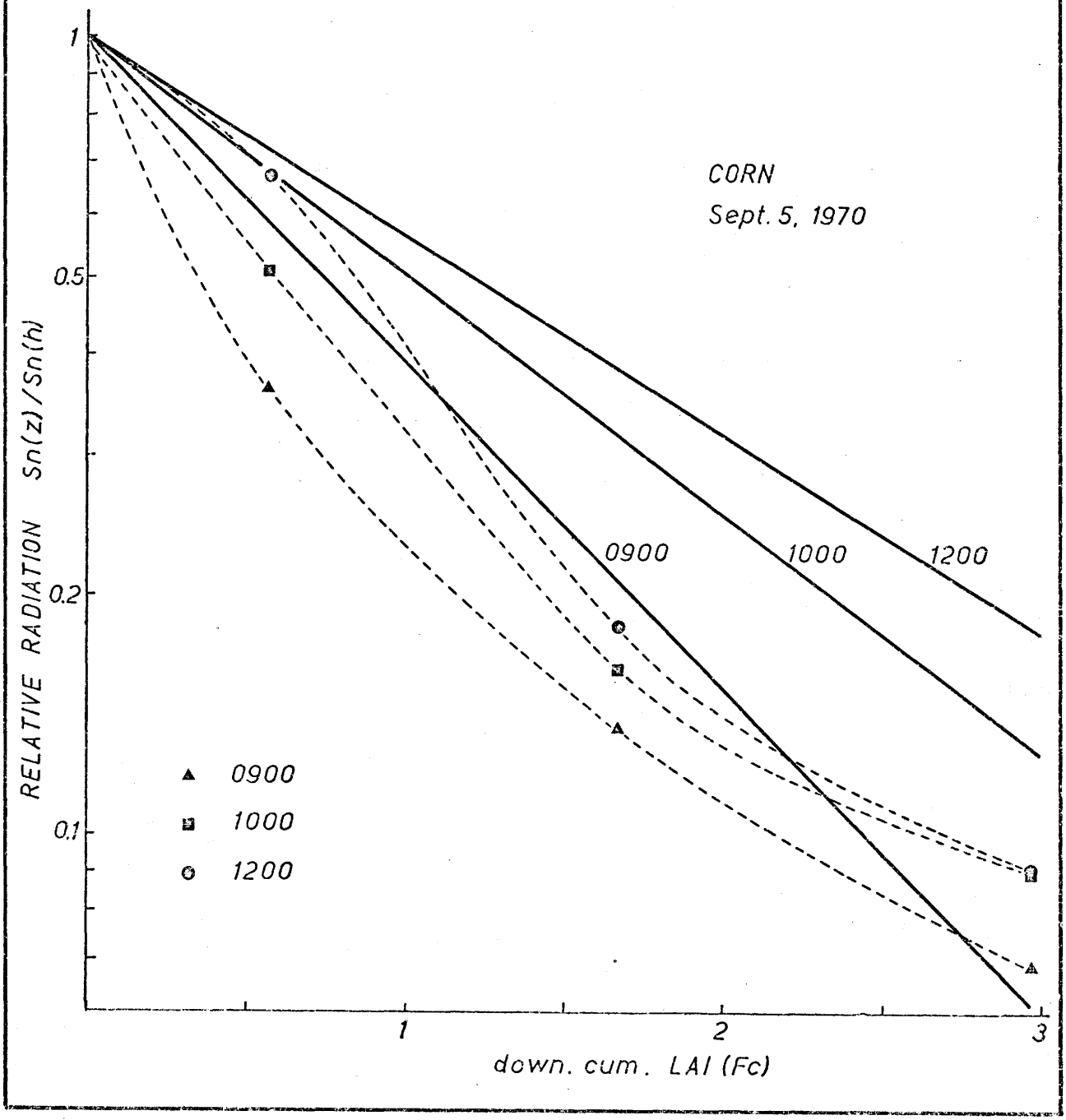

where h is canopy height, and z is the depth from the top of the canopy. Near the top of the canopy this term approaches unity and the equation reverts to Eq. 23. With increasing depth the effect of $(F'/F.\sec \zeta)$ is considerably reduced. Since this term may be considered analagous to k in the exponential model, the reduction in this term is consistent with the observations of Allen and Brown (1965) who found that k decreased with increasing leaf area.

The profiles obtained using this method are shown in Fig. 43. There is considerable improvement when the correction is applied. Maximum errors still occur in the area of maximum leaf density but are reduced to approximately 30%. In the top $^1/_3$ of the canopy at noon, when radiation intensities are highest, prediction is very good. Using this technique it may be possible to determine profiles with sufficient accuracy for some purposes. However, since the correction is essentially empirical it cannot explain the behaviour of the radiation after it enters the canopy.

The exponential model of Duncan et al., (1967) has the form

$$Sn(z) = Sn(h)^{I}_{\cdot} \exp\left[-(F'/F).\sec\zeta .Fc\right] + Sn(h)^{D}_{\cdot} \exp\left[-(F'/F).\sec\zeta .Fc\right], \qquad (25)$$

where the first exponent refers to the direct portion of the global radiation (I) and the second to the diffuse portion (D). The latter is computed for each sky zone (six in this case) and the total value of diffuse radiation in the middle of each foliage layer calculated as the sum of the values of $Sn(h)^{D}$ for each sky zone. Fig. 44 shows the predicted profiles using this model. The computed fluxes from this model are

FIG. 43. MODIFIED EXPONENTIAL MODEL WITH HEIGHT DEPENDENT FUNCTION (clear day)

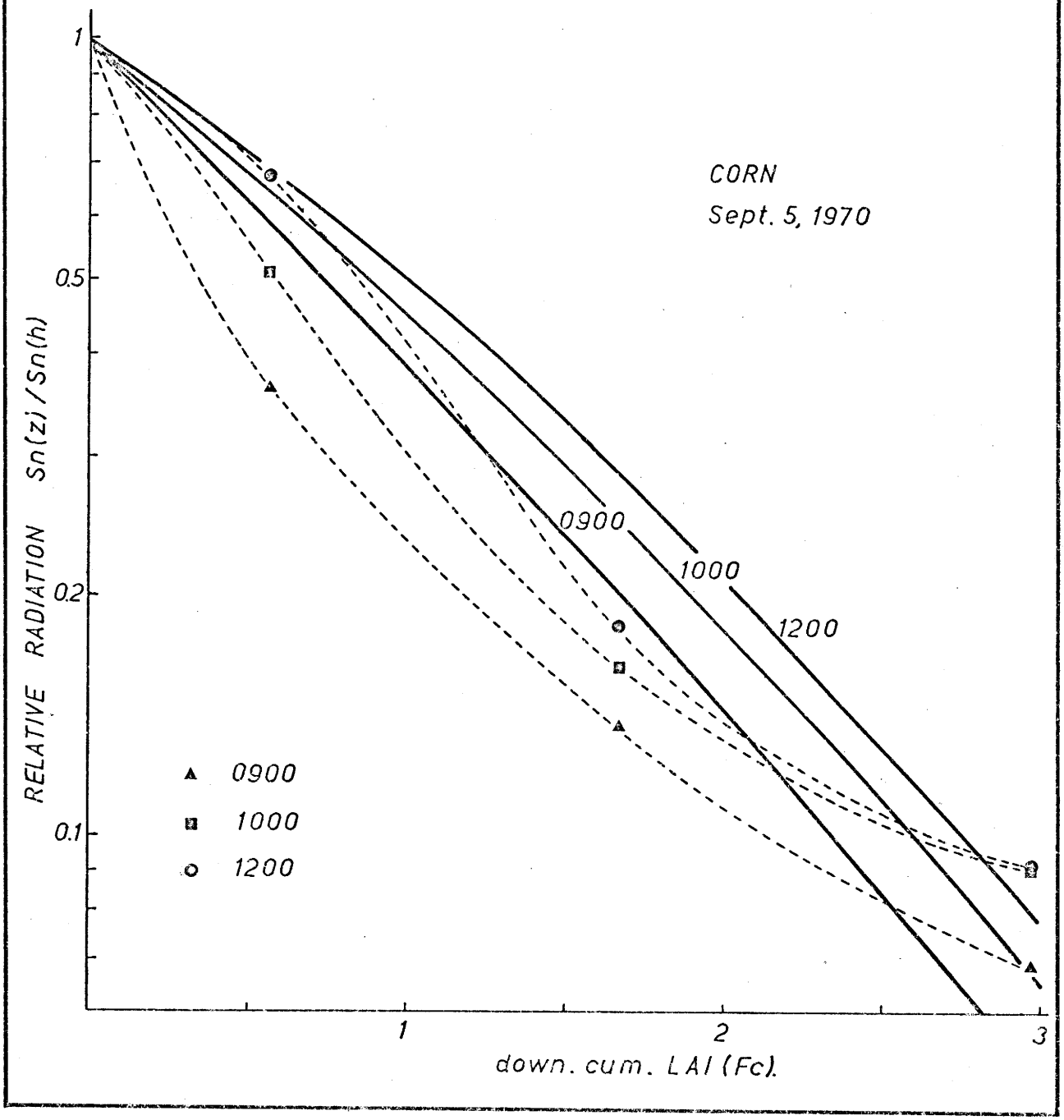

considerably better than any yet discussed. Errors in the upper and middle canopy layers, where most of the radiation is absorbed, are small (generally less than 10%) although prediction is less satisfactory in the lowest layer at higher zenith angles. However, since the magnitude of the measured fluxes at this level is small, large errors can be tolerated without appreciably altering the magnitude of the predicted flux. It should also be pointed out here that due to lack of data on the proportions of direct to diffuse radiation it was impossible to present a more rigorous evaluation than that presented here.

Although the model predicts well it has a number of disadvantages which, in the author's opinion, make it unsuitable. The equations used are cumbersome and require measurements of leaf angle to represent the canopy architecture. This is a difficult parameter to measure and even more difficult to ensure that a value obtained is representative of the crop under consideration. Furthermore, although the global radiation is divided into direct and diffuse at the top of the canopy, a significant improvement, no accomodation is provided for the proportion of the direct beam which appears as diffuse radiation at lower levels. Similarly, other important plant parameters such as leaf reflection, transmission and absorption are ignored. The substantial empiricism inherent in the model does not recommend it as a means of understanding the intricate role played by all these factors in determining the form of the short-wave radiation profile.

3. Monteith model

The model proposed by Monteith (1965b) was also evaluated,

FIG. 44. *DUNCAN et. al. (1967) MODEL (clear day)*

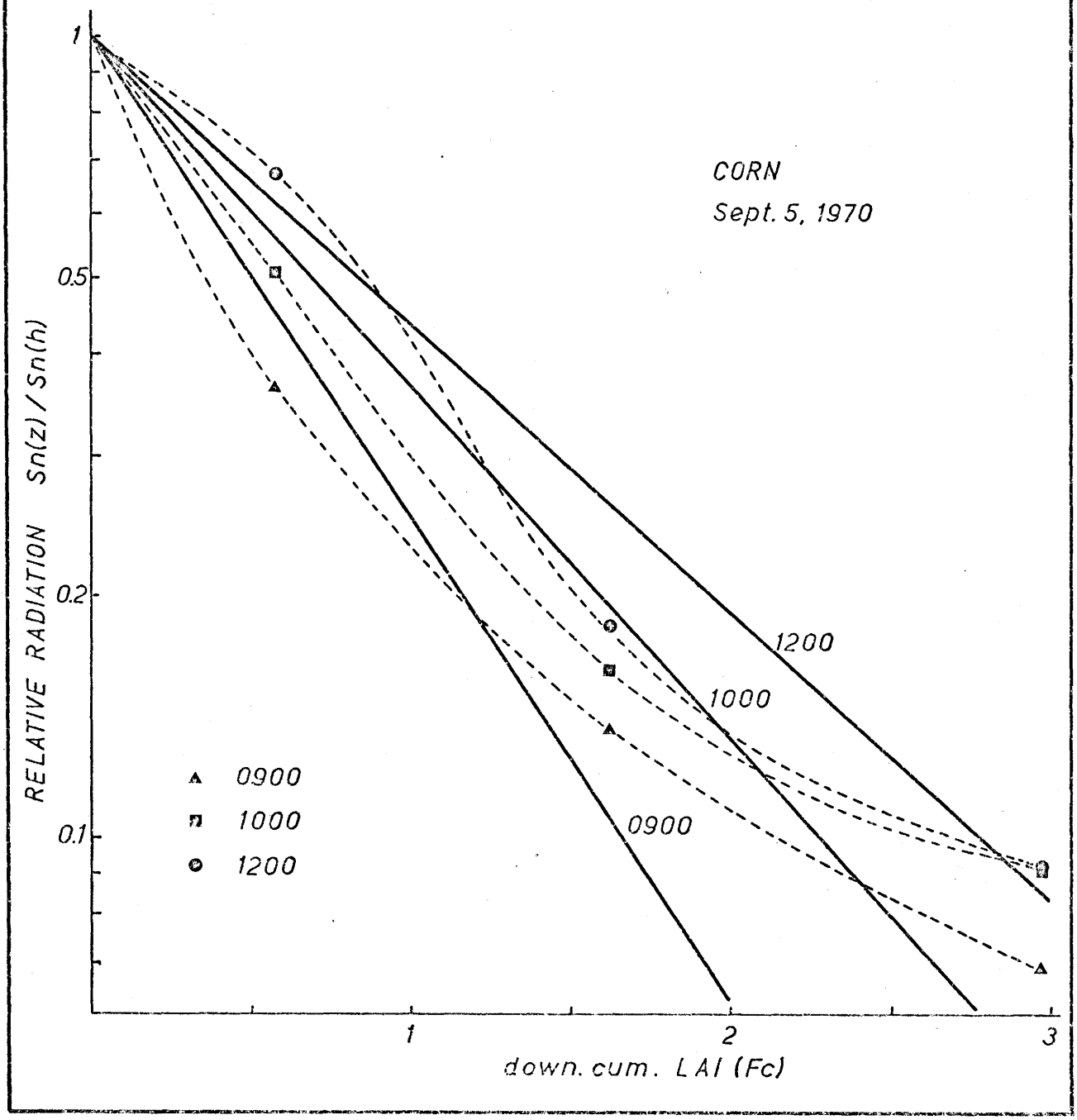

although it refers only to total global radiation. Data in this study consist of values of net global flux in the canopy. However, if we assume that the depletion of both follow a similar pattern (i.e. a conservative reflection coefficient within the canopy) the performance of the model may be evaluated.

Theoretical profiles were calculated using four layers, three of unit leaf-area-index and the other, the lowest, of the residual leaf-area-index, for values of s = 0.2, 0.4, 0.6, and 0.8 according to the binomial expansion

$$Sn\ (F) \quad = \quad \left[s \ + \ (1 - s)\ \tau\right]^{F} \ . \ Sn\ (h). \qquad (26)$$

In the expression, τ, the individual leaf transmission coefficient, was obtained by integrating the spectral transmission curve for corn (Yocum, Allen and Lemon, 1964) to give a weighted mean value for the solar spectrum.

Fig. 45 shows the theoretical curves for extinction of radiation with leaf-area-index F at four values of s. When comparisons are made between these theoretical curves and measured transmissions, the s values increased with depth in a similar fashion to those presented by Monteith for a clover sward. No direct comparison can be made concerning the absolute values of s but the behaviour is such that the assumption that s is independent of leaf-area-index is invalid. This was noted by Monteith, who attempted to explain this in terms of a change in leaf posture with height and suggested that s be allowed to vary exponentially with F using an expression of the form

$$s \quad = \quad a.\ \exp\ (-bF), \qquad (27)$$

FIG. 45. MONTEITH (1965) MODEL

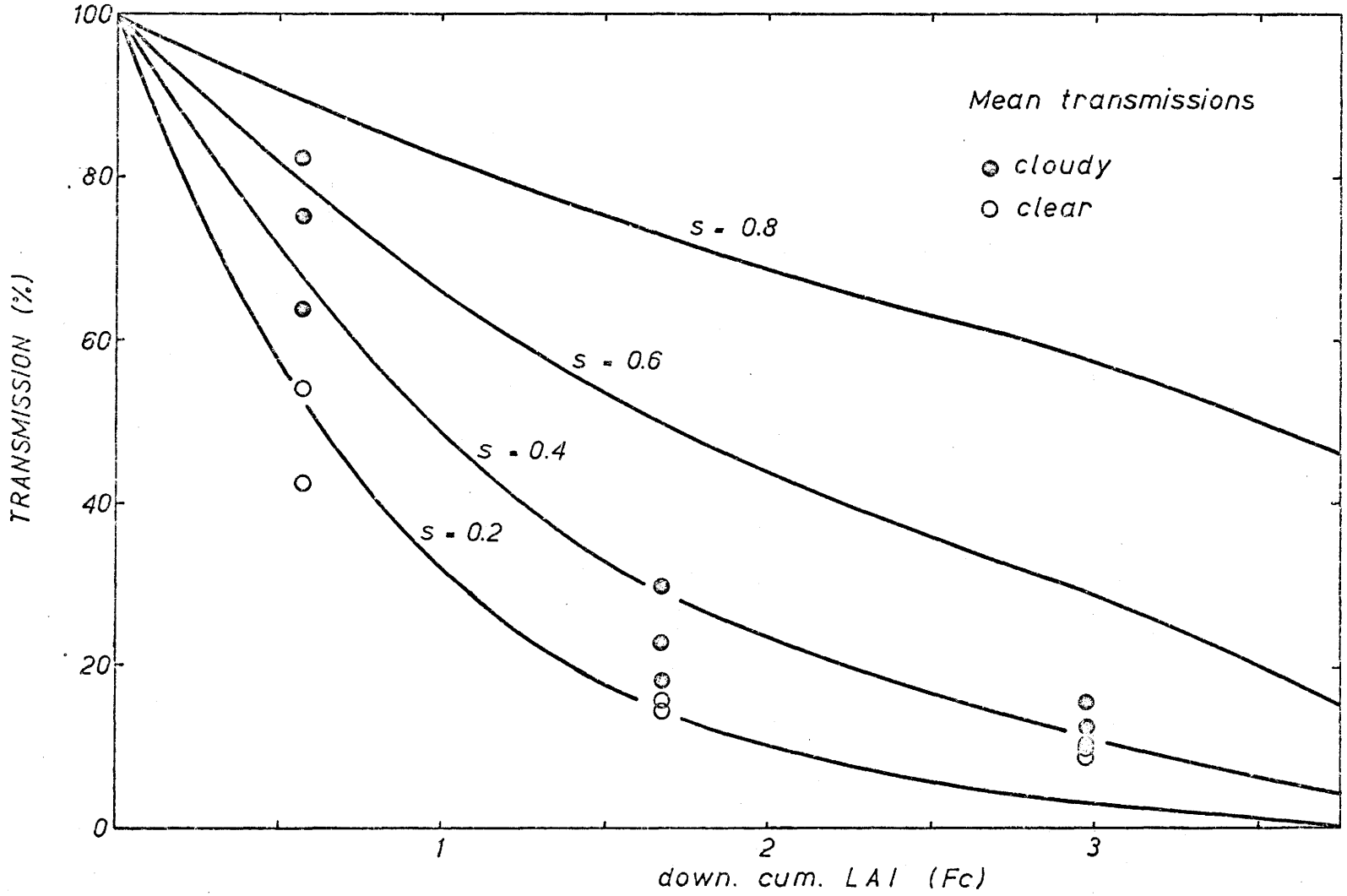

where a and b are empirically derived constants depending on the leaf distribution and posture.

A further possible cause for the change in s with depth is that the changing spectral composition of the radiation results in an incorrect transmission coefficient being assigned to the lower layers of the canopy. Larger amounts of green light near the base of the crop will bias the transmission coefficient so that the mean τ evaluated over the whole spectrum under-estimates the true transmission.

It is also noteworthy that the measured transmissions for cloudy days fall near the curves for higher values of s suggesting that the transmission is strongly affected by the amount of diffuse radiation. If this is the case, and evidence points to it, then it is incorrect to obtain a value of s unique to a particular crop at a specified stage of growth since this value will vary with prevailing weather conditions.

In addition s is specified as the area of sunflecks below the first layer. This can only refer to direct radiation and the study reveals the major shortcoming of the model; direct and diffuse radiation are not treated separately. On clear days, as shown in Fig. 45 the fit is fairly good. However, on cloudy days much more radiation is transmitted through the canopy. The model as formulated, with a constant s, does not take account of this very important term on days with considerable cloud amounts.

3. Net radiation profile models

1. The exponential model

In recent years a number of workers, Uchijima (1962), Inoue (1968),

Cowan and Milthorpe (1968) and others have stated that the extinction of of net radiation followed a similar law to that for short-wave radiation due to Monsi and Saeki (1953). According to this model, one can describe the distribution of net radiation in a plant community by an equation of the following form

$$Rn\ (z) \quad = \quad Rn\ (h) \quad \exp\ (-\kappa Fc), \tag{28}$$

in which Rn (z) is the net radiation at a height z within the canopy, Rn (h) is the net radiation at the top (h) of the canopy = net radiation above the crop, and κ is an empirical extinction coefficient.

Using Eq. 28 the extinction coefficients for clear and cloudy days were computed using a least squares fit procedure. Fig. 46 does not indicate a diurnal trend in κ, even on clear days. A marked diurnal trend was noted by Impens et al. (1969b) for corn. After accounting for the assymetrical course of his extinction curves, attributed to row orientation, there is a marked dependence of the extinction coefficient on azimuth angle. He attributed this to the more erectophile foliage distribution in corn. A diurnal trend in κ has also been found in corn at this site in previous studies (McCaughey, personal communication). The absence of any diurnal trend in these results suggests that the canopy was sufficiently uniform to minimise such row effects.

Fig. 47 and 48 show the mean daily profile predicted from the exponential model. The first point of note is that the values of the extinction coefficients are very similar, the difference between them being less than the diurnal range on a clear day (0.510 - 0.599). As noted by previous workers it is again revealed that an upward concave

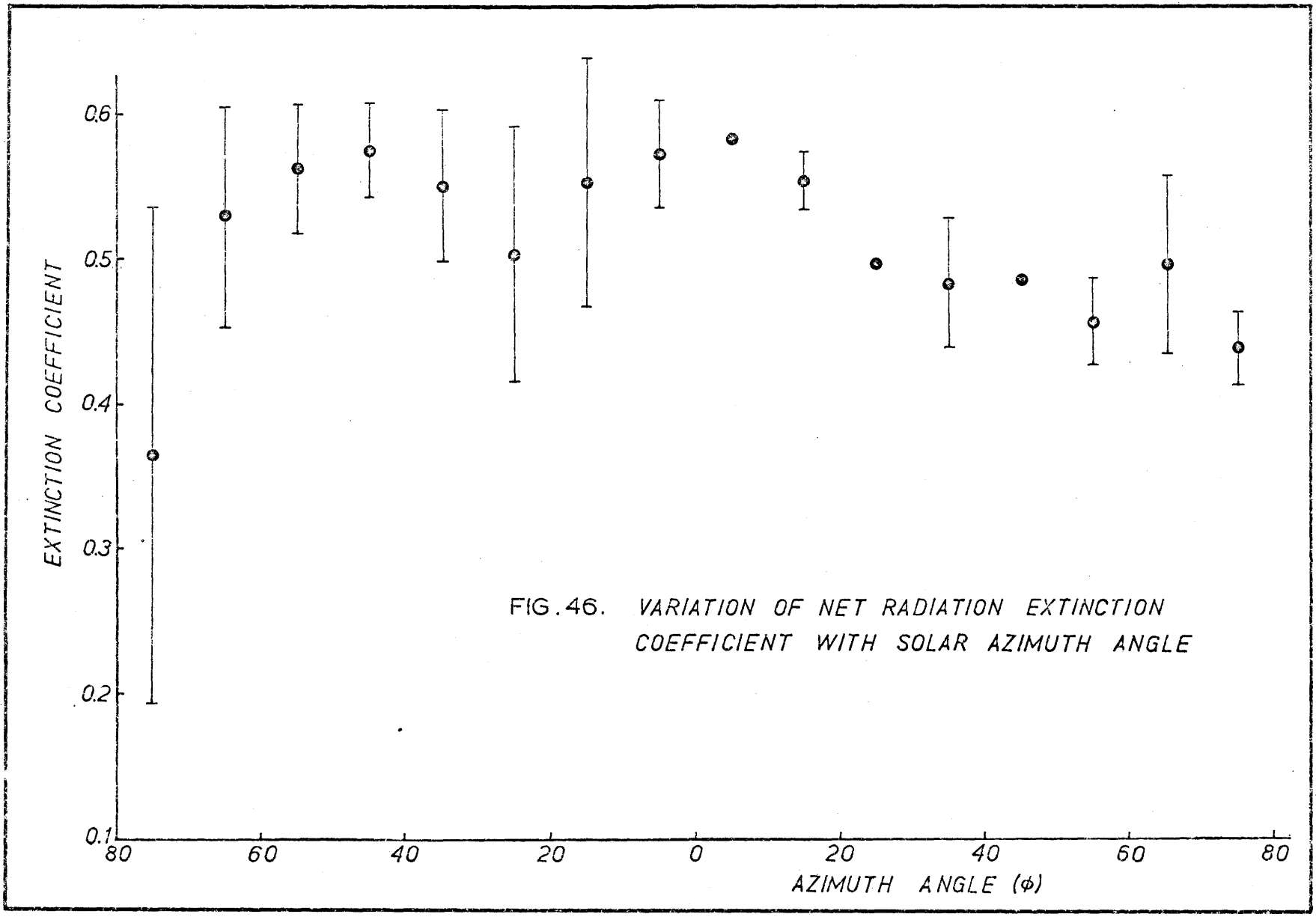

FIG. 46. VARIATION OF NET RADIATION EXTINCTION COEFFICIENT WITH SOLAR AZIMUTH ANGLE

FIG. 47. EXPONENTIAL MODEL FOR NET RADIATION (clear day)

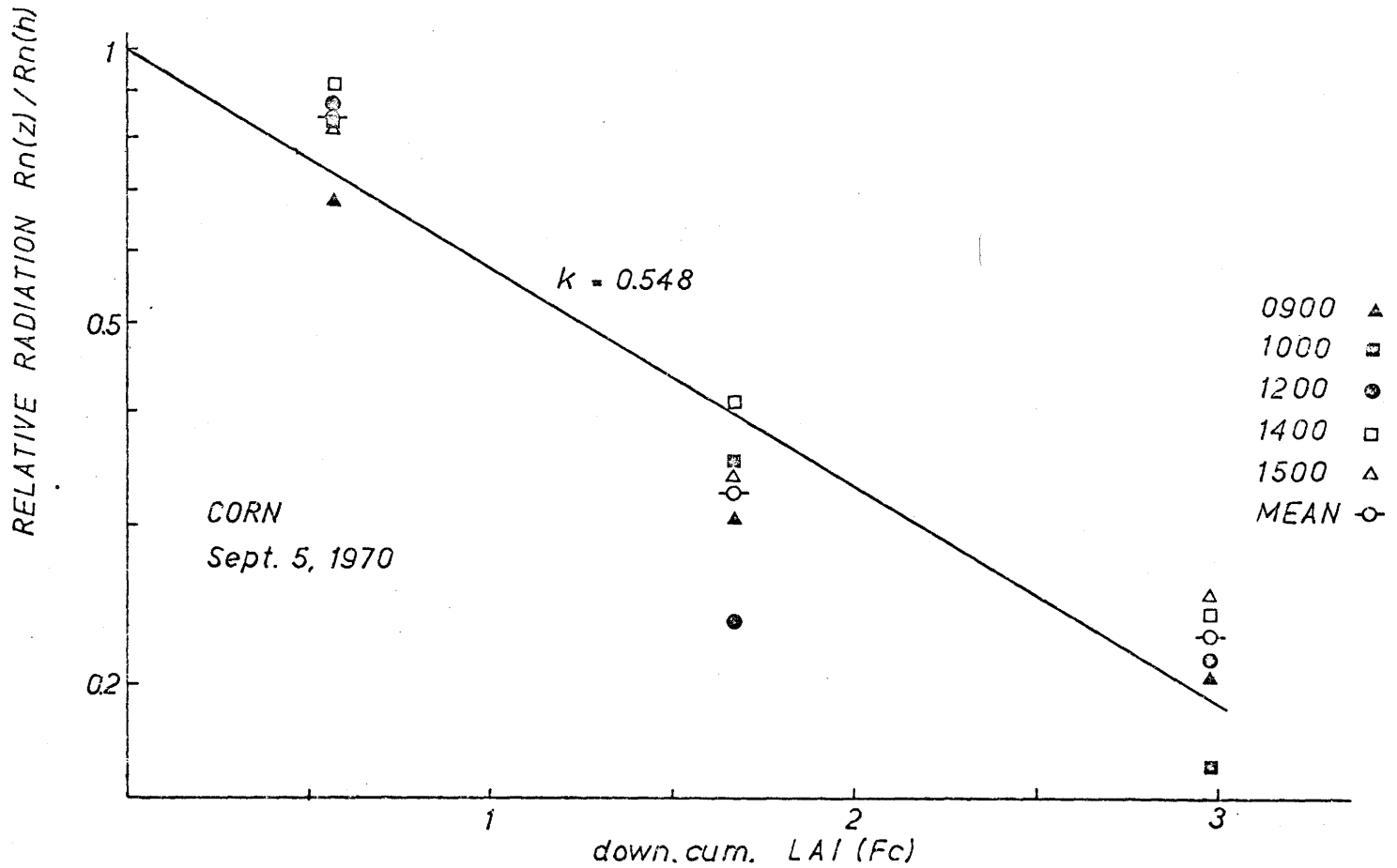

FIG. 48. *EXPONENTIAL MODEL FOR NET RADIATION (cloudy day)*

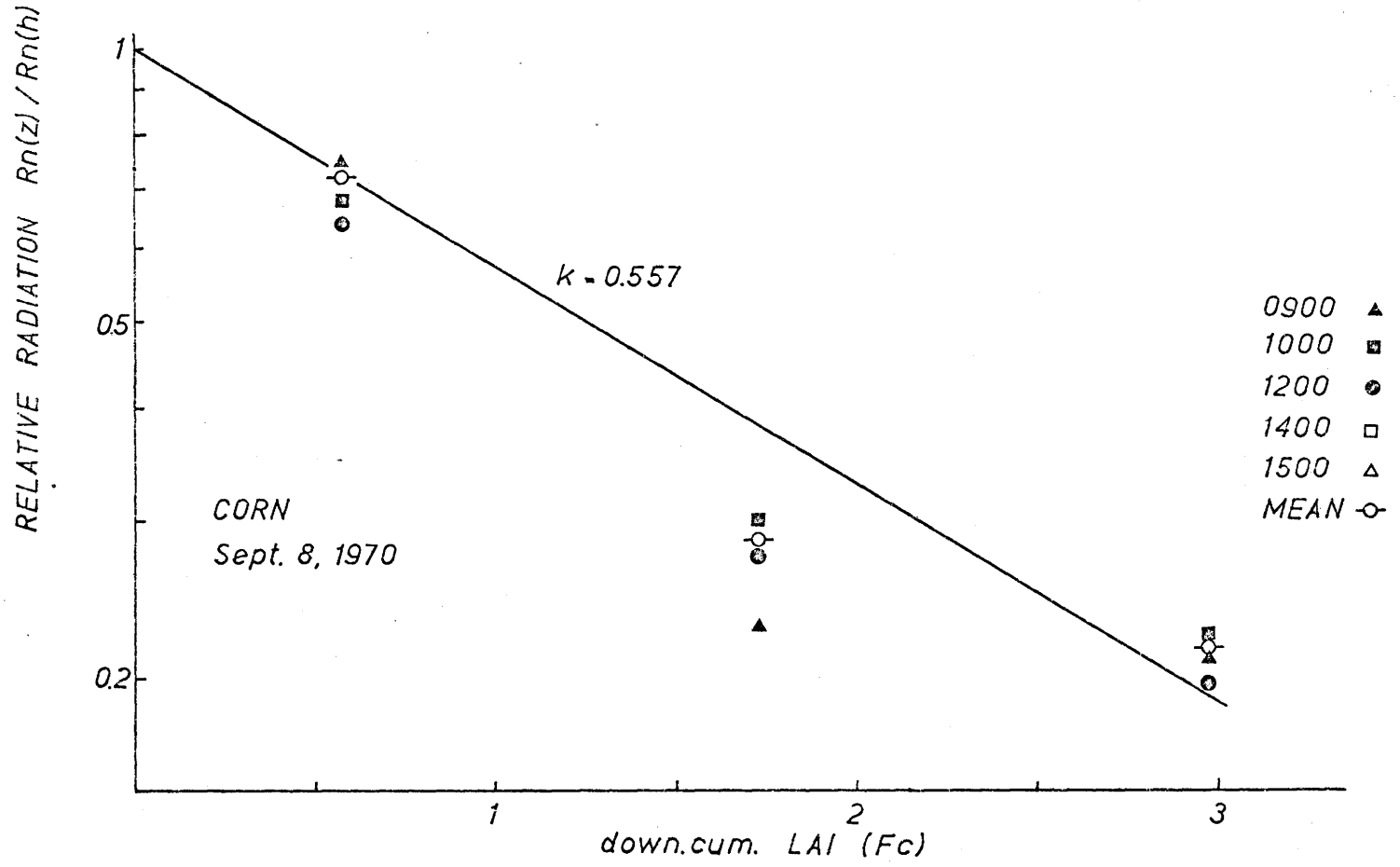

curve fits the data much better than does the exponential prediction line.

2. Modified exponential model

The downward curvature of the semi-log plot of relative radiation against cumulative leaf-area-index indicates a diminution of with depth in the canopy as a result of increasing downward cumulative leaf-area-index. Impens and Lemeur (1969b) attributed this to the high transmissive and reflective properties of foliage elements in the near infra-red and to the influence of soil characteristics on net radiation exchange within the lower part of the canopy. The strong departure from Beer's Law in the bottom part of the canopy suggested to them that net radiation attenuation in foliage should be described by an equation of the form

$$Rn\ (z) \quad = \quad Rn\ (h)\ \exp\ (-\kappa_1 Fc + \kappa_2 Fc^2) \quad , \qquad (29)$$

where κ_1 and κ_2 are extinction coefficients and other symbols are as in Eq. 28. This approach has also been used by Allen and Brown (1965) to characterise short-wave radiation depletion in corn.

Eq. 29 was solved to enable values of κ_1 and κ_2 to be calculated. The predicted relative net radiation is shown in Fig. 49 and 50. The line of best fit to the data points when the intercept is constrained is a regression equation with constants $\kappa_1 = -0.4967$ and $\kappa_2 = 0.0764$ for the clear day and $\kappa_1 = -0.6077$ and $\kappa_2 = 0.1158$ for the cloudy day. The standard errors of the estimate were 0.0542 and 0.0498 for cloudy and clear days respectively.

Measurements in corn from re-analysis of earlier data are also

FIG. 49. IMPENS MODEL FOR NET RADIATION (clear day)

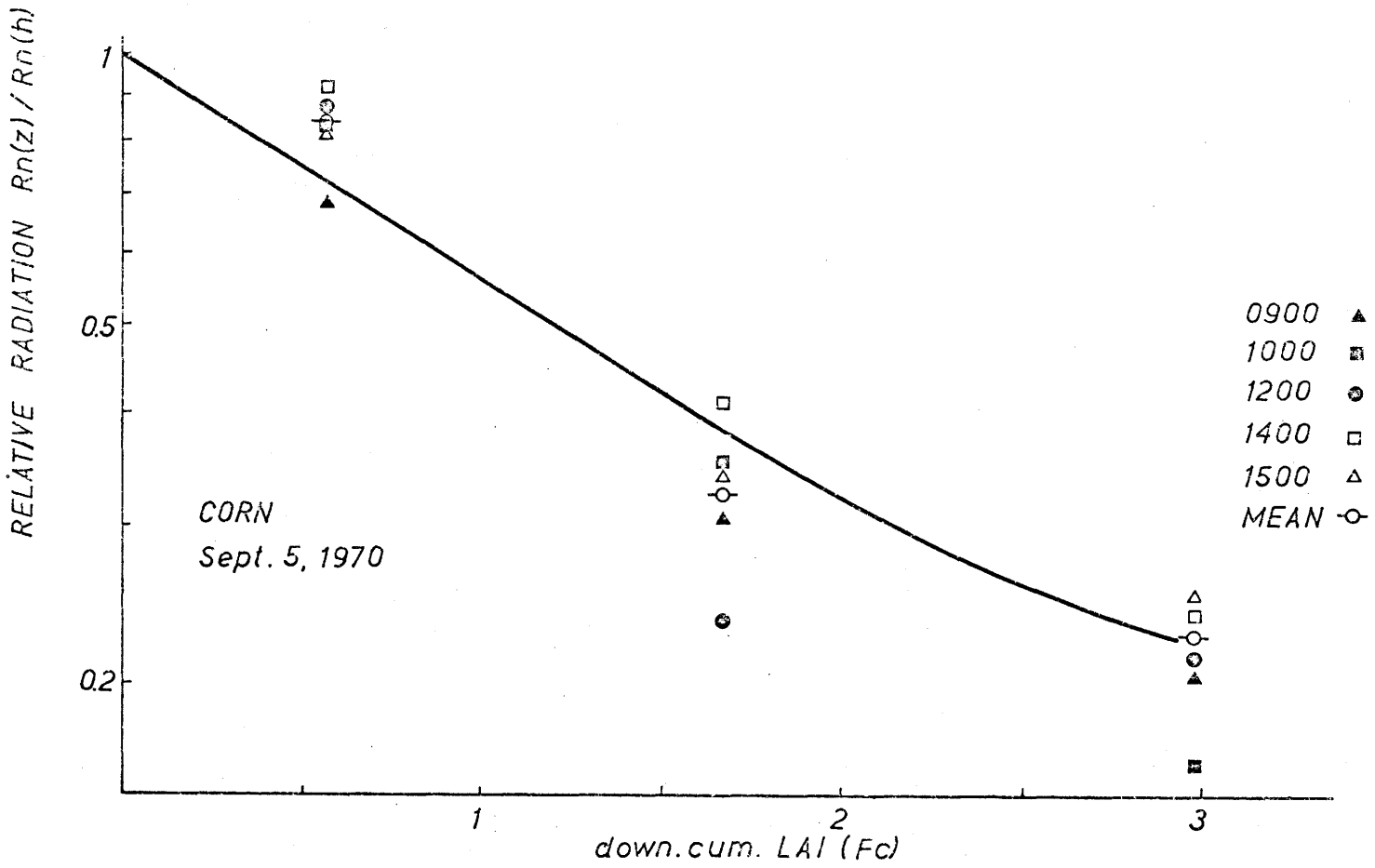

FIG. 50. *IMPENS MODEL FOR NET RADIATION (cloudy day)*

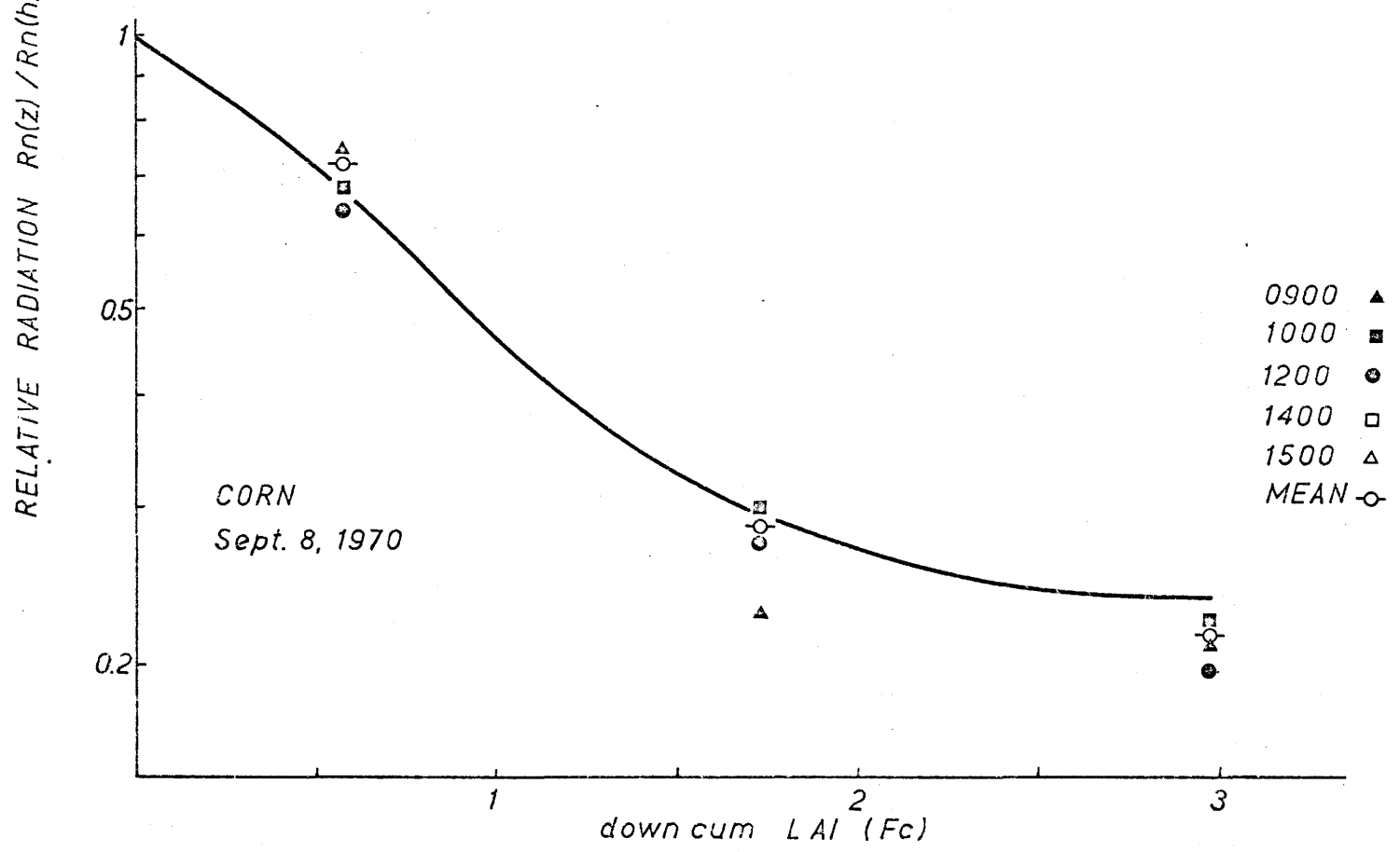

FIG. 51. *DAYTIME NET RADIATION TRANSMISSION IN CORN (Impens, 1969b)*

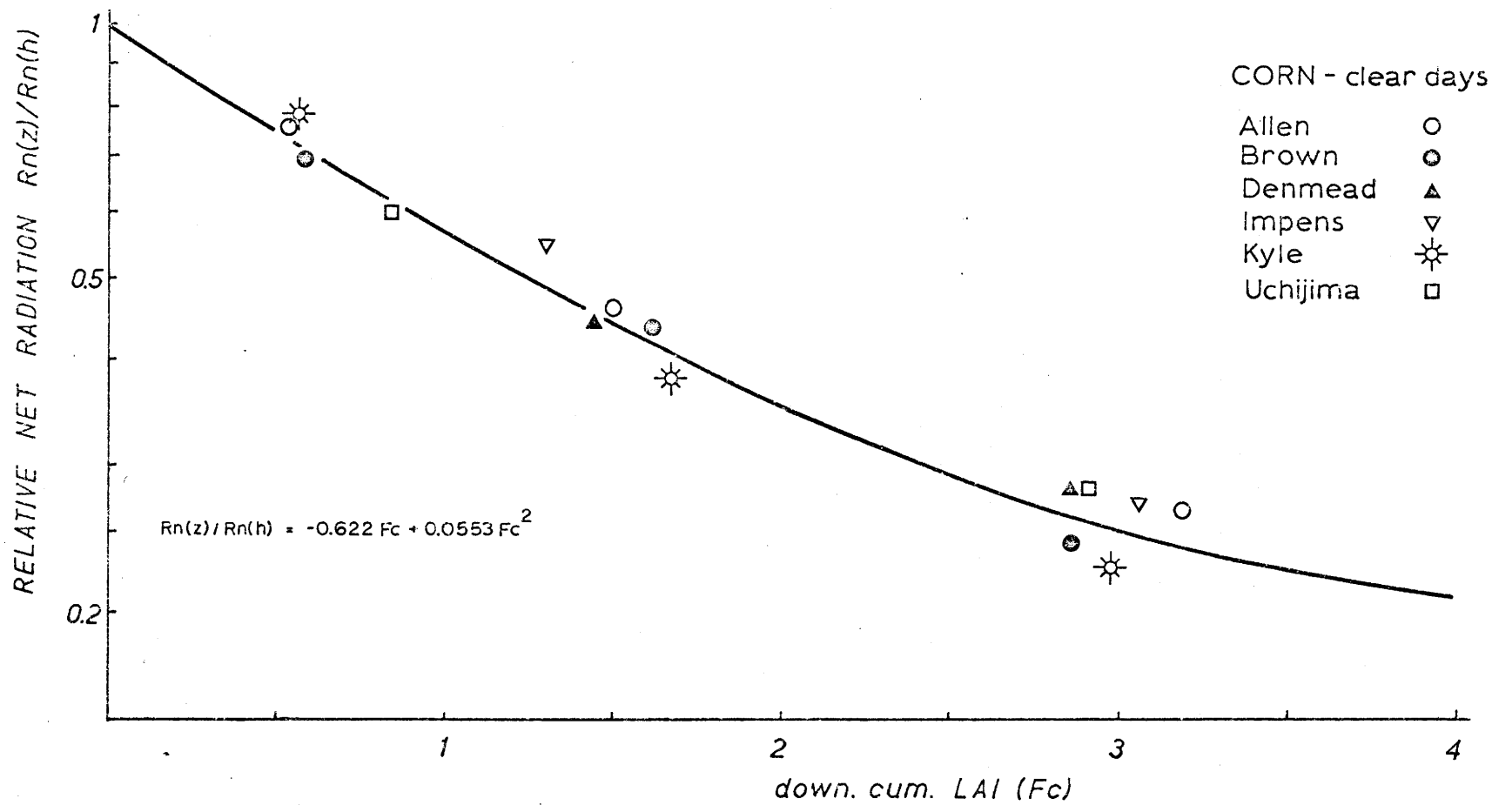

presented by Impens and Lemeur (1969b). Their line of best fit is a regression equation with constants $\kappa_1 = -0.6220$ and $\kappa_2 = 0.0553$. When the mean daytime ratios for clear days from the present study are plotted along with these data, (Fig. 51), they agree well with previous results obtained in corn.

This method, although empirical, produces very satisfactory results on a daily basis, particularly on clear days. On days with varying cloud amounts the whole problem is considerably more complex. In cases such as these, it may be necessary to study the mechanisms operating within the canopy, particularly the temperature regime, before any satisfactory prediction of relative net radiation can be made.

4. Summary

A number of conclusions follow from the preceding discussion. The exponential model for net short-wave radiation was found inadequate as a means of predicting radiation levels in the canopy, even on clear days. Various modifications provided better estimates. The Duncan et al., (1967) model was a considerable improvement, since it incorporates the diffuse radiation component. However, the basic assumption is still present that the decline is exponential and that the deviations must be accounted for by modifying the terms in the exponent. As a result the model is very unwieldy and difficult to manipulate since it requires a large number of parameters some of which can only be obtained with dubious accuracy. Monteith's (1965b) model attempted to simplify the number of variables and thus suffers from a lack of accuracy.

The study reveals the necessity to consider the direct and diffuse

components of the global radiation separately since their behaviour in the canopy is very different. There are also strong indications that it is necessary to consider the depletion of visible and near infra-red radiation as separate entities.

It was found that the Impens and Lemeur (1969b) model of net radiation in the canopy was quite successful and a considerable improvement over the exponential model.

CHAPTER VII

A NEW APPROACH TO DEPLETION OF SHORT-WAVE RADIATION

1. Introduction

In the exponential model of global radiation depletion it has been shown that the extinction coefficient k is not a constant, but varies with leaf angle j and the angle of penetration of the solar beam m (Anderson, 1966). This means that the depletion of the direct and diffuse components will be markedly different, hence the poor performance of the model under cloudy conditions. The necessity to treat the two components of the global radiation differently was realised by Duncan et al., (1967). However, they retained the framework of the exponential model and thus their model requires many complex variables some of which are difficult, if not impossible to specify. Although not very successful, Monteith's (1965) attempts to reduce the number of variables, by simplifying the canopy structure, is an admirable goal. His failure to separate the components is probably the major fault of the model.

The ultimate aim of a model for short-wave radiation in the plant canopy must be to provide an accurate prediction of the profile under a wide range of conditions given a minimum of input parameters. This is the attempted purpose of the model now presented.

2. Theory

Radiation estimates within a crop canopy are difficult and

subject to many sources of error. Fortunately we can measure global radiation fluxes above the crop with comparatively greater accuracy. By using measurements of incoming direct and diffuse radiation, sources of error above the canopy are minimised.

The object of the model is to predict global and net global radiation in the canopy by a numerical method using these radiation inputs. An attempt is made to simplify plant parameters influencing the depletion by using individual leaf properties rather than canopy properties. Data given by Lemon (1967) indicate that this assumption is fairly accurate. Absorption spectra for a corn leaf and a corn plant community do not vary widely, the community absorption tending to be higher. Canopy reflection coefficients tend to be lower (Monteith, 1959a) than individual leaf reflection coefficients due to trapping of radiation between the crop elements. The resultant sum of reflection and absorption is nearly constant for both the individual corn leaves and the crop community.

The following plant properties are used:

1. crop leaf-area-index (F),
2. leaf reflection coefficient (α),
3. leaf absorption coefficient (a),
4. ground reflection coefficient (αg).

It is proposed that the corn community can be represented by n horizontal layers of leaves with constant leaf-area-index F_1, F_2, F_3 ..... F_n over the complete depth of the canopy. Leaf area and position are described by the leaf-area-index within each layer. It is assumed that the leaves grow equally in all directions around the individual

stems and act as Lambertian surfaces, reflecting light non-directionally. Transmitted direct radiation is assumed to be transformed into diffuse radiation.

If I_i is the incoming direct radiation ($I \cos \zeta$), and D_i is the incoming diffuse radiation the interaction of these streams as they meet a layer F_i is as follows:

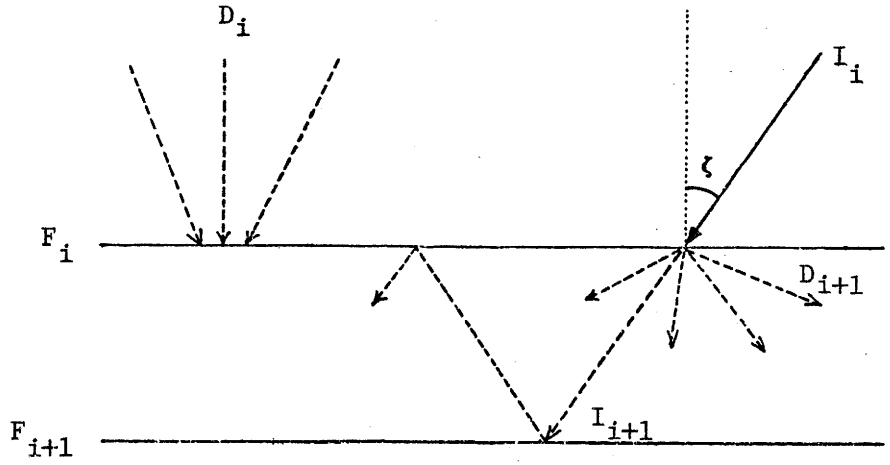

The change in the direct beam radiation ΔI_i is

$$\Delta I_i = -F_i . \sec \zeta . I_i , \tag{30}$$

where $F_i . \sec \zeta$ is the leaf-area-increment with a correction for foliage mass dependent on solar zenith angle. Hence, the direct radiation incident on the layer F_{i+1} is

$$I_{i+1} = I_i + \Delta I_i . \tag{31}$$

The change in the diffuse radiation ΔD_i after passing through the layer F has three components

1. diffuse radiation is absorbed by the leaves and some is reflected upwards,

$$-\left[D_i \cdot F_i \cdot (\alpha + a)\right] \quad ;$$

2. the unintercepted direct radiation is scattered within the layer,

$$\left[I_{i+1} \cdot \alpha F_{i+1} \cdot \alpha F_i\right] \quad ;$$

3. some intercepted direct radiation is transmitted as diffuse radiation within the layer,

$$\left[I_i \cdot F_i \sec\zeta \cdot 1 \quad - \quad (\alpha + a)\right] .$$

The total change in diffuse radiation is given by the algebraic sum of the components

$$D_i = -\left[D_i \cdot F_i (\alpha + a)\right] + \left[I_{i+1} \cdot \alpha F_i\right] + \left[I_i \cdot F_i \sec\zeta \cdot 1 - (\alpha + a)\right] , \tag{32}$$

and the incident diffuse radiation at the layer F_{i+1} by

$$D_{i+1} = D_i + \Delta D_i . \tag{33}$$

By incrementing I_i and D_i through each layer the global radiation profile is obtained. Flux values are calculated as the radiation passes through each layer, the height of which is found from the curve relating cumulative leaf-area-index to height.

Net global radiation at each level is then calculated by the

following procedure:

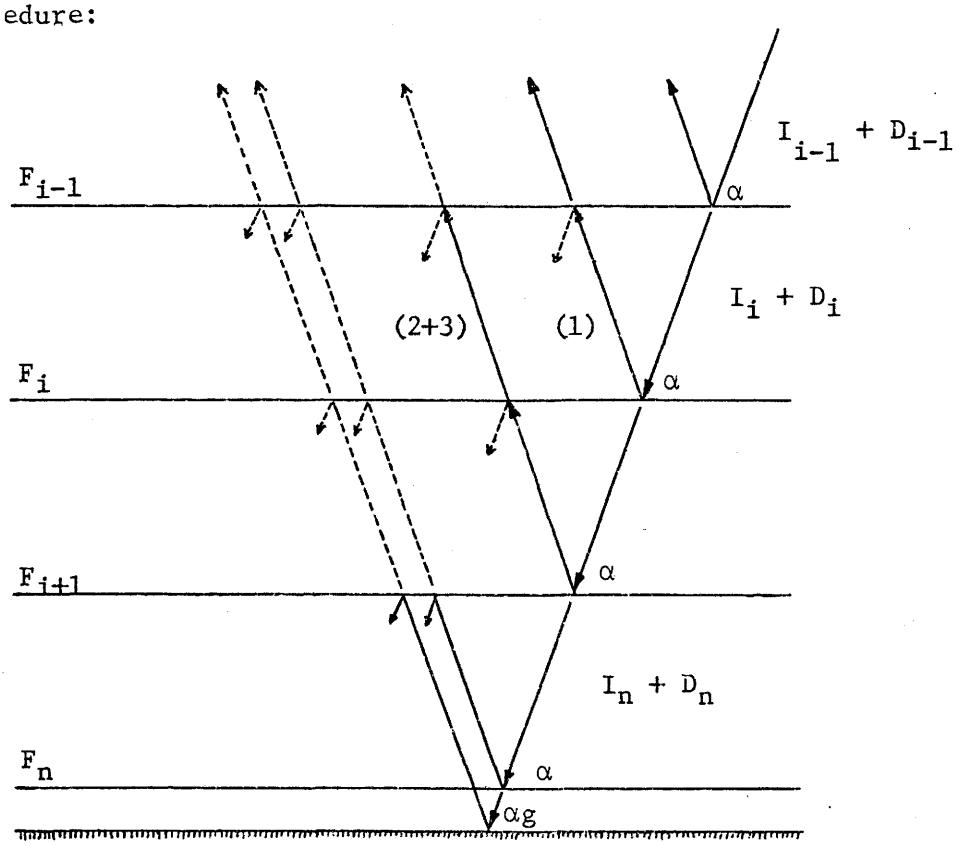

Reflection is considered to have three components

1. direct reflection from the F_i layer,

2. direct reflection from the F_{i+1} layer unintercepted by the F_i layer,

3. direct reflection from the F_{i+1} layer transmitted through the F_i layer.

Upward reflection from lower layers will be very small and may be ignored in the computations. The reflected radiation from the F_i layer is then

$$R_i = [(I_i + D_i).F_i] + [R_{i+1}(1 - F_i)] + \{R_{i+1}[1 - (\alpha + a)]F_i\} . \quad (34)$$

One special case has to be accounted for. This is the reflected radiation from the lowest canopy level F_n, which incorporates the ground reflection. The reflected radiation at this level is given by

$$R_n = [(I_n + D_n).F_n\alpha] + [(I_{n+1} + D_{n+1}). \alpha g.(1 - F_n)] \quad . \qquad (35)$$

The reflected radiation is subtracted from the global radiation at each level to obtain the net global profile.

3. Evaluation of the model

The model was tested using short-wave radiation data obtained under cloudless skies. No diffuse radiation estimates were available in this study. Consequently a further assumption was made that the diffuse radiation component was 10% of the global radiation. Further tests with the model indicated that this assumption was valid. Changing the proportions of diffuse radiation from 5 - 20%, the amounts normally found on clear days, did not noticeably alter the prediction. Values of leaf albedo for corn were obtained from previous work at Simcoe (Davies and Buttimor, 1969). Mean leaf absorption was calculated over the spectral range from the relations given by Yocum, Allen and Lemon (1964). The ground reflection coefficient at the measurement site was taken as the mean value obtained in previous studies at this site (Arnfield, unpublished data). The leaf-area-increment was eventually chosen on the basis of sampling the crop depth uniformly., (Fig. 52). A value of 0.3 permitted the height increment at the densest region in the canopy (100 - 50 cm above the ground) to be approximately 10 cm thick thus

FIG. 52. *LEAF-AREA-DENSITY PROFILE & DOWNWARD CUMULATIVE LEAF-AREA-INDEX IN CORN September, 5, 1970*

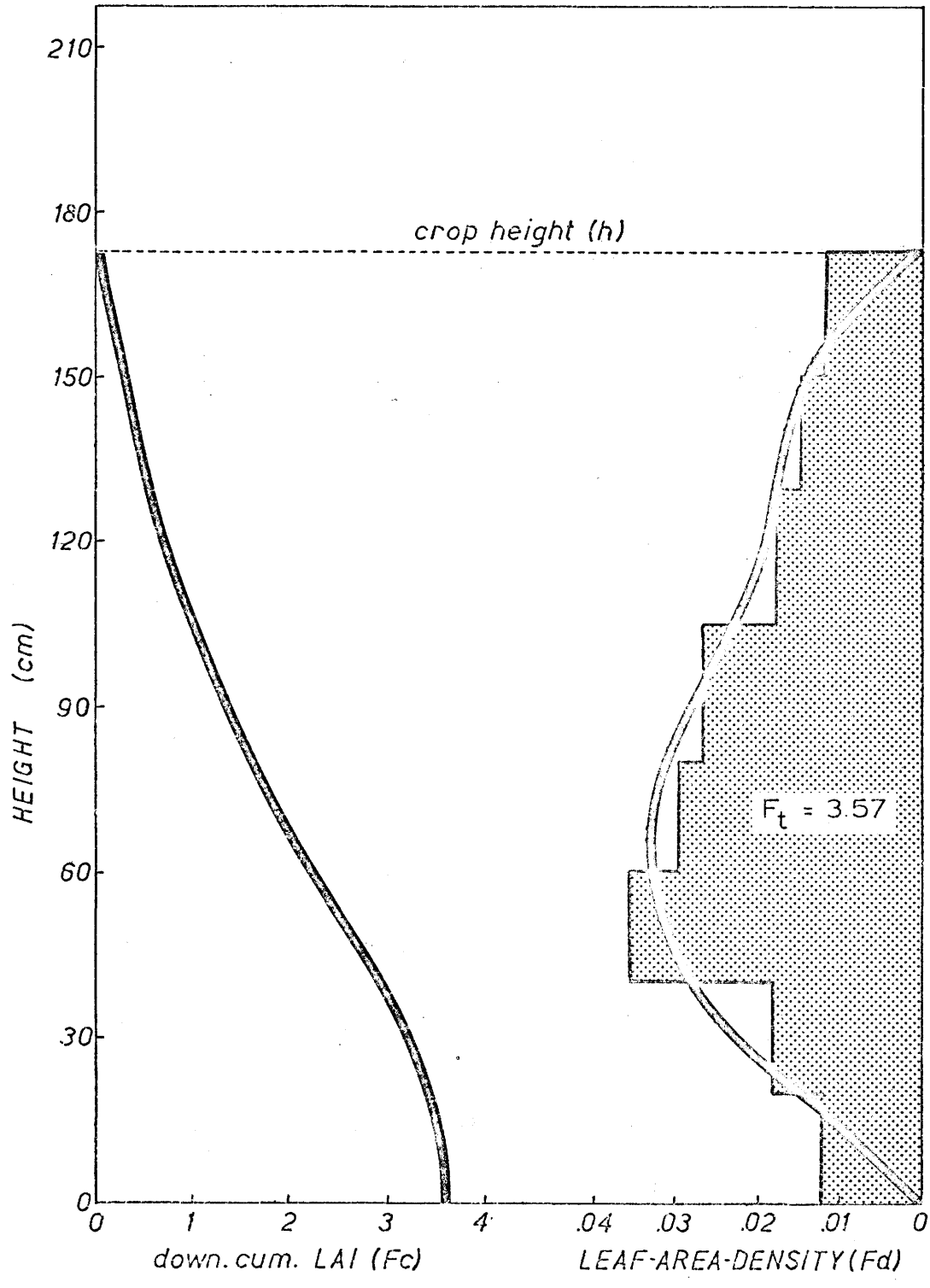

allowing adequate sampling in this zone.

The performance of the model is shown in Fig. 53. In general, the model succeeds very well in predicting net global radiation. A number of points may be raised concerning the divergence of the predicted from the measured profile. In the incomplete canopy region the model seriously under-predicts the fluxes of net global radiation at solar noon. The model as formulated here does not account for possible row effects evident when the sun is closest to the zenith. In addition to the multiple reflection of short-wave radiation along the rows at this time it should be pointed out that the measured profile at this time is subject to considerable errors. The upper sensor at 130 cm was sited in the incomplete canopy region, with part of its length between the rows. The net pyranometer thus received proportionately more radiation than it would have ordinarily. Before any modifications are made to the model to account for multiple reflection more data are required on an improved spatial sampling basis to ensure that the flux measured in this region is not a purely local effect of sensor siting.

The model also under-predicts in the lower region of the canopy but this is not so serious since flux intensities are considerably lower than in the higher layers. In this respect the model has a fault in common with the exponential model. The under-prediction may be attributed to two causes. With increasing depth in the canopy the spectral composition of the radiation changes markedly, (Allen and Brown, 1965), considerably larger proportions of near infra-red and green light being present. Individual leaf reflection in the spectral region 0.54 - 0.56 μm is twice that in the rest of the visible spectrum and in the near infra-red region

FIG. 53. *PERFORMANCE OF "PHYSICAL" MODEL (clear day)*

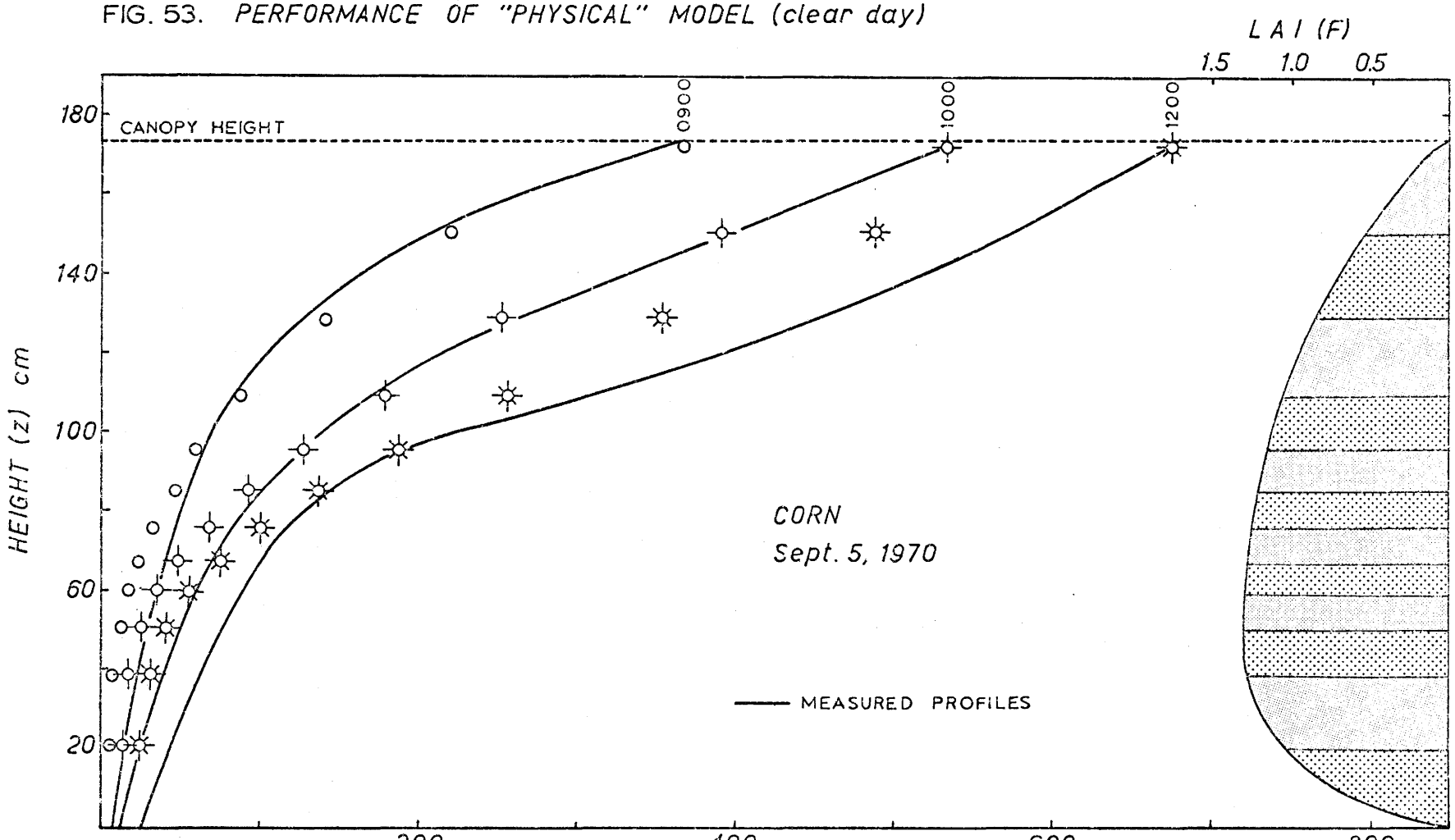

FIG. 54. *TRANSMISSION, REFLECTION AND ABSORPTION SPECTRA OF A CORN LEAF (after Yocum, Allen and Lemon, 1964)*

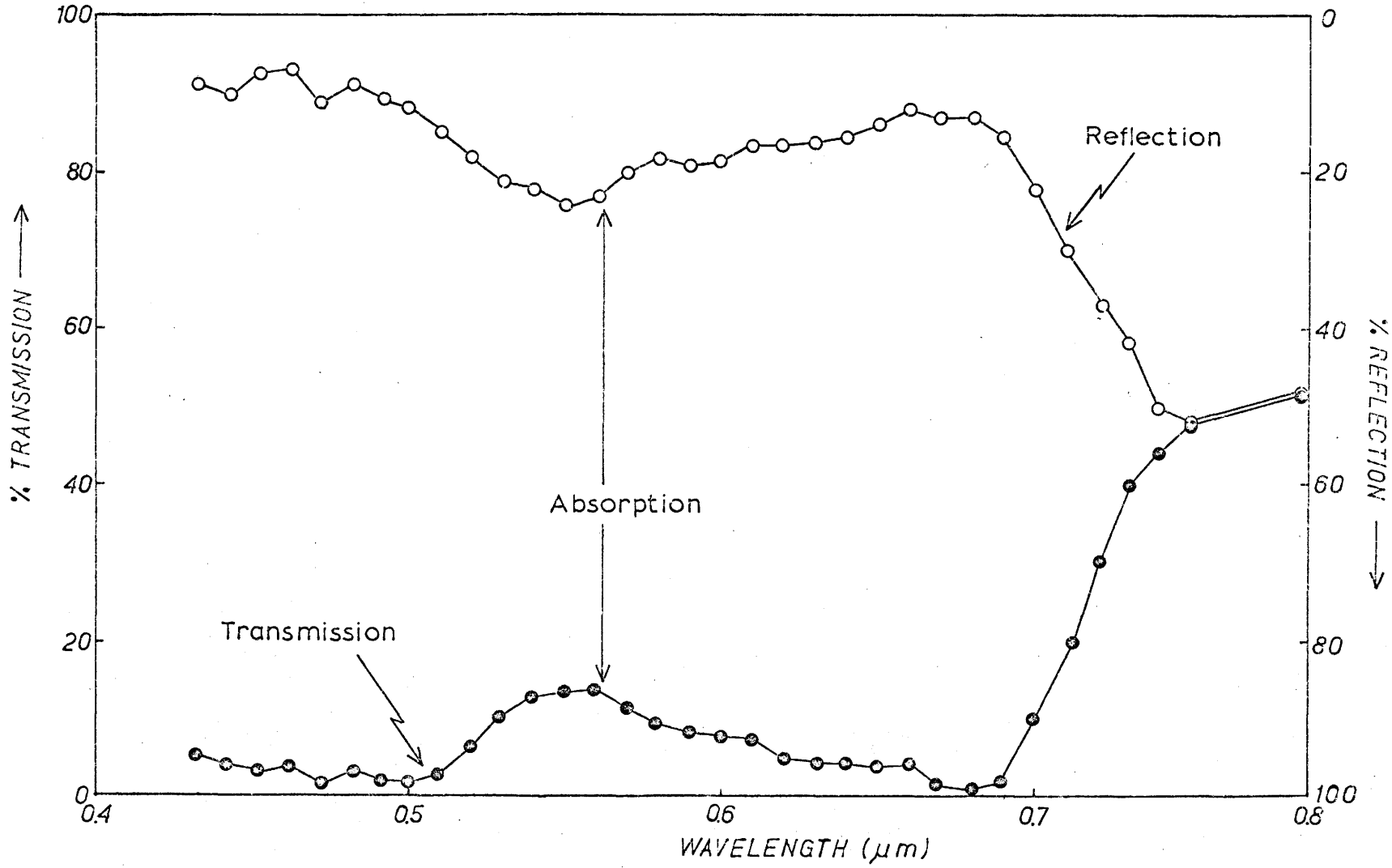

FIG. 55. *PERFORMANCE OF "PHYSICAL" MODEL (cloudy day)*

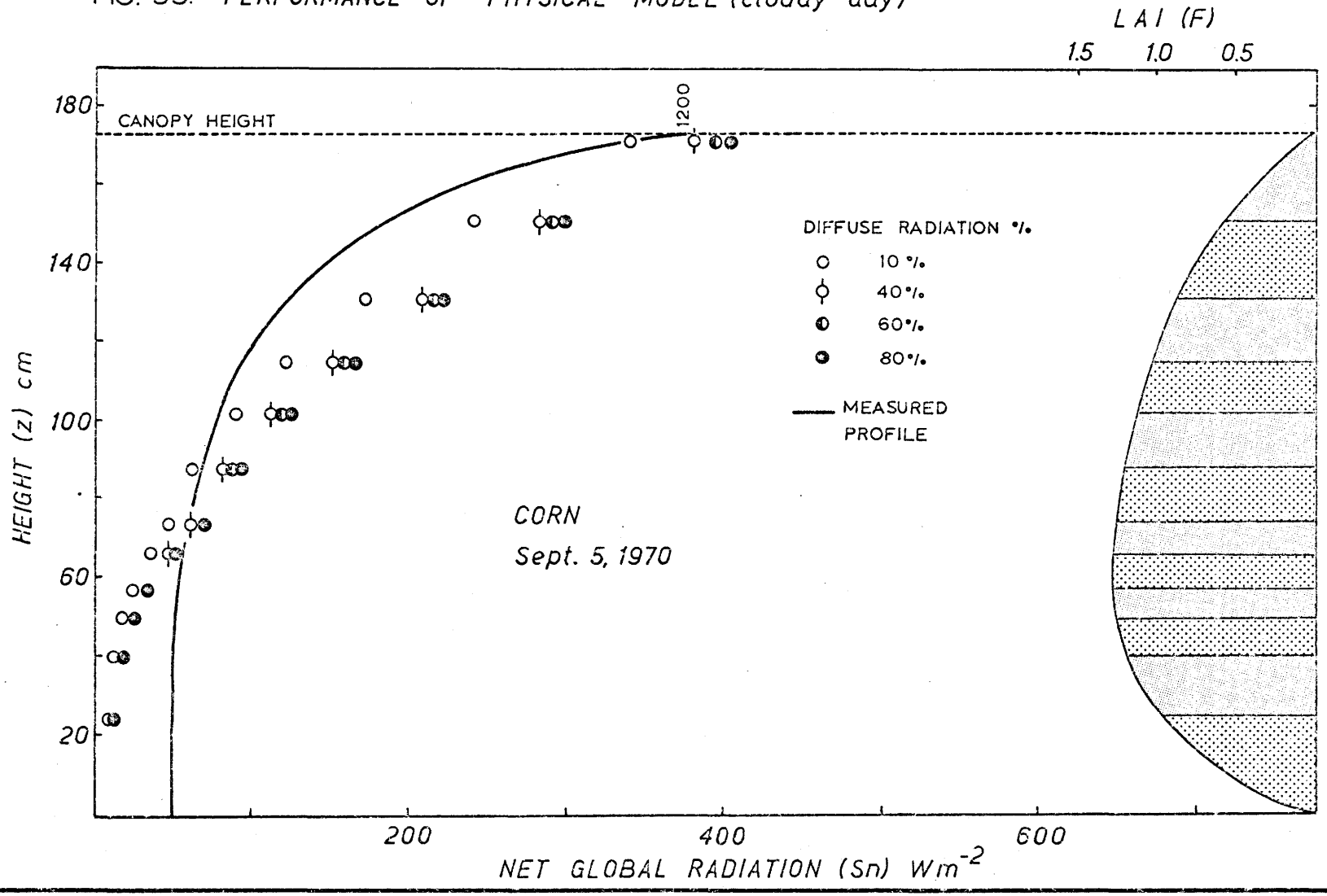

beyond 0.75 μm reflection is as high as 50% (Fig. 54). This is unaccounted for in the model, where a constant reflection coefficient is assumed, inevitably resulting in some under-prediction. In addition, in the lowest layers of the canopy the majority of the radiation is diffuse. If the depletion of the diffuse component is incorrectly handled in the formulation this will also contribute to the under-prediction.

The evaluation of the model under cloudy conditions supports the latter statement (Fig. 55). Varying proportions of diffuse radiation (10%, 40%, 60% and 80%) were assumed and the predicted profiles calculated using the model. In all cases prediction is poorer than that obtained under clear skies. This suggests that the model does not take account of the diffuse radiation depletion correctly, since accuracy decreases with increasing quantities of diffuse radiation present on cloudy days and at greater depths in the canopy.

Further studies are required to assess the mechanisms whereby diffuse radiation is depleted in the canopy before accurate cloudy day predictions can be made. However, on clear days when diffuse radiation proportions are small the model performs exceptionally well.

CHAPTER VIII

CONCLUSIONS AND FURTHER DEVELOPMENT

A number of conclusions may be drawn from the results of the investigation.

The net radiation above the canopy is a linear function of the global radiation incident on the surface as shown by previous workers (Davies, 1967; Linacre, 1968). Use of a reflection coefficient and a "heating coefficient" do not improve the relationship (Idso, 1968; Davies and Buttimor, 1969). Dependence of the reflection coefficient on solar zenith angle is also evident.

It was found that the exponential model of Monsi and Saeki (1953) was a poor predictor of relative net global radiation in the canopy. Addition of leaf and sun angle terms did not greatly improve the prediction. The model due to Monteith (1965) was also insufficiently accurate although the attempt to simplify the number of variables is noted as an admirable goal. The major shortcoming of these models appears to be the complete disregard of the fact that global radiation is composed of direct and diffuse components and that these behave differently within the canopy.

The improved exponential model of Duncan et al. (1967) produced much better results. However, the variables are many and difficult to estimate and as a result the model suffers from its own complexity. Since the diffuse component is treated separately from the direct radiation the

model has a distinct advantage over the exponential model.

Net radiation models were also investigated. The exponential model was found to be insufficiently accurate for prediction of net radiation on a time basis shorter than a day. The Impens and Lemeur (1969) model was a considerable improvement. The major criticism is the lack of process oriented models for the prediction of net radiation.

A new model introduced in the previous chapter predicts net global radiation in the canopy very well, especially when diffuse radiation amounts are small. The poorer prediction under cloudy skies suggests that the diffuse depletion is not correctly handled. To adequately test the model much more and better data are required. Studies of this nature require accurate instrumentation placed within a detailed sampling grid. One of the weak points of this study was the inadequate horizontal spatial sampling particularly in the variable, incomplete canopy region.

This study points to the need for further work to ascertain the behaviour of diffuse radiation in the canopy before it can be adequately modelled on a "physical"basis. Evidence also suggests that investigation of the changing spectral composition of radiation with depth may yield valuable information about the radiation regime within plant canopies.

REFERENCES

Allen, L. H. and K. W. Brown, 1965: Short-wave radiation in a corn crop, Agron. J., 57, 575-580.

Allen, L. H., C. S. Yocum and E. R. Lemon, 1964: Photosynthesis under field conditions VII. Radiant energy exchanges within a corn crop canopy and implications in water use efficiency, Agron. J., 56, 253-259.

Anderson, M. C., 1966: Stand structure and light penetration II. A theoretical analysis, J. Appl. Ecol., 3, 41-54.

_____, 1969a: Radiation and crop structure, IBP/PP Handbook, CSIRO, Canberra, 86 pp.

_____, 1969b: A comparison of two theories of scattering of radiation in crops, Agric. Meteor., 6, 399-405.

Brougham, R.W., 1958: Interception of light by the foliage of pure and mixed stands of pasture plants, Aust. J. Agric. Res., 9, 39-52.

Brown, K. W., 1964: Vertical fluxes within the vegetative canopy of a cornfield, Interim Rept., 64 - 1 - USDA - ARS - SWC (for USARDC, Ft. Huachuca), Ithaca, N.Y.

Brown, K. W. and W. Covey, 1966: The energy budget and micrometeorological transfer processes within a cornfield, Agric. Meteor., 3, 73-96.

Brown, K. W., N. J. Rosenberg and P. Doraiswamy, 1970: Shading inverted pyranometers and measurements of radiation reflected from an alfalfa crop, Water Resources Res., 6, 1782-1786.

Budyko, M. I., 1956: Teplovoi balans zemnoi poverkhnosti, Gidro. Izdatel'stvo, Leningrad. (Translated as: Stepanova, N.A., 1958. The heat balance of the earth's surface. US Dept. of Commerce, Office of Technical Services, Washington, D.C.) 259 pp.

Chang, Jen-Hu, 1961: Microclimate of sugar cane, Haw. Plant. Rec., 56, 195-223.

_____, 1968: Climate and agriculture - an ecological survey, Aldine, Chicago, 304 pp.

Cowan, I. R., 1966: Water transport and energetics in crop plants and their environment, Ph.D. Thesis, Univ. of Nottingham, England.

_____, 1968: The interception and absorption of radiation in plant stands, J. Appl. Ecol., 5, 367-379.

Cowan, I. R. and F. L. Milthorpe: Physiological responses in relation to the environment within the plant cover, Nat. Resources Res. V., Proc. Copenhagen Symp. UNESCO, 107-130.

Davies, J. A., 1967: A note on the relationship between net radiation and solar radiation, Quart. J. R. Meteor. Soc., 93, 109-115.

Davies, J. A. and P. H. Buttimor, 1969: Reflection coefficients heating coefficients and net radiation at Simcoe, S. Ontario, Agric. Meteor., 6, 373-386.

Decker, W. L., 1964: Research Bulletin No. 854, Agric. Expt. Sta., Missouri.

Denmead, O. T., 1967: A strip net radiometer, Aust. J. Instr. Control, 61.

Denmead, O. T., L. J. Fritschen and R. H. Shaw, 1962: Spatial distribution of net radiation in a cornfield, Agron. J., 54, 505-510.

Duncan, W. G., R. S. Loomis, W. A. Williams and R. Hanau, 1967: A model for simulating photosynthesis in plant communities, Hilgardia, 38, 181-205.

Ekern, P. C., 1965: The fraction of sunlight retained as net radiation in Hawaii, J. Geophys. Res., 70, 785-793.

Fitzpatrick, E. A. and W. R. Stern, 1965: Components of radiation balance of irrigated plots in a dry monsoonal climate, J. Appl. Meteor., 4, 649-660.

Fritschen, L. J., 1963: Construction and evaluation of a miniature net radiometer, J. Appl. Meteor., 2, 165-172.

_____, 1967: Net and solar radiation relations over irrigated field crops, Agric. Meteor., 4, 55-62.

Funk, J. P., 1959: Improved polyethylene shielded net radiometer, J. Sci. Instr., 36, 267-370.

_____, 1962: A net radiometer designed for optimum sensitivity and a ribbon thermopile used in a miniaturised version, J. Geophys. Res., 67, 2753-2760.

Gates, D. M., 1965: Energy, plants and Ecology, Ecol., 46, 1-13.

_____, 1966: Characteristics of soil and vegetated surfaces to reflected and emitted radiation, Proc. 4th Symp. Remote Sens. Environ., Univ. of Michigan, Ann Arbor, 573-600.

Gates, D. M., H. J. Keegan, J. C. Schleter and V. R. Weidner, 1965: Spectral properties of plants, Appl. Opt.,4, 11-20.

Gier, J. T. and R. V. Dunkle, 1951: Total hemispherical radiometers, Trans. Amer. Inst. Elect. Engrs., 70, 339-343.

Graham, W. G. and K. M. King, 1961: Short-wave reflection coefficient for a field of maize, Quart. J. R. Meteor. Soc., 87, 425-428.

Hanau, R., 1967: Appendix on theory for the computation of leaf illumination by skylight, (in A model for simulating photosynthesis in plant communities, by W. G. Duncan et al.), Hilgardia, 38, 202-205.

Idso, S. B., 1968: An analysis of the heating coefficient concept, J. Appl. Meteor., 7, 716-717.

Idso, S. B., D. G. Baker and B. L. Blad, 1969: Relations of radiation fluxes over natural surfaces, Quart. J. R. Meteor. Soc., 95, 244-257.

Impens, I. I., 1970: Daytime distribution of energy sinks and sources and transfer processes within a sunflower canopy, Proc. Paris Symp. UNESCO, 1-19.

Impens, I. I. and R. Lemeur, 1969a: The radiation balance of several field crops, Arch. Meteor. Geophys. Bioklim. B17, 261-268.

_____, 1969b: Extinction of net radiation in different crop canopies, Arch. Meteor. Geophys. Bioklim. B17, 403-412.

Impens, I. I., R. Lemeur and R. Moermans, 1970: Spatial and temporal variation of net radiation in crop canopies, Agric. Meteor., 7, 335-337.

Inoue, E., 1968: The CO_2 concentration profile within crop canopies and its significance for the productivity of plant communities, Nat. Resources Res. V., Proc. Copenhagen Symp. UNESCO, 359-366.

Isobe, S., 1962: Preliminary studies on physical properties of plant communities, Bull. Nat. Inst. Agric. Sci., Tokyo, A9, 29-67.

Kasanaga, H. and M. Monsi, 1954: On the light transmission of leaves and its meaning for the production of matter in plant communities, Jap. J. Bot., 14, 304-324.

Lemon, E. R., 1967: Aerodynamic studies of CO_2 exchange between the atmosphere and the plant, in Harvesting the Sun, ed. A. San Pietro, F.A. Greer and T. J. Army, Academic Press, New York, 263-290.

Linacre, E. T., 1968: Estimating the net radiation flux, Agric. Meteor., 5, 49-63.

Maharajh Singh, D. B. Peters and J. W. Pendleton, 1968: Net and spectral radiation in soybean canopies, Agron. J., 60, 542-545.

Monsi, M. and T. Saeki, 1953: Uber den Lichtfaktor in den Planzengesellschaften und seine Bedeutung für die Stoffproduktion, Jap. J. Bot., 14, 22-52.

Monteith, J. L., 1958: The heat balance of soil beneath crops, in Climatology and microclimatology, UNESCO, New York.

_____, 1959a: The reflection of short-wave radiation by vegetation, Quart. J. R. Meteor. Soc., 85, 386-392.

_____, 1959b: Solarimeter for field use, J. Sci. Instr., 230, 583-617.

_____, 1965a: Radiation and crops, Exp. Agric., 1, 241-251.

_____, 1965b: Light distribution and photosynthesis in field crops, Ann. Bot. (N.S.), 29, 17-37.

_____, 1966: The photosynthesis and transpiration of crops, Exp. Agric., 2, 1-14.

Monteith, J. L. and G. Szeicz, 1961: The radiation balance of bare soil and vegetation, Quart. J. R. Meteor. Soc., 87, 159-170.

_____, 1962: Radiative temperature in the heat balance of natural surfaces, Quart. J. R. Meteor. Soc., 88, 496-507.

Oguntoyinbo, J. S., 1970a: Reflection coefficient of natural vegetation, crops, and urban surfaces in Nigeria, Quart. J. R. Meteor. Soc., 96, 430-441.

_____, 1970b: Surface measurements of albedo over different agricultural crop surfaces in Nigeria and their spatial and seasonal variability, J. Geog. Assoc. Nigeria, 13, 39-55.

Penman, H. L., 1948: Natural evaporation from open water, bare soil and grass, Proc. Roy. Soc., London, A193, 120-145.

Reeve, J. E., 1960: Appendix on derivation of formulae, (in Inclined point quadrats, by J. Warren Wilson), New Phytol., 59, 8.

Rose, C. W., 1966: Agricultural Physics, Pergamon Press, London. 226 pp.

Saeki, T., 1963: Light relations in plant communities, in Environmental Control of Plant Growth, ed. L. T. Evans, Academic Press, New

Stanhill, G., G. J. Hofstede and J. D. Kalma, 1966: Radiation balance of natural and agricultural vegetation, Quart. J. R. Meteor. Soc., 92, 128-140.

Stanhill, G. and M. Fuchs, 1968: The climate of the cotton crop. Physical characteristics and microclimate relationships, Agric. Meteor., 5, 183-202.

Stern, W. R. and C. M. Donald, 1962: Light relationship in grass-clover swards, Aust. J. Agric. Res., 13, 599-614.

Szeicz, G., J. L. Monteith and J. M. Dos Santos, 1964: Tube solarimeter to measure radiation among plants, J. Appl. Ecol., 1, 169-174.

Tanner, C. B., 1963: Basic instrumentation and measurements for plant environment and micrometeorology, Soils Bulletin 6, Univ. of Wisconsin, Madison, Wisc.

Tanner, C. B., A. E. Peterson and J. R. Love, 1960: Radiant energy exchange in a corn field, Agron. J., 52, 373-379.

Uchijima, Z., 1962: Studies on the microclimate within plant communities, J. Agric. Meteor., Japan, 18, 1-9.

Warren Wilson, J., 1960: Inclined point quadrats, New Phytol., 59, 1-8.

Watson, D. J., 1947: Comparative physiological studies on the growth of field crops. I. Variation in net assimilation rate and leaf area between species and varieties, and within and between years, Ann. Bot., (N.S.), 11, 41-76.

Yocum, C. S., L. H. Allen and E. R. Lemon, 1964: Photosynthesis under field conditions VI. Solar radiation balance and photosynthetic efficiency, Agron. J., 56, 249-253.